"Modélisation 1D des écoulements, exemples en biomécanique, en hydrodynamique fluviale et en écoulements granulaires"

Lagrée Pierre-Yves DR CNRS (∂'Alembert UMR 7190 CNRS-Sorbonne Université)

Félix Lecomte (1737-1817)
D'Alembert (1717-1783), auteur de l'Encyclopédie
Avant 1786 Sculpture Marbre
H. 1,50 m ; l. 0,95 m ; pr. 0,92 m
Don de Napoléon Ier à l'Institut de France, 1807

en arrière plan:
Eugène Delacroix
La Liberté guidant le peuple, 1830
260 × 325 cm

Dans de nombreux cas ayant des applications évidentes (santé : écoulement du sang dans les artères, ou environnement : écoulements dans les fleuves, inondations, ressauts, glissements de terrains…) les phénomènes se produisent sur une échelle longitudinale bien plus grande que l'épaisseur caractéristique de l'écoulement. Cela permet de simplifier les équations, puis on les moyenne sur l'épaisseur ce qui donne les équations de type Saint-Venant. Nous discuterons la notion d'équations simplifiées moyennées sur l'épaisseur sur ces cas précédents et l'influence des fermetures. Pour rajouter de la précision, on peut envisager des méthodes multicouches que nous détaillerons, en rajoutant les effets non hydrostatiques on peut même revenir à Navier Stokes (à surface libre).

Masashi Saito, Xiaofei Wang, Arthur Ghigo, Jeanne Ventre, Teresa Politi, Fanshuo Ma,…

Geoffroy Kirstetter, Olivier Delestre, Mathilde Tavares,…

Stéphane Popinet, Jose Maria Fullana, Stéphanie Lebœuf…

d'Alembert

UMA

∂'Alembert
Institut Jean le Rond d'Alembert

SCIENCES SORBONNE UNIVERSITÉ

cnrs

Many interesting problems in fluid mechanics are one dimensional the most simple way to deal with fluids is to do a 1D approximation

(as in solids: beams/ rods… are very useful in engineering science)

at leat useful for engineers (CNRS-ingénierie), fast computations…

small aspect ratio, use a mean velocity… many details are lost

loss of details on velocity and shear stress

method to solve 1D problems and some comparisons to 2D

Three examples in this talk

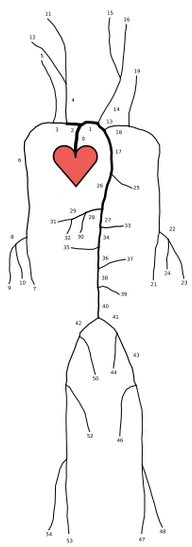

Blood flow
in arteries

hydraulic jump

granular avalanches flows

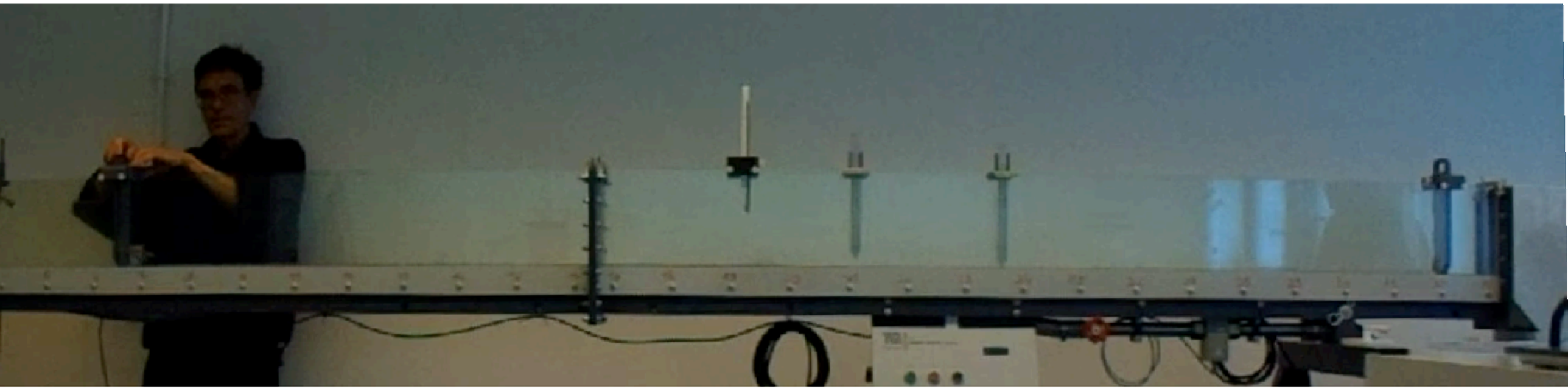

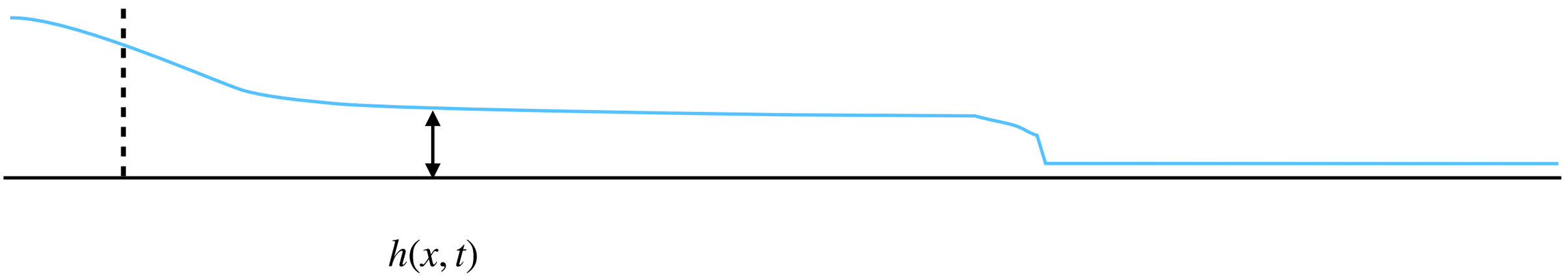

Saint-Venant (Shallow Water) 1871

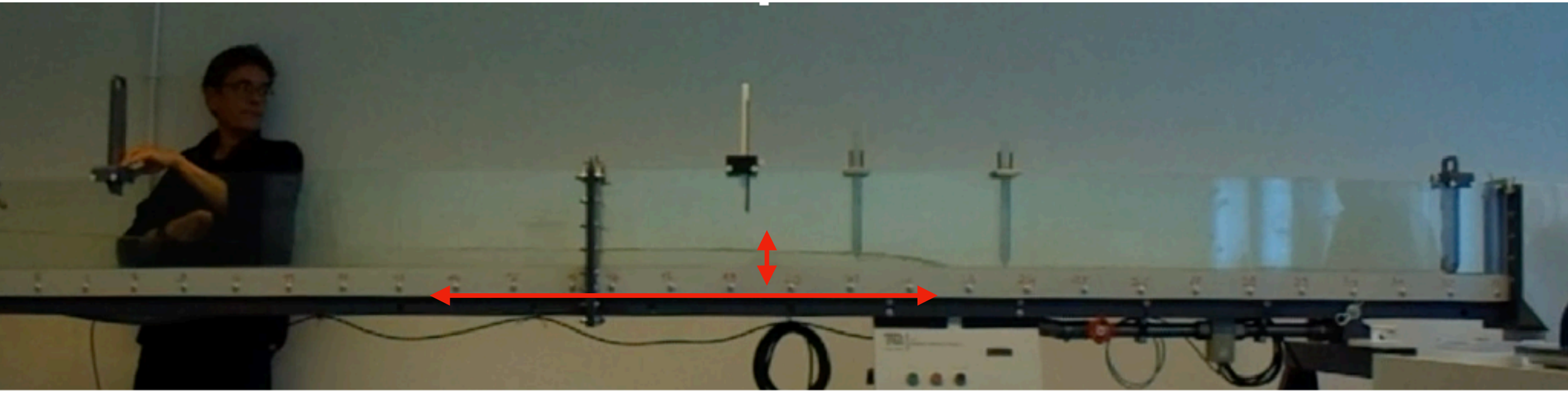

ε

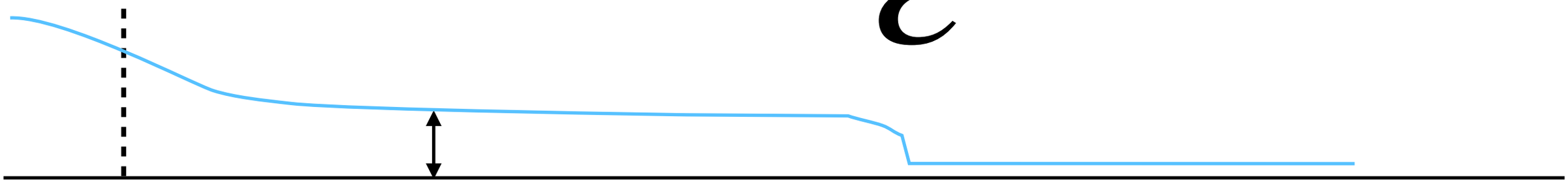

$h(x,t)$

Saint-Venant (Shallow Water) 1871

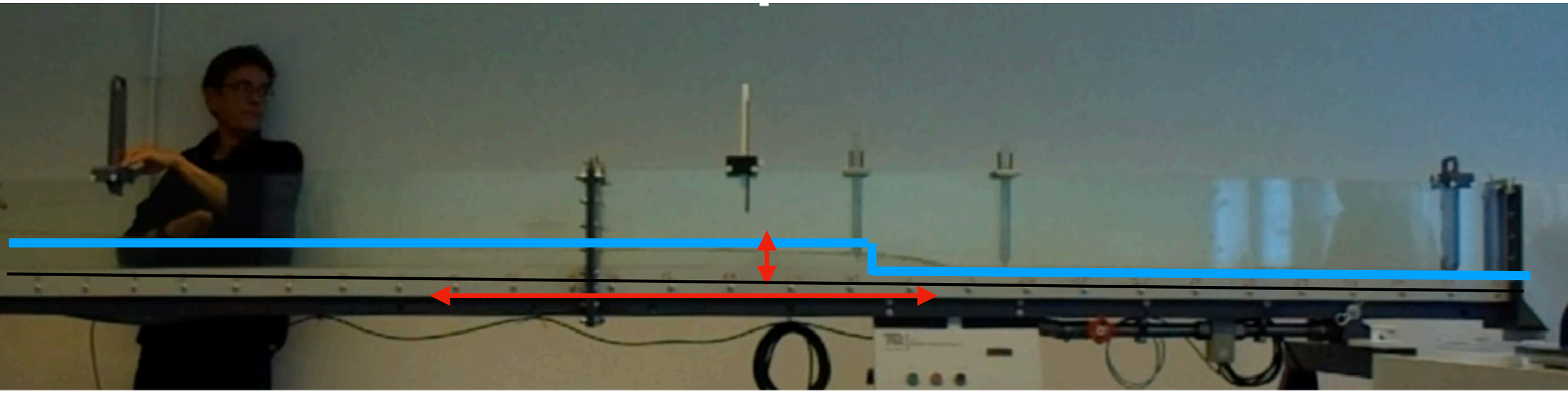

ε

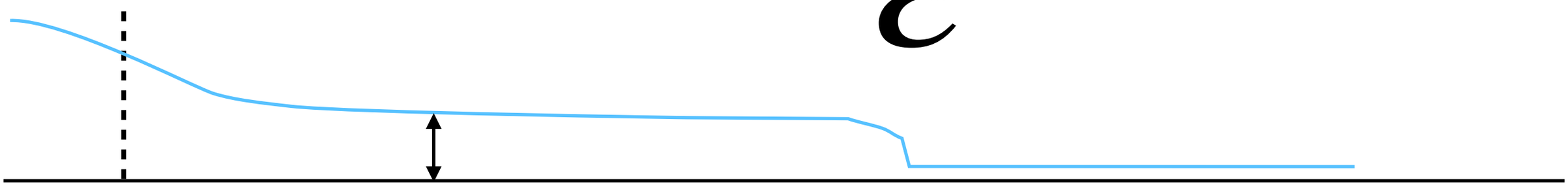

$h(x,t)$

Saint-Venant (Shallow Water) 1871

ε

mud flow (Bingham)

granular avalanches, μ(I) rheology

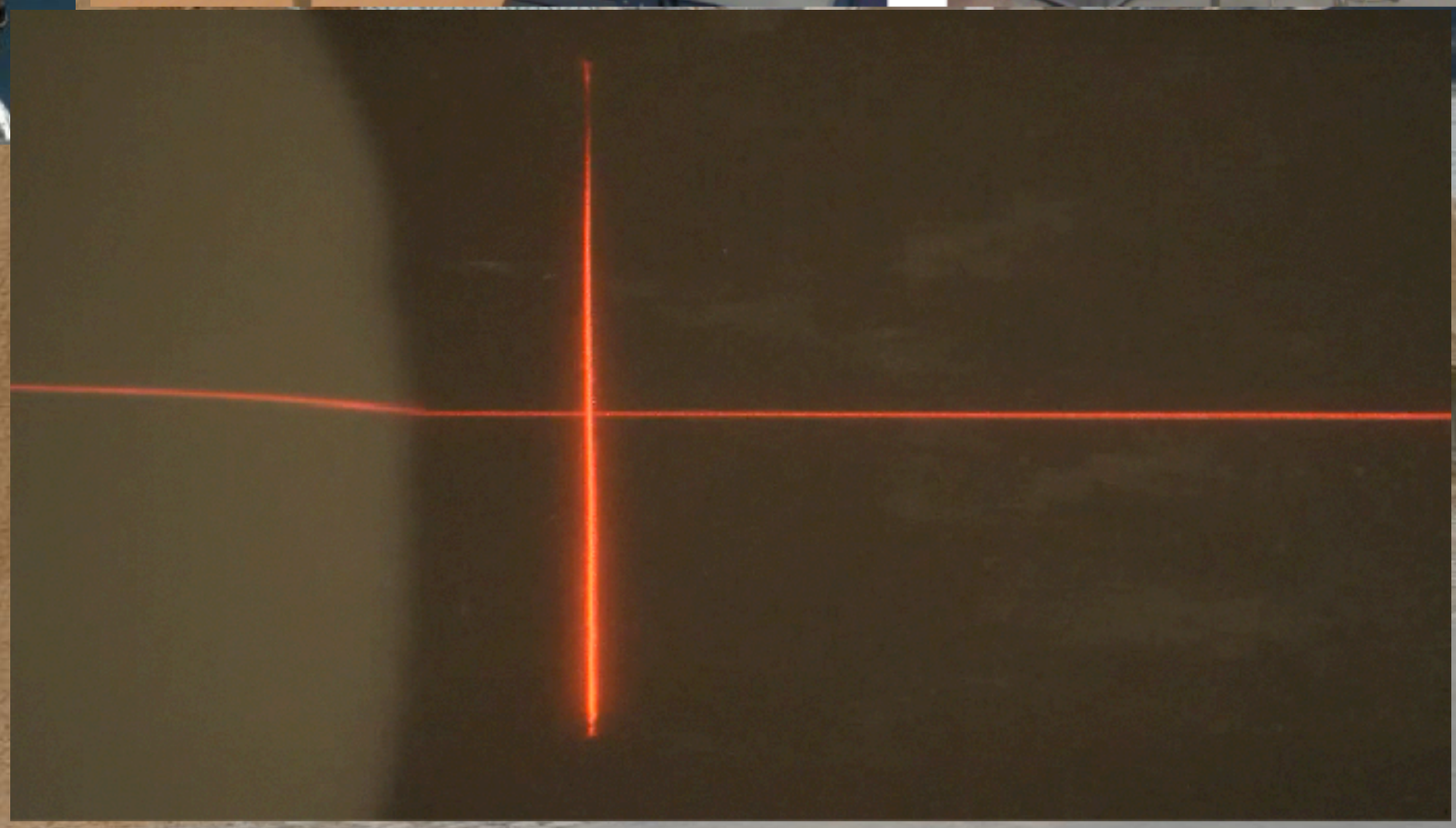

Saingier et al. Phys of Fluids 2016

granular avalanches, μ(I) rheology

ε

another one ?

(A)

ε

floods (contract with AXA)

another one ?

BETON

FARGE
ETONS
ANULATS

de la Seine
DEBLAI

concrete flow (CEMEX quai de Seine)

Blood flow - Multiscale models

Network size

Local accuracy

3D

1D

0D

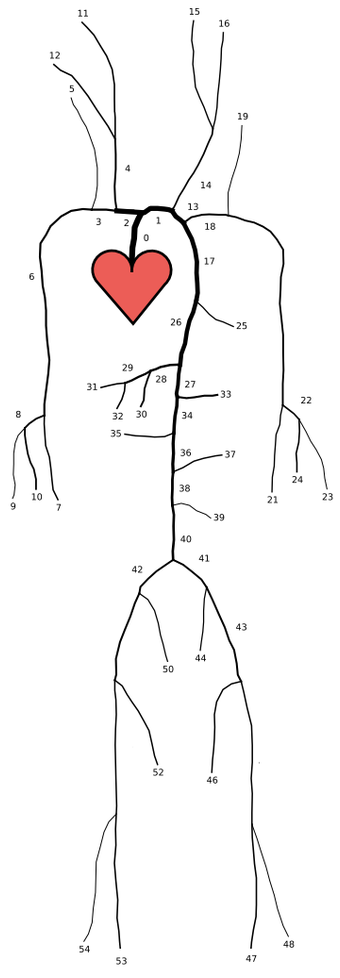

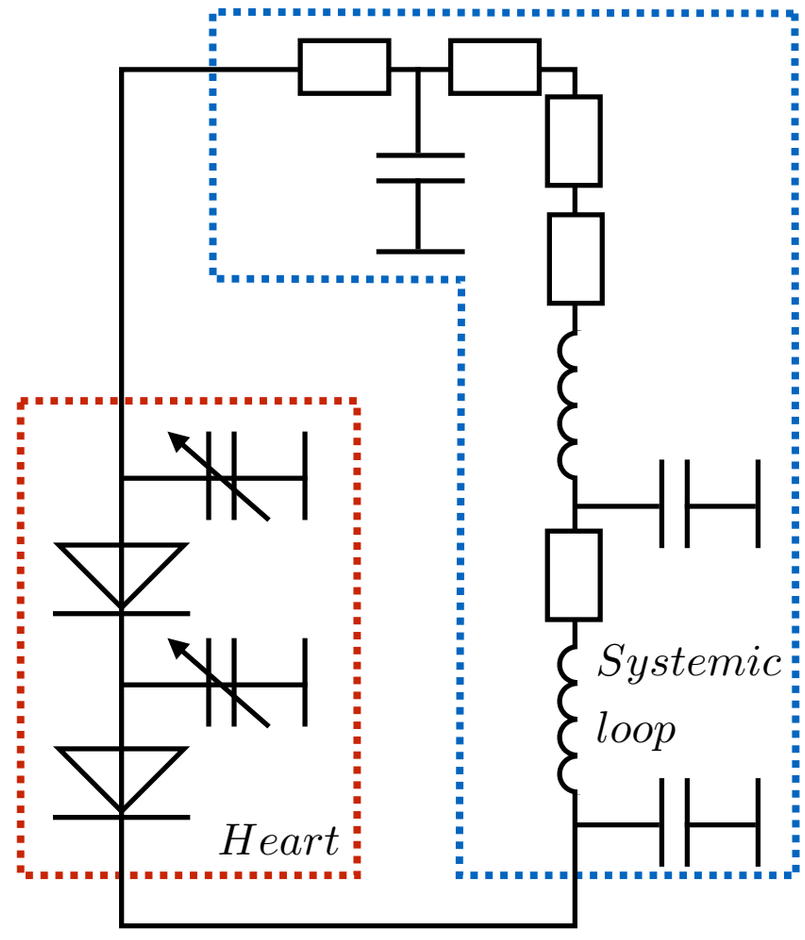

Kim & al., Ann Biomed Eng (2009)

blood flow in "realistic" networks

3D : Full NS

2D : Full NS

in between : Prandtl equations are 2D

1D : 2 equations Shallow water,

1D : 1 equation, lubrication, kinetic/flood wave

discuss 1D approximation and "**closures**"
(relations between for example the shear stress and the mean velocity)

continuous interest on that:

Christian Ruyer Quil, Jean-Paul Vila, Sergey Gavrilyuk, Gaël Richard, …
- system of equations, Weighted residual method, "regularized reduced model" .
- equation of momentum + equation of the shear (enstrophy)

we do not use their methods

Exemples of problems we are interested in:

all share common features

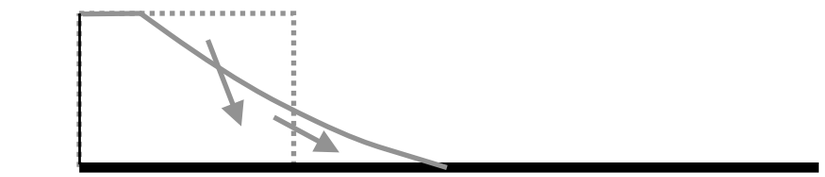

collapse of viscous flows
collapse of granular flows
collapse of Bingham flows

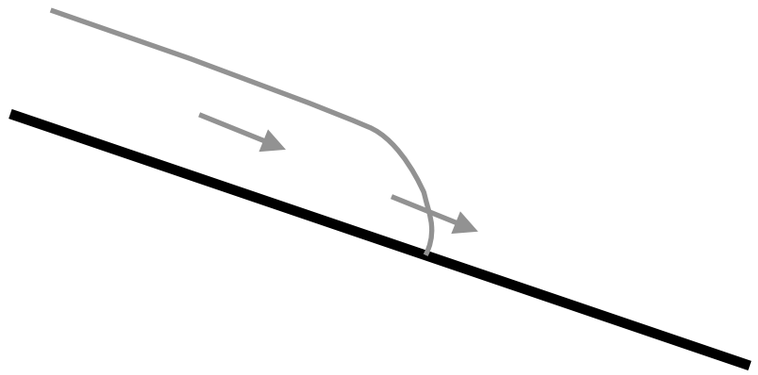

avalanches of viscous flows
avalanches of granular flows
avalanches of Bingham flows

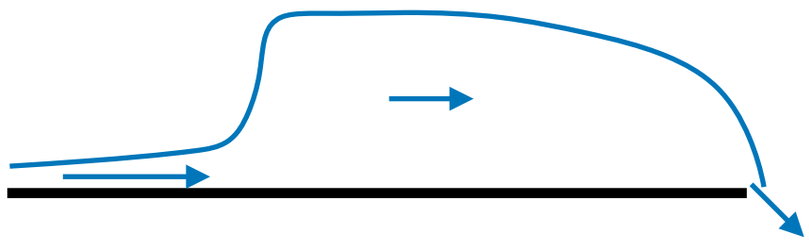

hydraulic jump

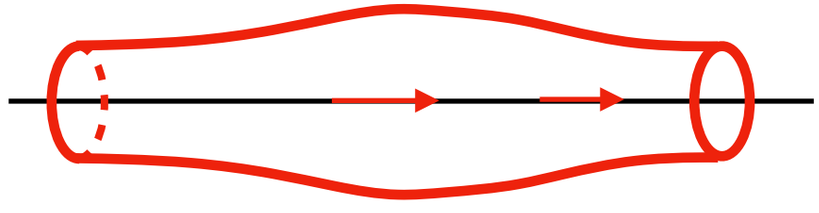

flows in elastic tubes

discuss 1D approximation and "closures"

Exemples of problems we are interested in:

all share common features

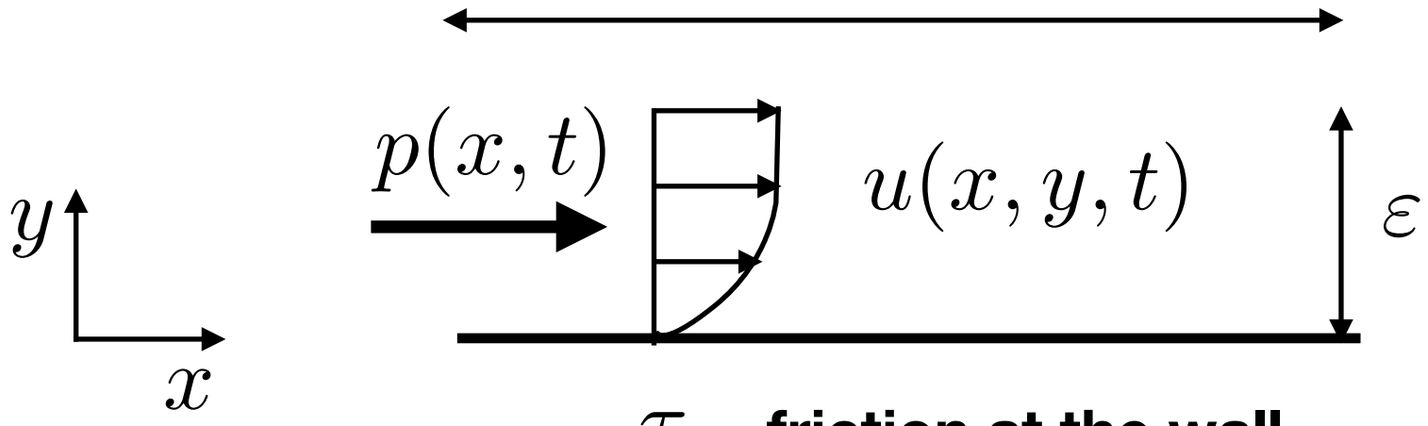

τ **friction at the wall**

dominant balance:

unsteady effects/ non linearities/ pressure/ viscosity

$$\rho\frac{\partial u}{\partial t} \sim \rho u\frac{\partial u}{\partial x} \sim -\frac{\partial p}{\partial x} \sim \frac{\partial \tau}{\partial y}$$

Rheology

viscous flows

$$\tau = \eta\frac{\partial u}{\partial y}$$

Bingham flows

$$\tau = \tau_y + \eta\frac{\partial u}{\partial y}$$

granular flows

$$\tau = \mu(I)p$$

Exemples of problems we are interested in:

all share common features

define an effective viscosity, function of shear rate

$$\tau = \eta_{eff} \frac{\partial u}{\partial y} \qquad \eta_{eff} = F(\frac{\partial u}{\partial y})$$

Rheology

viscous flows

$$\eta_{eff} = \eta$$

Bingham flows

$$\eta_{eff} = \frac{\tau_y}{\frac{\partial u}{\partial y}} + \eta$$

granular flows

$$\eta_{eff} = \frac{\mu(I)p}{\frac{\partial u}{\partial y}}$$

$\frac{\partial u}{\partial y} \to 0, \quad \eta_{eff} \to \infty$ **+ regularisation:** $\eta_{eff} \leq \eta_{max}$

Exemples of problems we are interested in:

all share common features

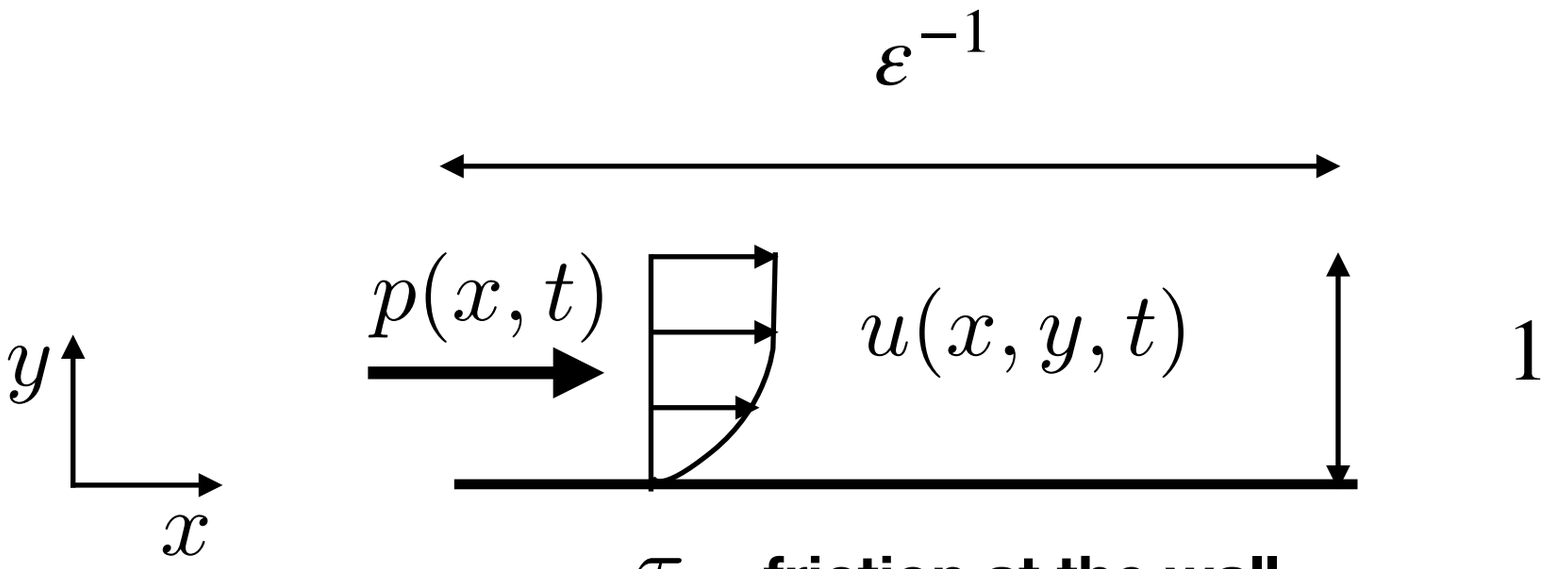

τ **friction at the wall**

dominant balance:

unsteady effects/ non linearities/ pressure/ viscosity

$$\rho\frac{\partial u}{\partial t} \sim \rho u\frac{\partial u}{\partial x} \sim -\frac{\partial p}{\partial x} \sim \frac{\partial \tau}{\partial y}$$

viscous Newtonien flows

Navier Stokes

starting from 2D Navier Stokes laminar **free surface flow**

$$\varepsilon = \frac{h_0}{L}$$ thin layer

$$x = \frac{h_0}{\varepsilon}\tilde{x}, \quad y = \tilde{y}h_0, \quad t = \frac{h_0}{\varepsilon c_0}\tilde{t}, \quad u = c_0\tilde{u} \quad \text{and} \quad v = \varepsilon c_0\tilde{v}$$

$$p = \rho c_0^2 \tilde{p} \qquad c_0^2 = gh_0$$

rescaled system of the Navier-Stokes equations:

$$\frac{\partial \tilde{u}}{\partial \tilde{x}} + \frac{\partial \tilde{v}}{\partial \tilde{y}} = 0$$

$$\frac{\partial \tilde{u}}{\partial \tilde{t}} + \frac{\partial \tilde{u}^2}{\partial \tilde{x}} + \frac{\partial \tilde{u}\tilde{v}}{\partial \tilde{y}} = -\frac{\partial \tilde{p}}{\partial \tilde{x}} + \frac{\mu}{\varepsilon \rho c_0 h_0}\left(\frac{\partial^2 \tilde{u}}{\partial \tilde{y}^2} + \varepsilon^2 \frac{\partial^2 \tilde{u}}{\partial \tilde{x}^2}\right),$$

$$\varepsilon\left(\frac{\partial \tilde{v}}{\partial \tilde{t}} + \frac{\partial \tilde{u}\tilde{v}}{\partial \tilde{x}} + \frac{\partial \tilde{v}^2}{\partial \tilde{y}}\right) = -\frac{\partial \tilde{p}}{\partial \tilde{y}} - 1 + \varepsilon\frac{\mu}{\varepsilon \rho c_0 h_0}\left(\frac{\partial^2 \tilde{v}}{\partial \tilde{y}^2} + \varepsilon^2 \frac{\partial^2 \tilde{v}}{\partial \tilde{x}^2}\right).$$

full 2D equations

Reduced Navier Stokes / Prandtl equations (RNSP)

free surface flow

$$\varepsilon = \frac{h_0}{L}$$ thin layer

$$x = \frac{h_0}{\varepsilon}\tilde{x}, \quad y = \tilde{y}h_0, \quad t = \frac{h_0}{\varepsilon c_0}\tilde{t}, \quad u = c_0\tilde{u} \quad \text{and} \quad v = \varepsilon c_0\tilde{v}$$

$$p = \rho c_0^2 \tilde{p} \qquad c_0^2 = gh_0$$

rescaled system of the Navier-Stokes equations:

$$\frac{\partial \tilde{u}}{\partial \tilde{x}} + \frac{\partial \tilde{v}}{\partial \tilde{y}} = 0$$

$$\frac{\partial \tilde{u}}{\partial \tilde{t}} + \frac{\partial \tilde{u}^2}{\partial \tilde{x}} + \frac{\partial \tilde{u}\tilde{v}}{\partial \tilde{y}} = -\frac{\partial \tilde{p}}{\partial \tilde{x}} + \frac{\mu}{\varepsilon \rho c_0 h_0} \frac{\partial^2 \tilde{u}}{\partial \tilde{y}^2},$$

$$0 = -\frac{\partial \tilde{p}}{\partial \tilde{y}} - 1.$$

+ boundary conditions: no slip at the bottom, no shear at the interface

no more full 2D equations

Reduced Navier Stokes / Prandtl equations (RNSP)

$$\varepsilon = \frac{h_0}{L}$$ thin layer

$$x = \frac{h_0}{\varepsilon}\tilde{x}, \quad y = \tilde{y}h_0, \quad t = \frac{h_0}{\varepsilon c_0}\tilde{t}, \quad u = c_0\tilde{u} \quad \text{and} \quad v = \varepsilon c_0\tilde{v}$$

$$p = \rho c_0^2 \tilde{p} \qquad c_0^2 = gh_0$$

rescaled system of the Navier-Stokes equations:

$$\frac{\partial \tilde{u}}{\partial \tilde{x}} + \frac{\partial \tilde{v}}{\partial \tilde{y}} = 0$$

$$\frac{\partial \tilde{u}}{\partial \tilde{t}} + \frac{\partial \tilde{u}^2}{\partial \tilde{x}} + \frac{\partial \tilde{u}\tilde{v}}{\partial \tilde{y}} = -\frac{\partial \tilde{p}}{\partial \tilde{x}} + \frac{1}{Re}\frac{\partial^2 \tilde{u}}{\partial \tilde{y}^2},$$

$$\tilde{p} = \tilde{h} - \tilde{y}.$$

+ boundary conditions: no slip at the bottom, no shear at the interface

2D equations

Lubrication

$$\varepsilon = \frac{h_0}{L}$$ thin layer

$$x = \frac{h_0}{\varepsilon}\tilde{x}, \quad y = \tilde{y}h_0, \quad t = \frac{h_0}{\varepsilon c_0 Re}\tilde{t}, \quad u = Rec_0\tilde{u} \quad \text{and} \quad v = \varepsilon c_0\tilde{v}$$

$$p = \rho c_0^2 \tilde{p} \qquad c_0^2 = gh_0$$

rescaled system of the Navier-Stokes equations:

$$\frac{\partial \tilde{u}}{\partial \tilde{x}} + \frac{\partial \tilde{v}}{\partial \tilde{y}} = 0$$

$$0 = -\frac{\partial \tilde{p}}{\partial \tilde{x}} + \frac{\partial^2 \tilde{u}}{\partial \tilde{y}^2},$$

$$\tilde{p} = \tilde{h} - \tilde{y}.$$

+ boundary conditions: no slip at the bottom, no shear at the interface

almost 1D equations

Reduced Navier Stokes / Prandtl equations (RNSP)

$$\varepsilon = \frac{h_0}{L}$$ thin layer

$$x = \frac{h_0}{\varepsilon}\tilde{x}, \quad y = \tilde{y}h_0, \quad t = \frac{h_0}{\varepsilon c_0}\tilde{t}, \quad u = c_0\tilde{u} \quad \text{and} \quad v = \varepsilon c_0\tilde{v}$$

$$p = \rho c_0^2 \tilde{p} \qquad c_0^2 = gh_0$$

rescaled system of the Navier-Stokes equations:

$$\frac{\partial \tilde{u}}{\partial \tilde{x}} + \frac{\partial \tilde{v}}{\partial \tilde{y}} = 0$$

$$\frac{\partial \tilde{u}}{\partial \tilde{t}} + \frac{\partial \tilde{u}^2}{\partial \tilde{x}} + \frac{\partial \tilde{u}\tilde{v}}{\partial \tilde{y}} = -\frac{\partial \tilde{p}}{\partial \tilde{x}} + \frac{1}{Re}\frac{\partial^2 \tilde{u}}{\partial \tilde{y}^2},$$

$$\tilde{p} = \tilde{h} - \tilde{y}.$$

+ boundary conditions: no slip at the bottom, no shear at the interface

2D equations

Reduced Navier Stokes / Prandtl equations (RNSP)

$$\varepsilon = \frac{h_0}{L}$$ thin layer

$$x = \frac{h_0}{\varepsilon}\tilde{x}, \quad y = \tilde{y}h_0, \quad t = \frac{h_0}{\varepsilon c_0}\tilde{t}, \quad u = c_0\tilde{u} \quad \text{and} \quad v = \varepsilon c_0\tilde{v}$$

$$p = \rho c_0^2 \tilde{p} \qquad c_0^2 = gh_0$$

rescaled system of the Navier-Stokes equations:

$$\int d\tilde{y}\,\{ \quad \frac{\partial \tilde{u}}{\partial \tilde{x}} + \frac{\partial \tilde{v}}{\partial \tilde{y}} = 0$$

$$\int d\tilde{y}\,\{ \quad \frac{\partial \tilde{u}}{\partial \tilde{t}} + \frac{\partial \tilde{u}^2}{\partial \tilde{x}} + \frac{\partial \tilde{u}\tilde{v}}{\partial \tilde{y}} = -\frac{\partial \tilde{p}}{\partial \tilde{x}} + \frac{1}{Re} \frac{\partial^2 \tilde{u}}{\partial \tilde{y}^2} \,,$$

$$\tilde{p} = \tilde{h} - \tilde{y} \,.$$

+ boundary conditions: no slip at the bottom, no shear at the interface

2D equations

Reduced Navier Stokes / Prandtl equations (RNSP)

$$\varepsilon = \frac{h_0}{L}$$ thin layer

$$x = \frac{h_0}{\varepsilon}\tilde{x}, \quad y = \tilde{y}h_0, \quad t = \frac{h_0}{\varepsilon c_0}\tilde{t}, \quad u = c_0\tilde{u} \quad \text{and} \quad v = \varepsilon c_0 \tilde{v}$$

$$c_0^2 = gh_0$$

rescaled system of the Navier-Stokes equations:

$$\frac{\partial \tilde{h}}{\partial \tilde{t}} + \frac{\partial}{\partial \tilde{x}} \int_0^h \tilde{u} d\tilde{z} = 0$$

$$\frac{\partial}{\partial \tilde{t}} \int_0^{\tilde{h}} \tilde{u} d\tilde{z} + \frac{\partial}{\partial \tilde{x}} \int_0^{\tilde{h}} \tilde{u}^2 d\tilde{z} = -\tilde{h}\frac{\partial \tilde{h}}{\partial \tilde{x}} - \frac{1}{Re}\left(\frac{\partial \tilde{u}}{\partial \tilde{y}}\right)_b,$$

+ boundary conditions: no slip at the bottom, no shear at the interface

2D equations

SHALLOW WATER Saint-Venant

integral system:

$$\frac{\partial \tilde{h}}{\partial \tilde{t}} + \frac{\partial}{\partial \tilde{x}} \int_0^{\tilde{h}} \tilde{u} d\tilde{z} = 0$$

$$\frac{\partial}{\partial \tilde{t}} \int_0^{\tilde{h}} \tilde{u} d\tilde{y} + \frac{\partial}{\partial \tilde{x}} \int_0^{\tilde{h}} \tilde{u}^2 d\tilde{y} = -\tilde{h}\frac{\partial \tilde{h}}{\partial \tilde{x}} - \frac{1}{Re}\left(\frac{\partial \tilde{u}}{\partial \tilde{y}}\right)_b,$$

if we define: **flow rate** **shear** at the wall **Boussinesq** or shape coeff.

$$\tilde{Q} = \int_0^{\tilde{h}} \tilde{u}\, d\, \tilde{y} \qquad \tilde{\tau}_b = \frac{1}{Re}\left(\frac{\partial \tilde{u}}{\partial\, \tilde{y}}\right)_b, \qquad \Gamma = \frac{\frac{1}{\tilde{h}}\int_0^{\tilde{h}} \tilde{u}^2(\tilde{y}) d\tilde{y}}{\left(\frac{1}{\tilde{h}}\int_0^{\tilde{h}} \tilde{u}(\tilde{y}) d\tilde{y}\right)^2},$$

classical Shallow Water/ Saint Venant

$$\frac{\partial \tilde{h}}{\partial \tilde{t}} + \frac{\partial \tilde{Q}}{\partial \tilde{x}} = 0$$

$$\frac{\partial \tilde{Q}}{\partial \tilde{t}} + \frac{\partial}{\partial \tilde{x}}\left(\Gamma \frac{\tilde{Q}^2}{\tilde{h}} + \frac{\tilde{h}^2}{2}\right) = -\tilde{\tau}_b$$

1D equations


ST VENANT

SHALLOW WATER Saint-Venant

Closure: relation between Γ and τ small Reynolds

In practice **Poiseuille**

$$\Gamma = \frac{\frac{1}{h}\int_0^h u^2 dy}{\left(\frac{1}{h}\int_0^h u dy\right)^2} = \frac{6}{5}$$ but use $\Gamma = 1$

In practice **shear** at the wall is $\tau = 3\frac{\mu Q}{h^2}$

$$u = \frac{3Q}{2h}\left((\frac{y}{h})(2 - \frac{y}{h})\right)$$

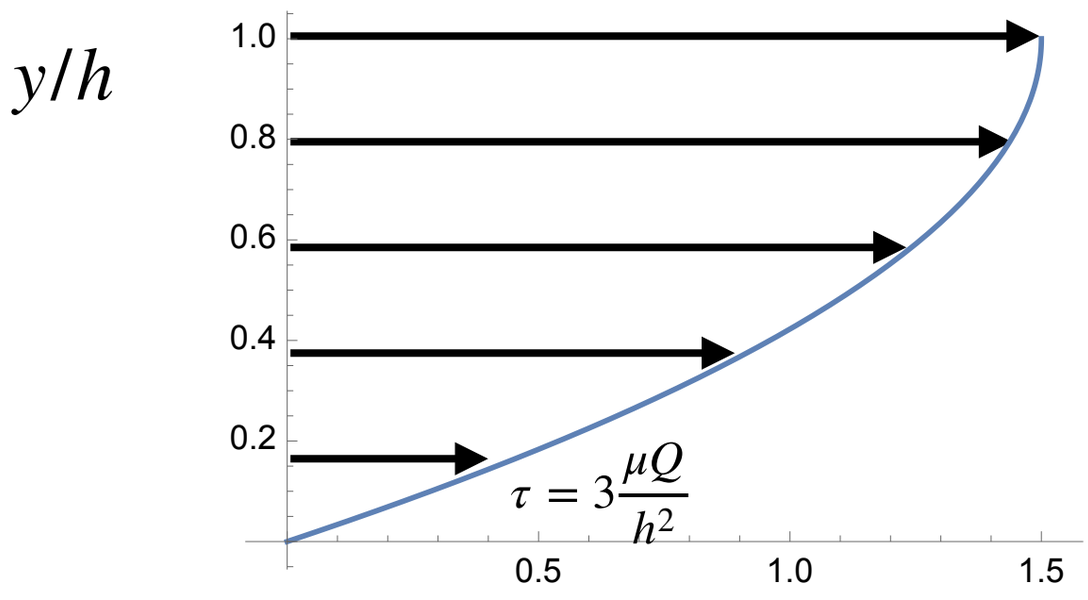

SHALLOW WATER Saint-Venant

Closure: relation between Γ and τ large Reynolds

In practice **Boussinesq** or shape coefficient is taken to 1 (Galilean invariance)

$$\Gamma = \frac{\frac{1}{h}\int_0^h u^2 dy}{\left(\frac{1}{h}\int_0^h u dy\right)^2} = 1$$

In practice **shear** at the wall is $\tau = \rho \frac{c_f}{2}\left(\frac{Q}{h}\right)^2$

Numerical resolution:

Riemann solver (see after)
Well balanced (equilibrium of the lake, see after)

Modeling rain-driven overland flow: friction terms in the Saint-Venant

Kirstetter et al. J.Hyd 2016

for good comparison between rain experiments and simulations

$$\Gamma = 1$$

$$Q/\nu < Re_c \qquad \tau = 3\mu \left(\frac{Q}{h^2} \right)$$

$$Q/\nu > Re_c \qquad \tau = \rho \frac{c_f}{2} \left(\frac{Q}{h} \right)^2$$

Fanning/ Darcy-Weisbach/Chézy

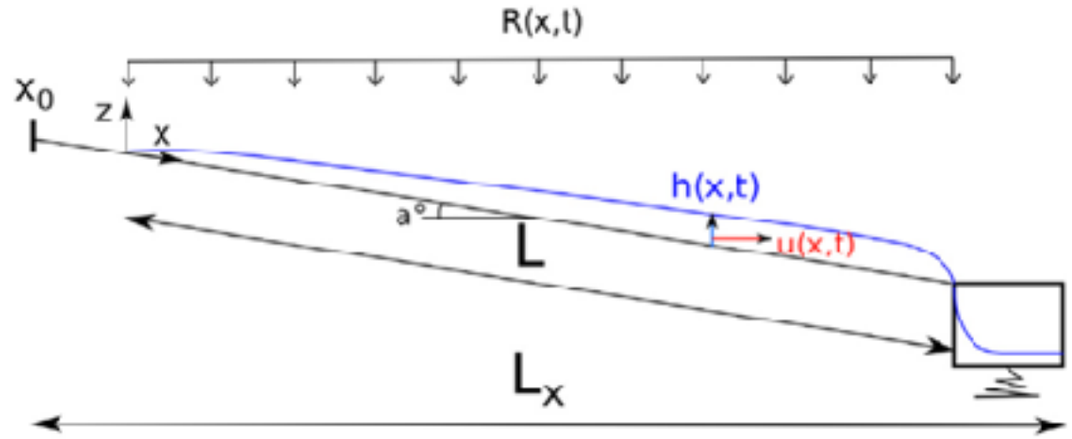

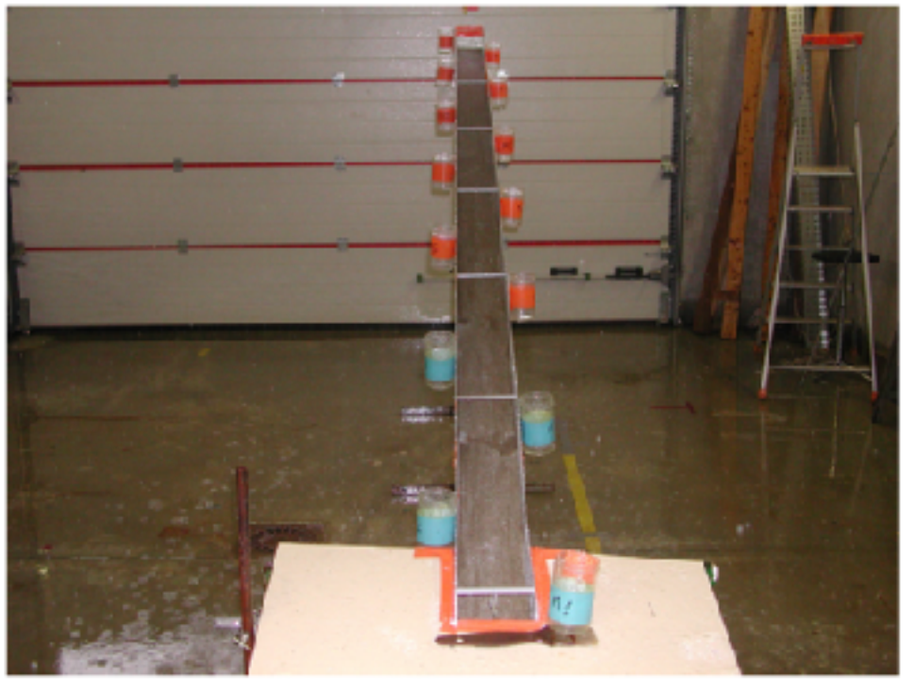

INRAe Val de Loire

hydrograph at output

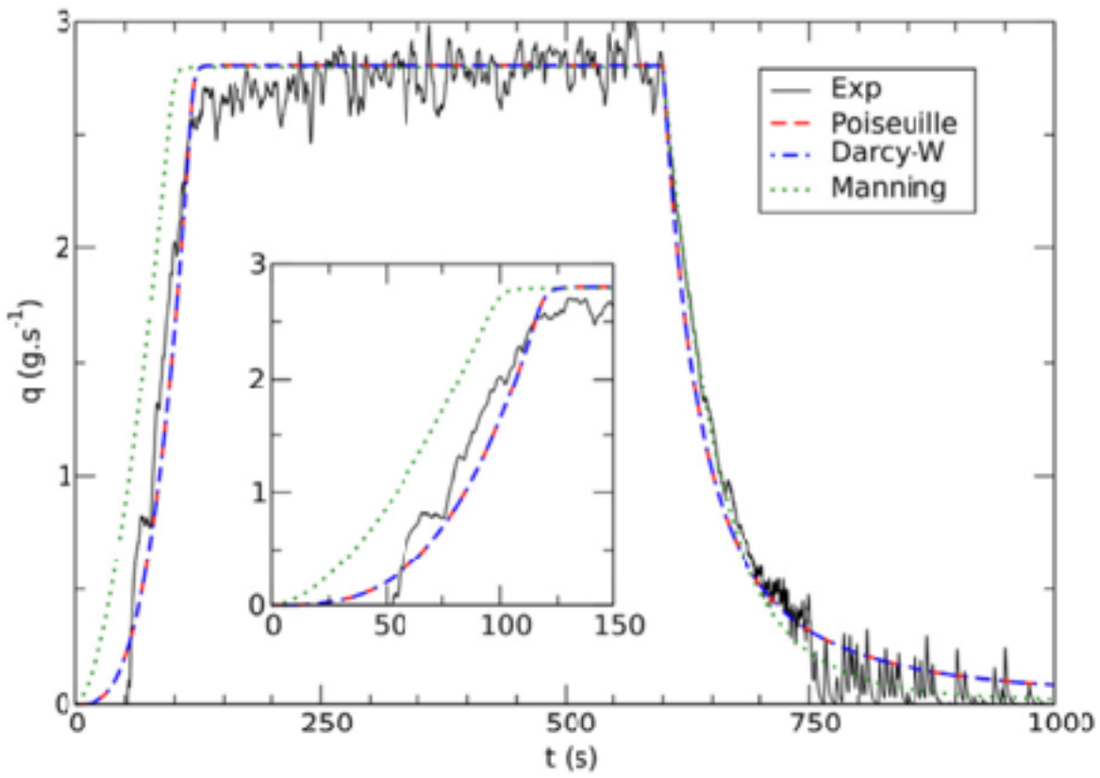

(a) Slope = 2 %, Rain = 25 $mm.h^{-1}$

∂'Alembert
Institut Jean le Rond d'Alembert
SCIENCES SORBONNE UNIVERSITÉ
cnrs

Numerical simulations of flood waves

Kirstetter et al. GMD 2021

$$\Gamma = 1$$

Mannning Strickler $$\tau = \rho g n^2 \frac{u^2}{h^{1/3}} = \rho g n^2 \frac{Q|Q|}{h^{7/3}}$$

+ test case 1:100 Toce river

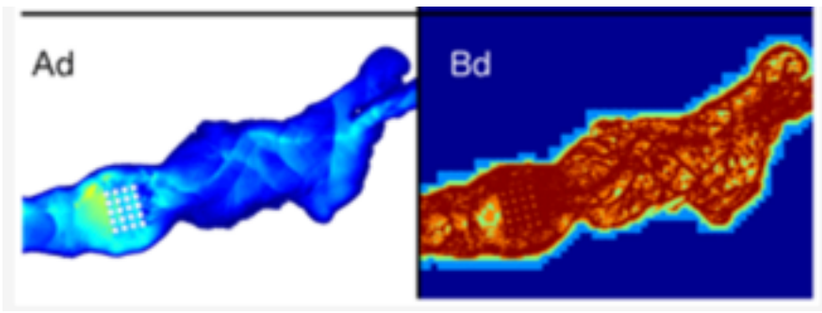

flood of the Seine 1910

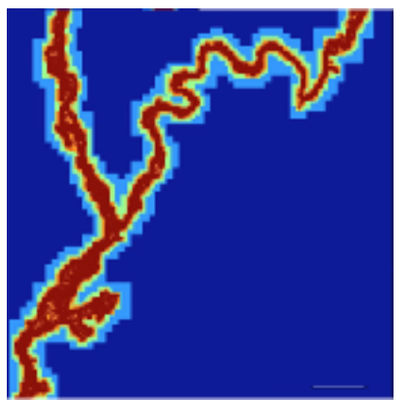

flood of Severn and Avon
Tewkesbury 20/07/2007

founding AXA

flood Cannes 03/10/2015

Basilisk


INONDATION DE
CANNES
3/10/2015 19H30

Simulations of flood over the Roya Valley topography

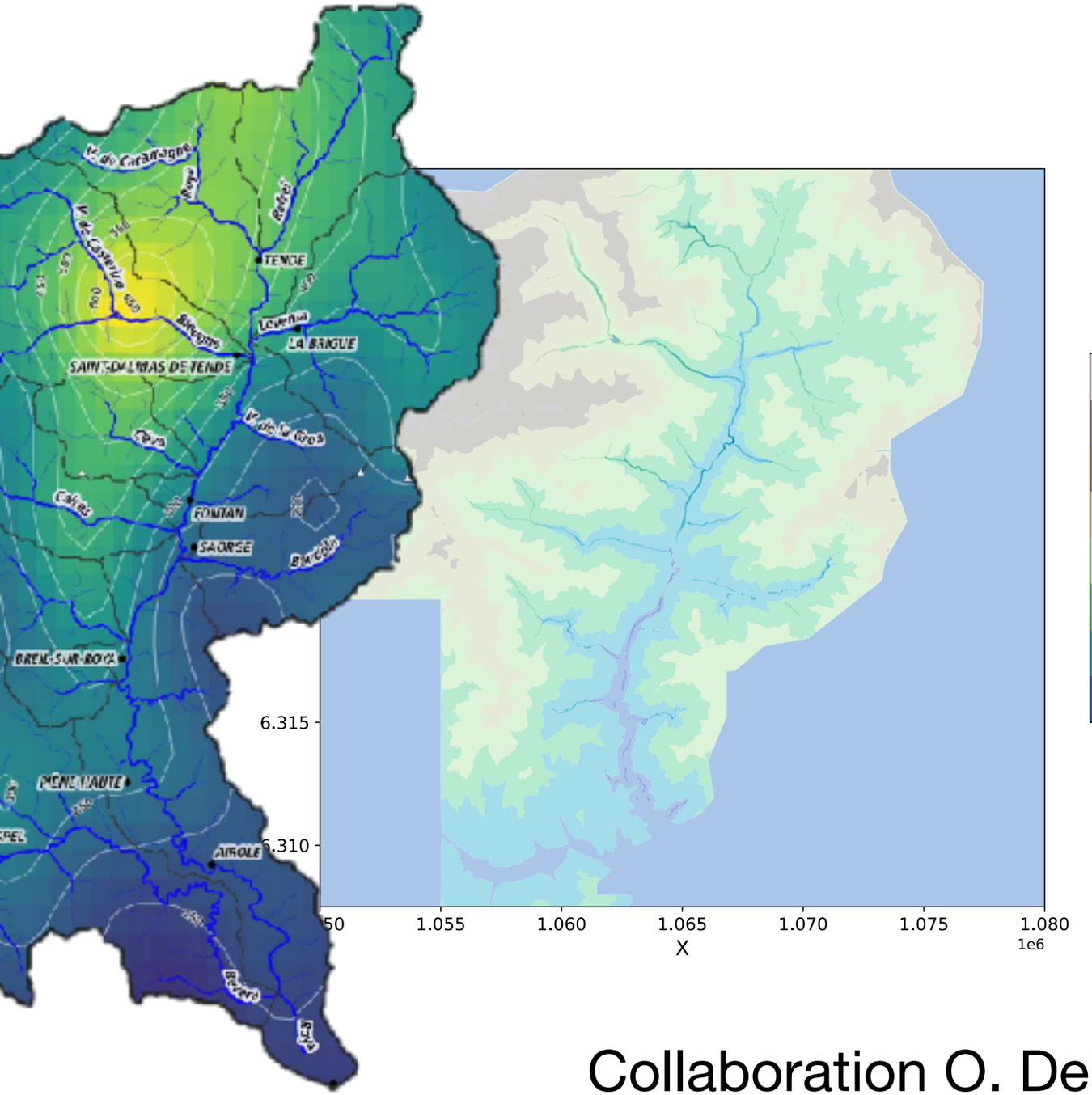

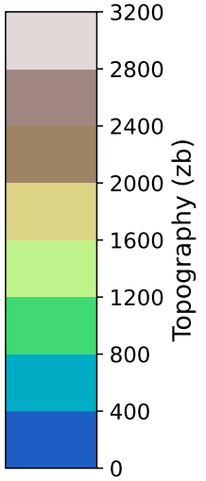

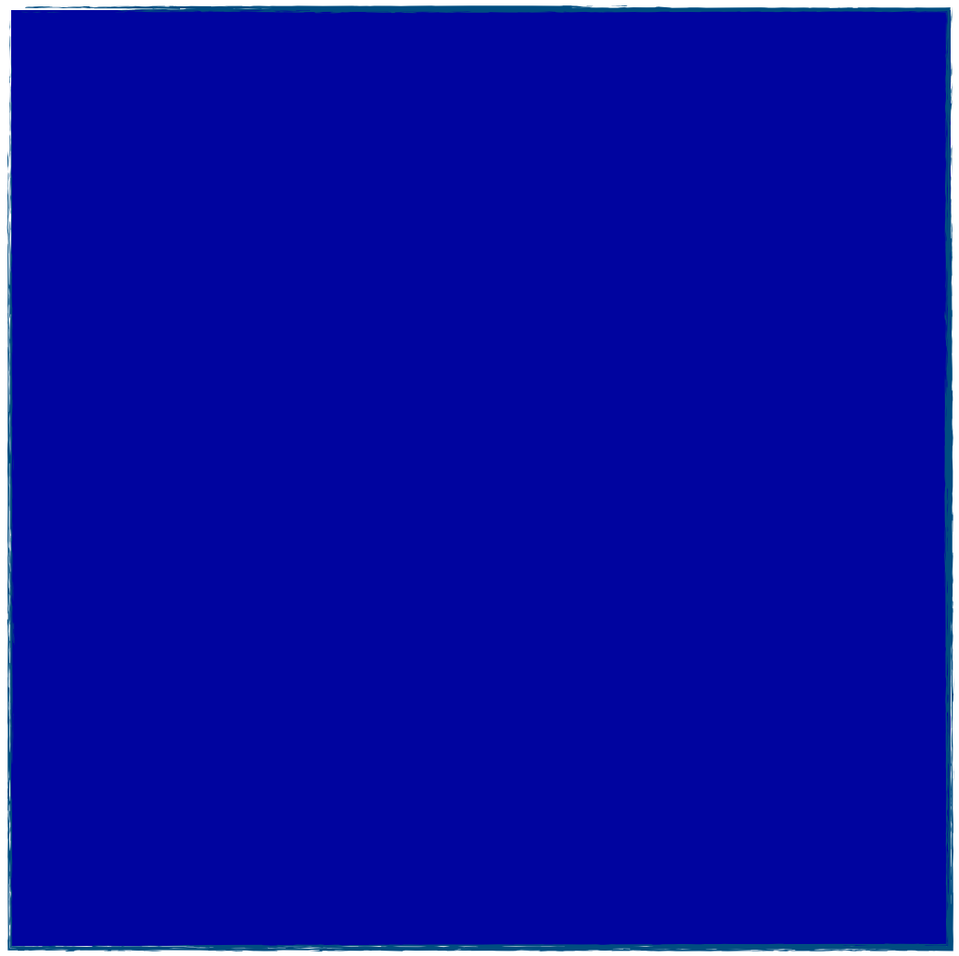

Collaboration O. Delestre Nice
and with ISTeP (on going)

1D unsteady flow in arteries

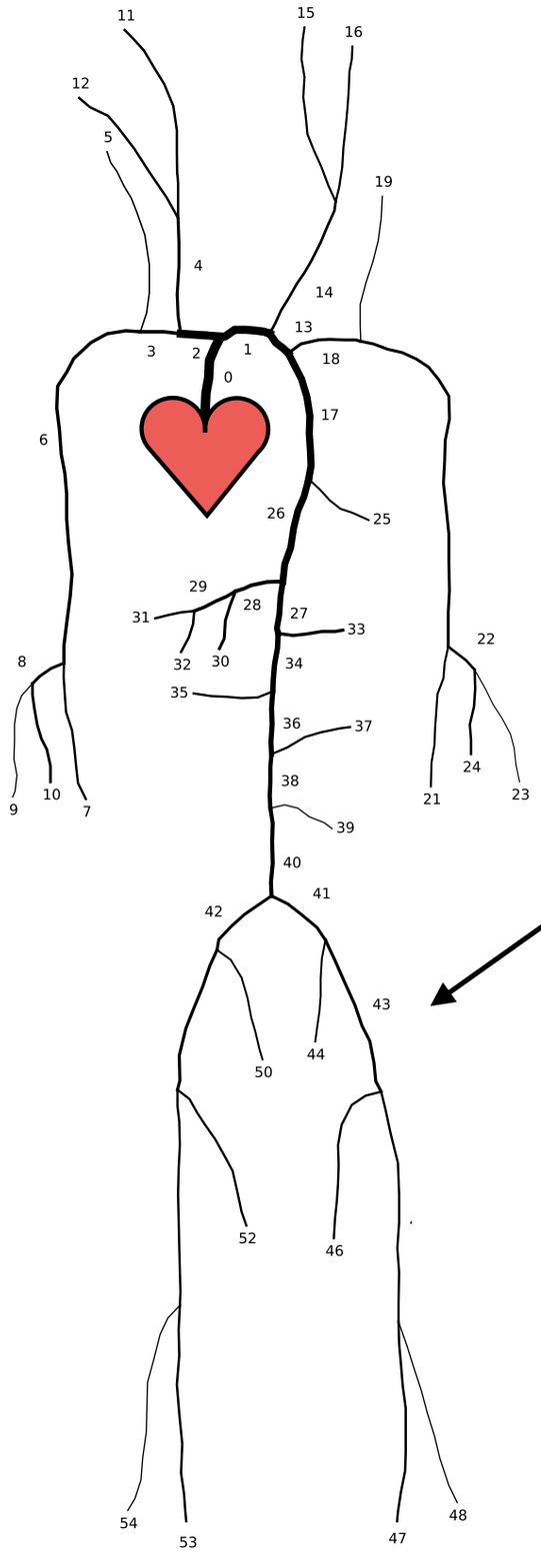

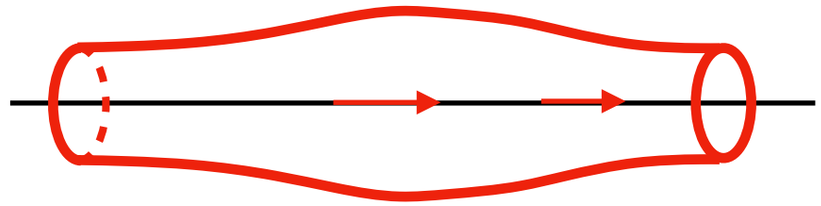

new subject, same equations
same problems, same methods !

1D unsteady flow in arteries

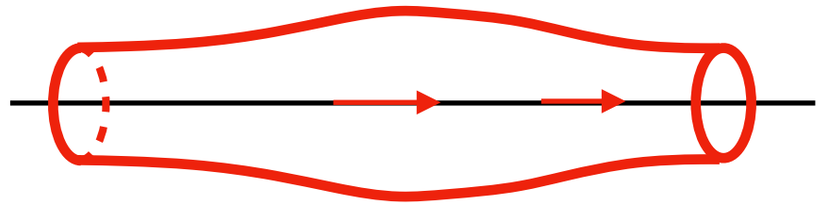

flow in ~ straight tubes

"boundary layer"/ long wave approximation in elastic tubes

$$2\pi \int_0^R dr \cdot \{$$

$$\frac{1}{r}\frac{\partial}{\partial r}\left[r u_r\right] + \frac{\partial u_x}{\partial x} = 0$$

$$\frac{\partial u_x}{\partial t} + u_r \frac{\partial u_x}{\partial r} + u_x \frac{\partial u_x}{\partial x} = -\frac{1}{\rho}\frac{\partial p}{\partial x} + \frac{\nu}{r}\frac{\partial}{\partial r}\left[r\frac{\partial u_x}{\partial r}\right]$$

$$p\,(x,t) - p_0 = K(R(x,t) - R_0)$$

section averaged equations

$$\frac{\partial A}{\partial t} + \frac{\partial Q}{\partial x} = 0$$

$$\frac{\partial Q}{\partial t} + \Gamma\frac{\partial}{\partial x}\left(\frac{Q^2}{A}\right) = -\frac{A}{\rho}\frac{\partial p}{\partial x} - \frac{\tau}{\rho}$$

same problem of closure

$$\Gamma = \frac{\frac{1}{R^2}\int_0^R u^2 r dr}{\left(\frac{1}{R^2}\int_0^R u r dr\right)^2} = F(Q,A)?$$

$$\tau = G(Q,A)?$$

1D unsteady flow in arteries

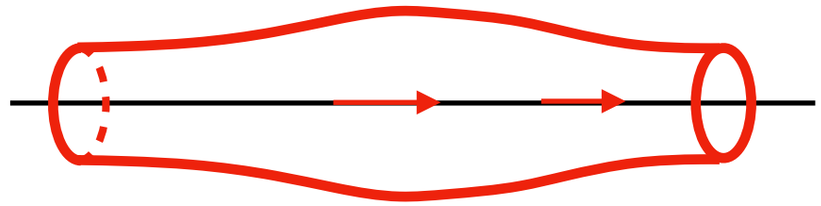

flow in ~ straight tubes

section averaged equations

$$\frac{\partial A}{\partial t} + \frac{\partial Q}{\partial x} = 0$$

$$\frac{\partial Q}{\partial t} + \Gamma \frac{\partial}{\partial x}\left(\frac{Q^2}{A}\right) = -\frac{A}{\rho}\frac{\partial p}{\partial x} - \frac{\tau}{\rho}$$

same problem of closure as in flood

$$\Gamma = \frac{\frac{1}{R^2}\int_0^R u^2 r dr}{\left(\frac{1}{R^2}\int_0^R u r dr\right)^2} = \frac{4}{3} \rightarrow 1$$

Poiseuille 4/3 - Flat 1 / Galilean invariance

Poiseuille: 8 , should be Womersley… but in practice: 22 !

$$\tau/\rho = 2\pi\nu R\left(\frac{\partial u}{\partial r}\right)_R = 8\pi\nu\frac{Q}{A} \rightarrow 22\pi\nu\frac{Q}{A}$$

Litterature + (Wang et al. JB 2016)

Numerical resolution

Wang et al. CMBBE 2015

Verification and comparison of four numerical schemes
for a 1D viscoelastic blood flow model

- finite differences (MacCormack)
- finite volumes
- finite elements
- discontinuous Galerkin

$$\frac{U_i^{n+1} - U_i^n}{\Delta t} + \frac{F_{i+1/2}^n - F_{i-1/2}^n}{\Delta x} = 0,$$

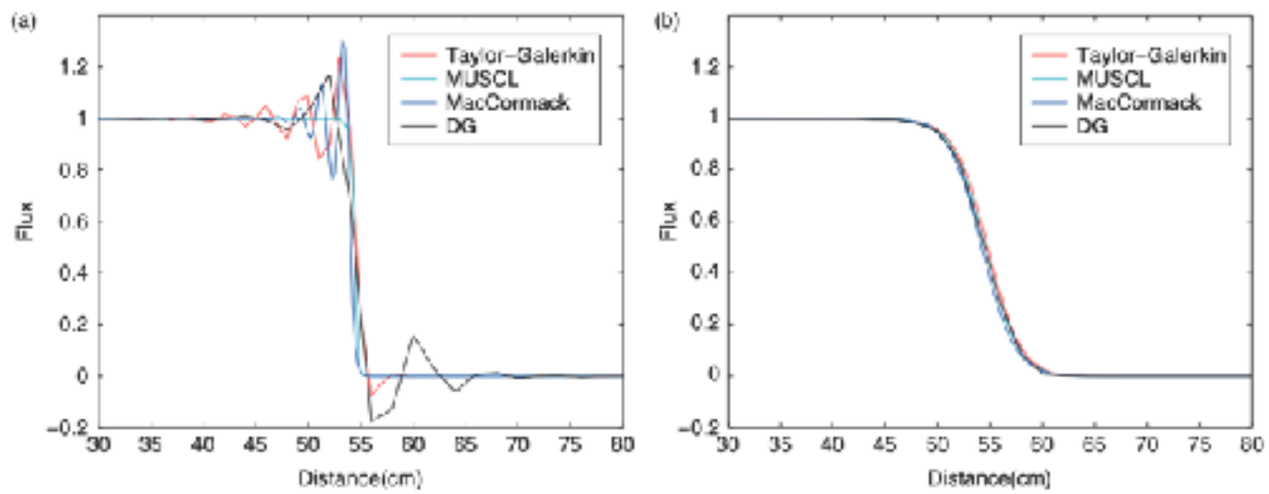

results almost the same (except shocks…)

Blood flow in a realistic network

Wang et al. CMBBE 2015

Nonlinear hyperbolic– parabolic system,
solved four numerical schemes,
- MacCormack,
- Taylor–Galerkin,
- Finite Volumes
- local discontinuous Galerkin.

Numerical schemes tested on a network with 55 arteries.

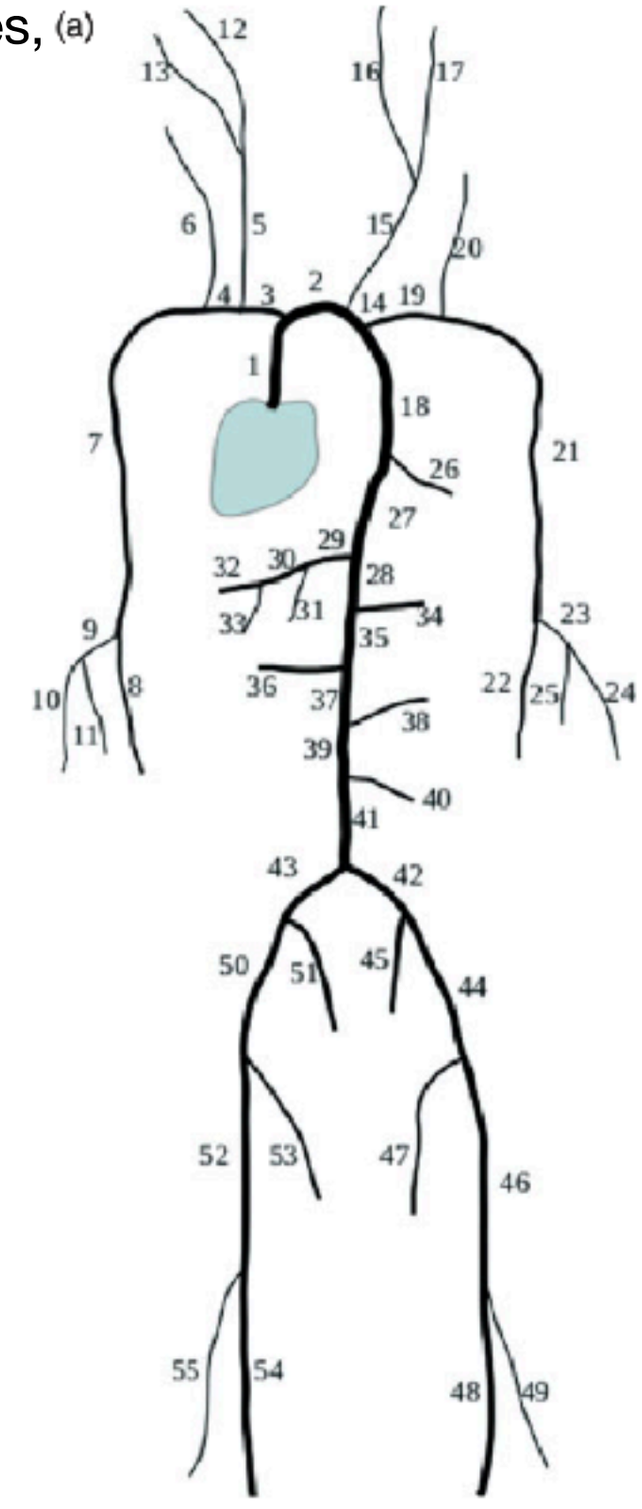

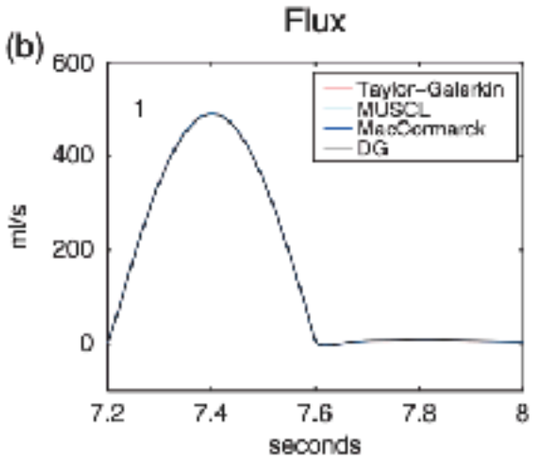

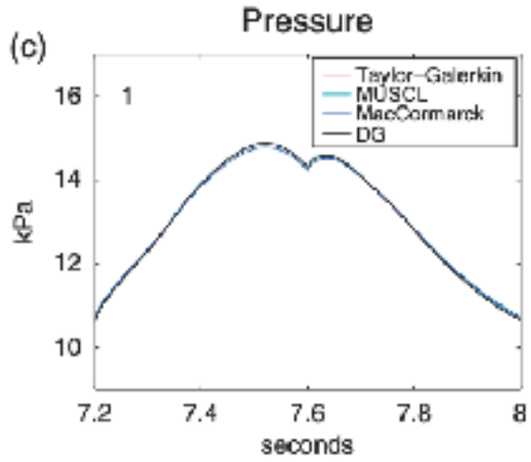

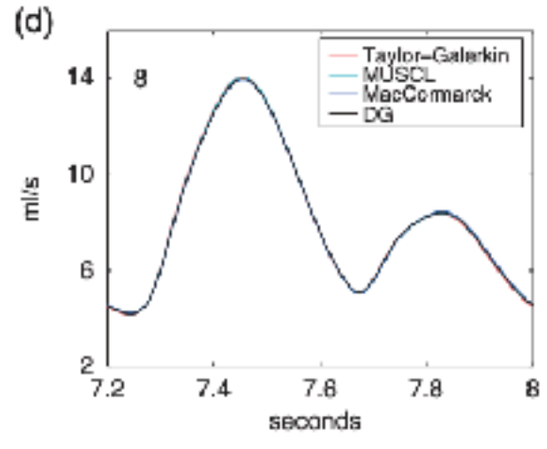

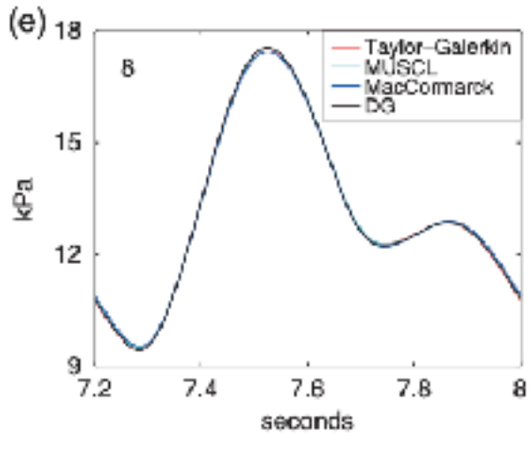

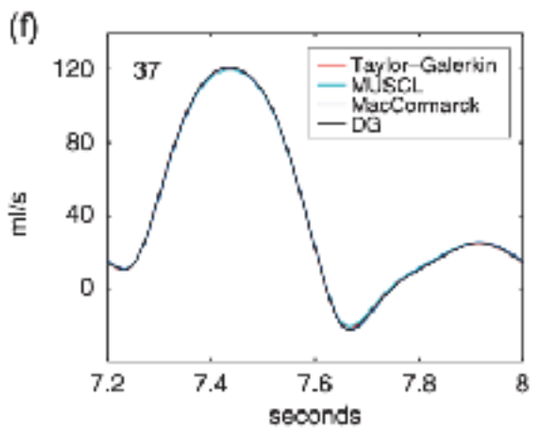

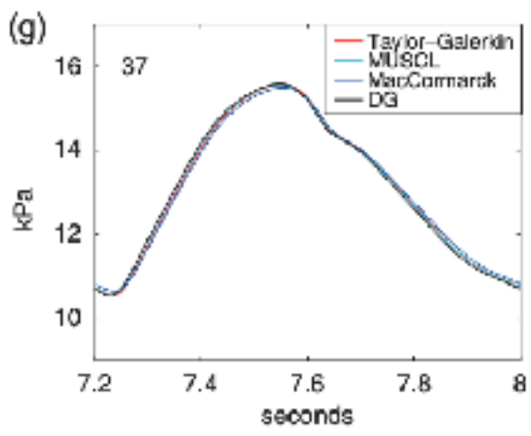

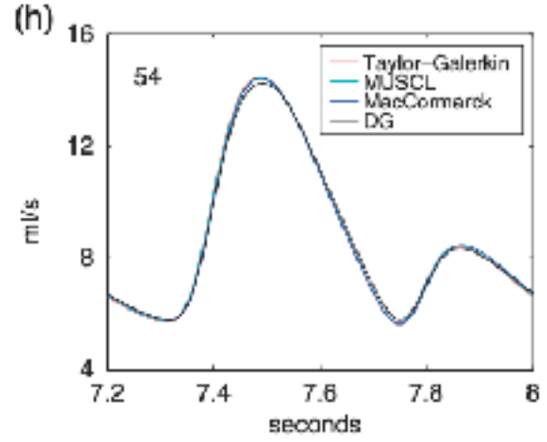

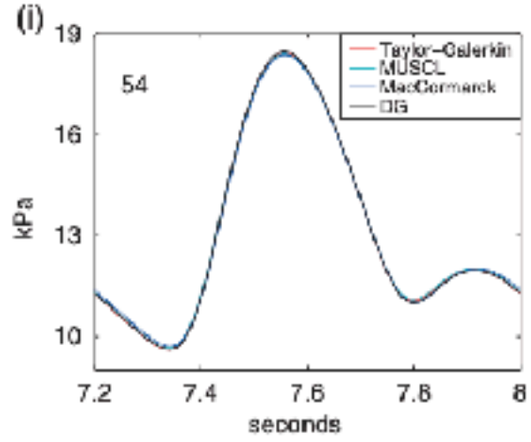

Table 1: *Arterial network: Data adapted from [13] and [4]*

ID	Name	l (cm)	A_0 (cm^2)	β (10^6Pa/cm)	C_v (10^4cm^2/s)	R_t
1	Ascending aorta	4.0	6.789	0.023	0.352	–
2	Aortic arch I	2.0	5.011	0.024	0.317	–
3	Brachiocephalic	3.4	1.535	0.049	0.363	–
4	R.subclavian I	3.4	0.919	0.069	0.393	–
5	R.carotid	17.7	0.703	0.085	0.423	–
6	R.vertebral	14.8	0.181	0.470	0.595	0.906
7	R. subclavian II	42.2	0.833	0.076	0.413	–
8	R.radius	23.5	0.423	0.192	0.372	0.82
9	R.ulnar I	6.7	0.648	0.134	0.322	–
10	R.interosseous	7.9	0.118	0.895	0.458	0.956
11	R.ulnar II	17.1	0.589	0.148	0.337	0.893
12	R.int.carotid	17.6	0.458	0.186	0.374	0.784
13	R. ext. carotid	17.7	0.458	0.173	0.349	0.79
14	Aortic arch II	3.9	4.486	0.024	0.306	–
15	L. carotid	20.8	0.536	0.111	0.484	–
16	L. int. carotid	17.6	0.350	0.243	0.428	0.784
17	L. ext. carotid	17.7	0.350	0.227	0.399	0.791
18	Thoracic aorta I	5.2	3.941	0.026	0.312	–
19	L. subclavian I	3.4	0.706	0.088	0.442	–
20	L. vertebral	14.8	0.129	0.657	0.704	0.906
21	L. subclavian II	42.2	0.650	0.097	0.467	–
22	L. radius	23.5	0.330	0.247	0.421	0.821
23	L. ulnar I	6.7	0.505	0.172	0.364	–
24	L. interosseous	7.9	0.093	1.139	0.517	0.956
25	L. ulnar II	17.1	0.461	0.189	0.381	0.893
26	intercoastals	8.0	0.316	0.147	0.491	0.627
27	Thoracic aorta II	10.4	3.604	0.026	0.296	–
28	Abdominal aorta I	5.3	2.659	0.032	0.311	–
29	Celiac I	2.0	1.086	0.056	0.346	–
30	Celiac II	1.0	0.126	0.481	1.016	–
31	Hepatic	6.6	0.659	0.070	0.340	0.925
32	Gastric	7.1	0.442	0.096	0.381	0.921
33	Splenic	6.3	0.468	0.109	0.444	0.93
34	Sup. mensenteric	5.9	0.782	0.083	0.439	0.934
35	Abdominal aorta II	1.0	2.233	0.034	0.301	–
36	L. renal	3.2	0.385	0.130	0.481	0.861
37	Abdominal aorta III	1.0	1.981	0.038	0.320	–
38	R. renal	3.2	0.385	0.130	0.481	0.861
39	Abdominal aorta IV	10.6	1.389	0.051	0.358	–
40	Inf. mesenteric	5.0	0.118	0.344	0.704	0.918
41	Abdominal aorta V	1.0	1.251	0.049	0.327	–
42	R. com. iliac	5.9	0.694	0.082	0.405	–
43	L. com. iliac	5.8	0.694	0.082	0.405	–
44	L. ext. iliac	14.4	0.730	0.137	0.349	–
45	L. int. iliac	5.0	0.285	0.531	0.422	0.925
46	L. femoral	44.3	0.409	0.231	0.440	–
47	L. deep femoral	12.6	0.398	0.223	0.419	0.885
48	L. post. tibial	32.1	0.444	0.383	0.380	0.724
49	L. ant. tibial	34.3	0.123	1.197	0.625	0.716
50	L. ext. iliac	14.5	0.730	0.137	0.349	–
51	R. int. iliac	5.0	0.285	0.531	0.422	0.925
52	R. femoral	44.4	0.409	0.231	0.440	–
53	R. deep femoral	12.7	0.398	0.223	0.419	0.888
54	R. post. tibial	32.2	0.442	0.385	0.381	0.724
55	R. ant. tibial	34.4	0.122	1.210	0.628	0.716

Sherwin et al 2003

"Well Balanced" numerical resolution

Delestre & Lagrée IJNMF 2012
Ghigo et al. JCP 2016

problem when tubes are not straight… spurious flow

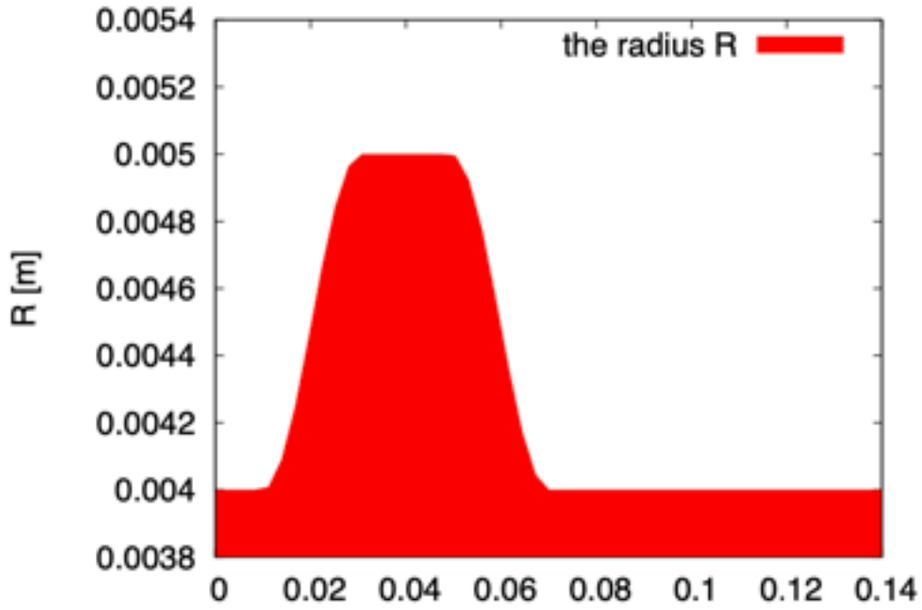

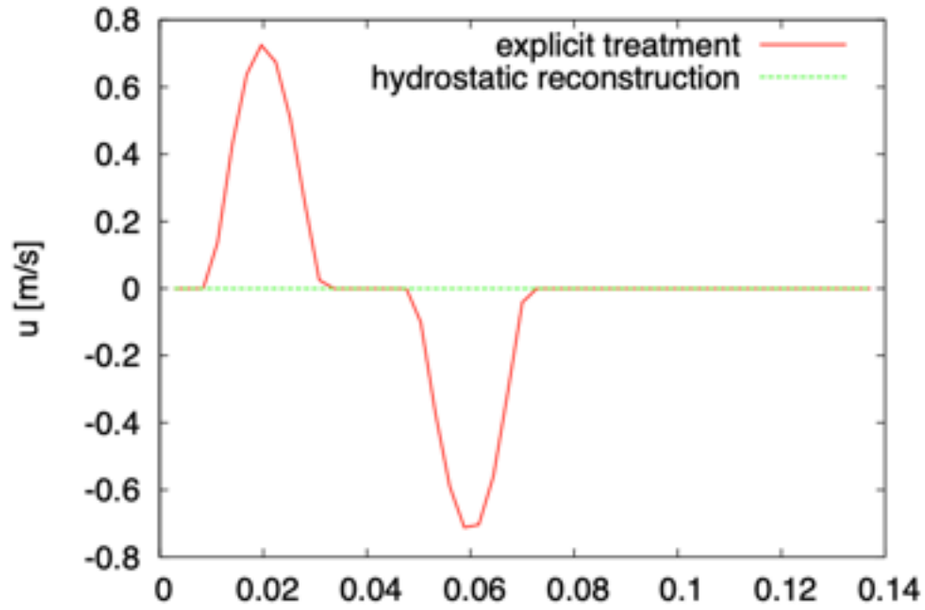

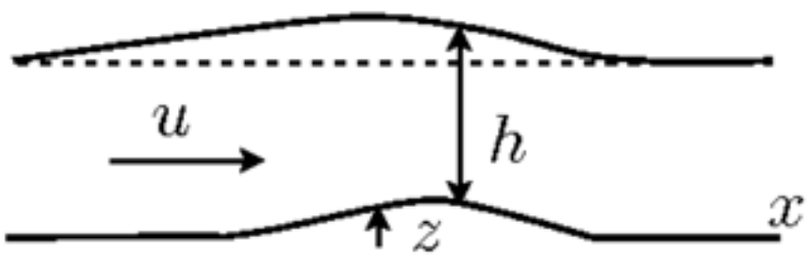

$$\begin{cases} q = u = 0 \\ \partial_x (h + z\,(x)) = \partial_x \eta = 0\,, \end{cases}$$

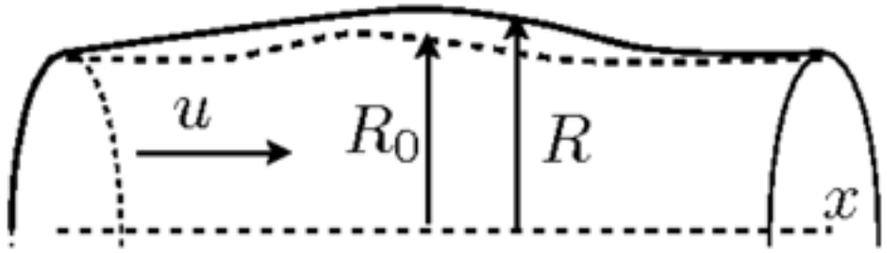

$$\begin{cases} Q = u = 0 \\ \partial_x \left(b\sqrt{A} - b\sqrt{A_0\,(x)} \right) = 0\,. \end{cases}$$

by analogy with the **”lake at rest”**
(hydrostatic equilibrium for the shallow water),
we introduced **"man at eternal rest”**

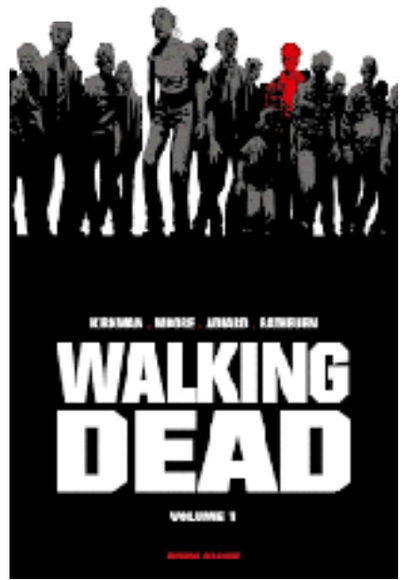

Kirkman R, Moore T, Adlard C. The Walking Dead. Image Comics, 2003.

Experimental Validation

Saito et al JBE 2011

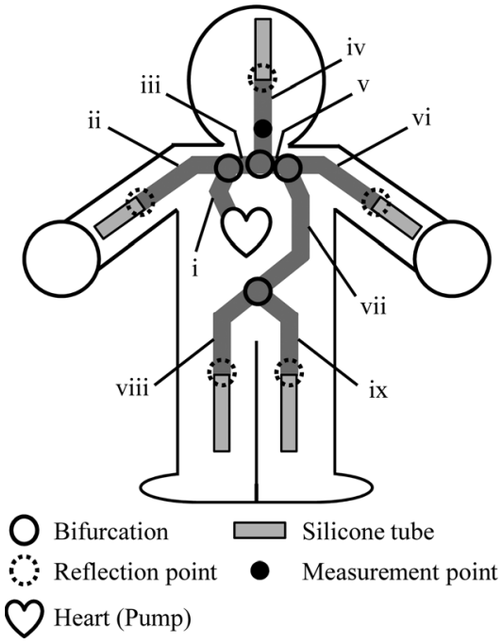

	Name	Length [mm]	Diameter [mm]	Thickness [mm]
i	Aorta arch A	35	12	2
ii	R.subclavian radial artery	800	6	1.5
iii	Aorta arch B	20	11	2
iv	L.carotid artery	675	6	1.5
v	Aorta arch C	40	10	2
vi	L.Subclavian radial artery	710	6	1.5
vii	Aorta	470	8	1.5
viii	R.femoral artery	365	6	1.5
ix	L.femoral artery	365	6	1.5

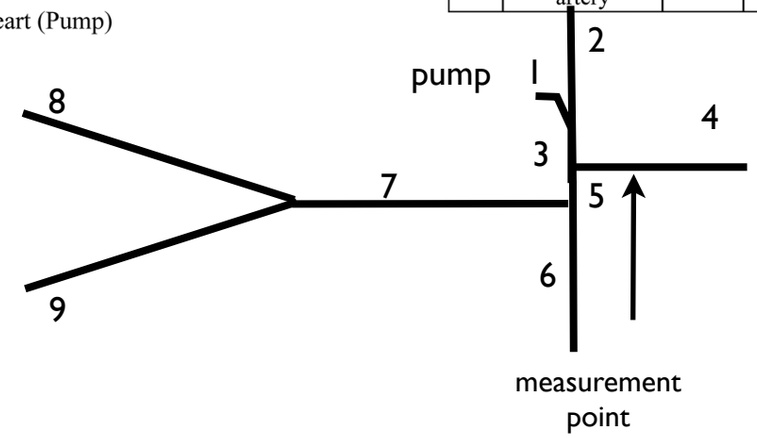

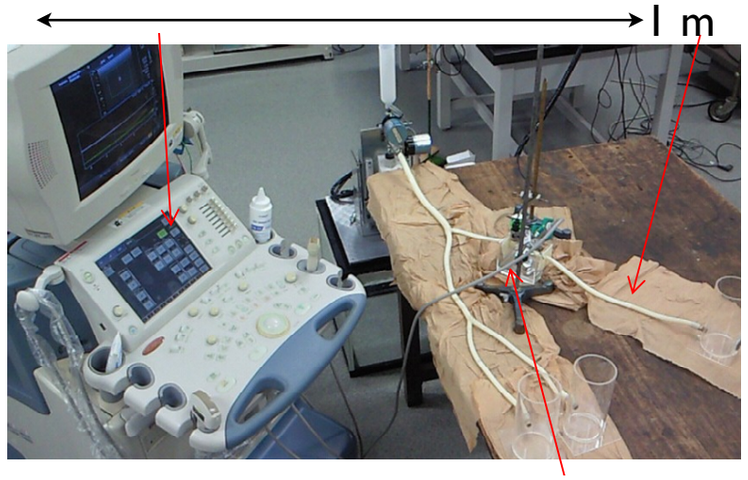

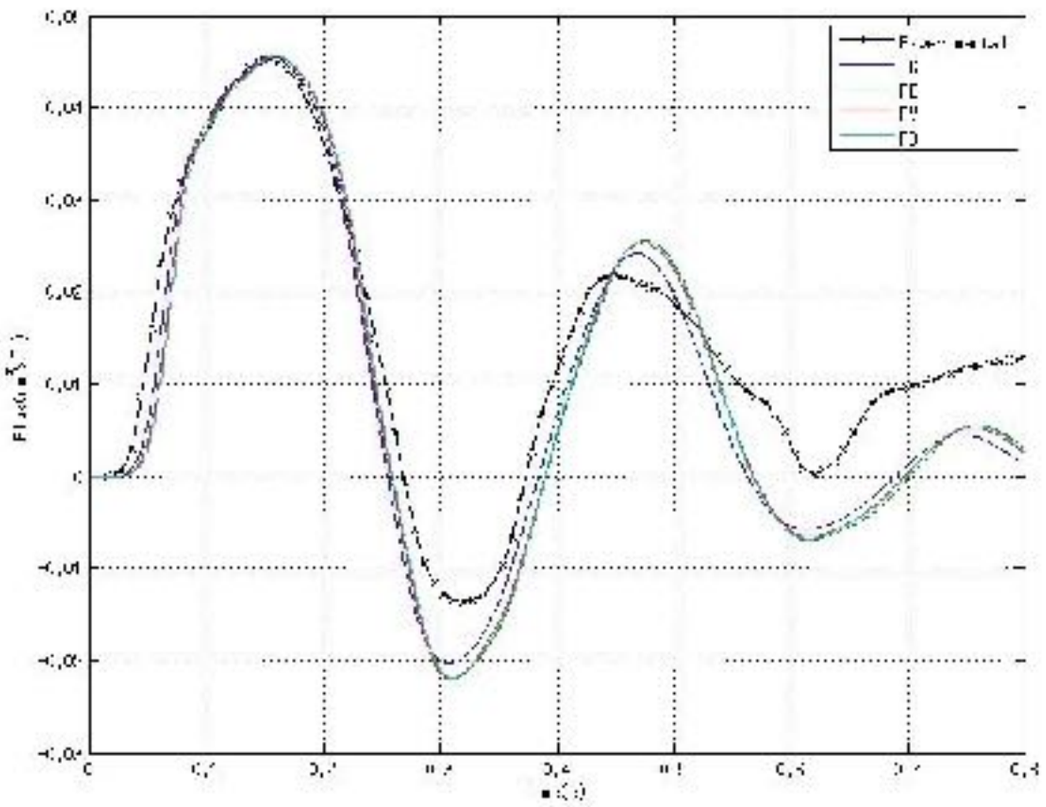

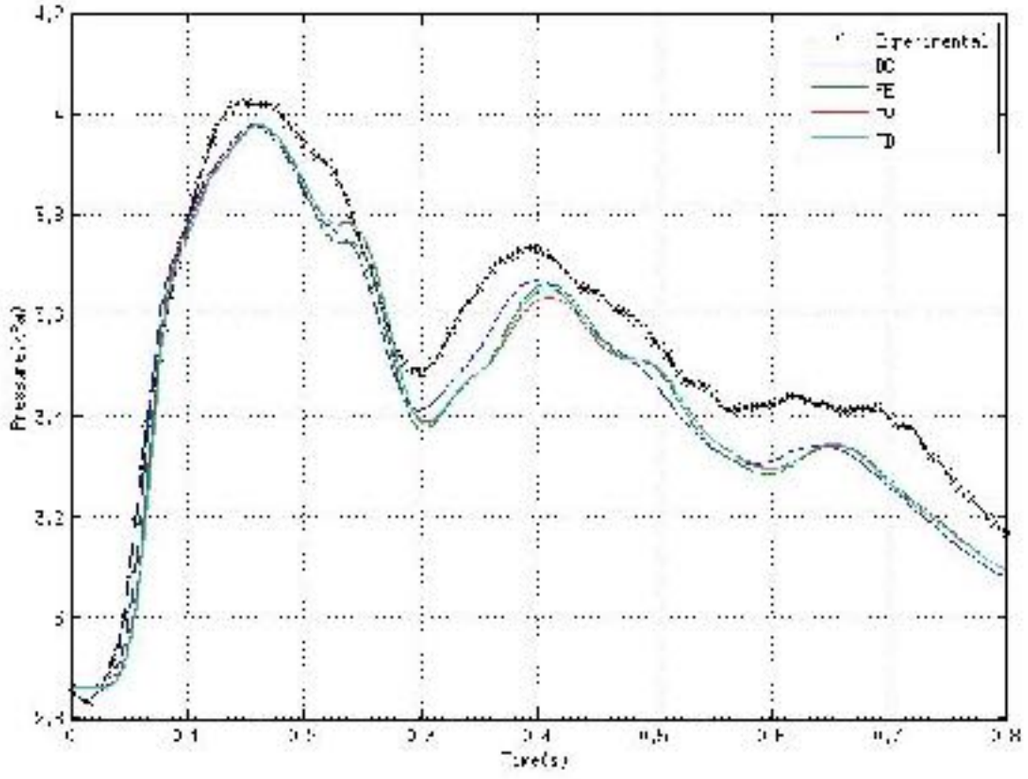

In vitro networks

9 arteries network

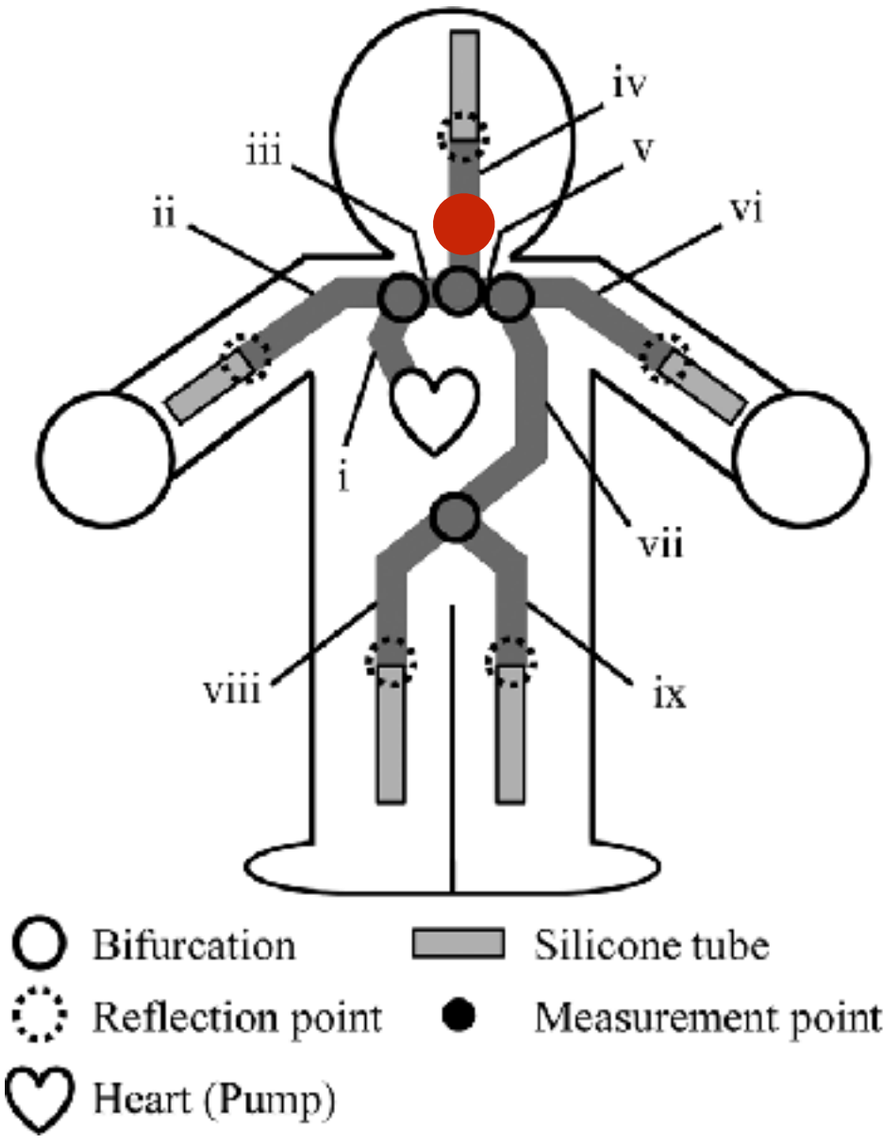

Saito & al., J Biomech Eng (2011)

37 arteries network

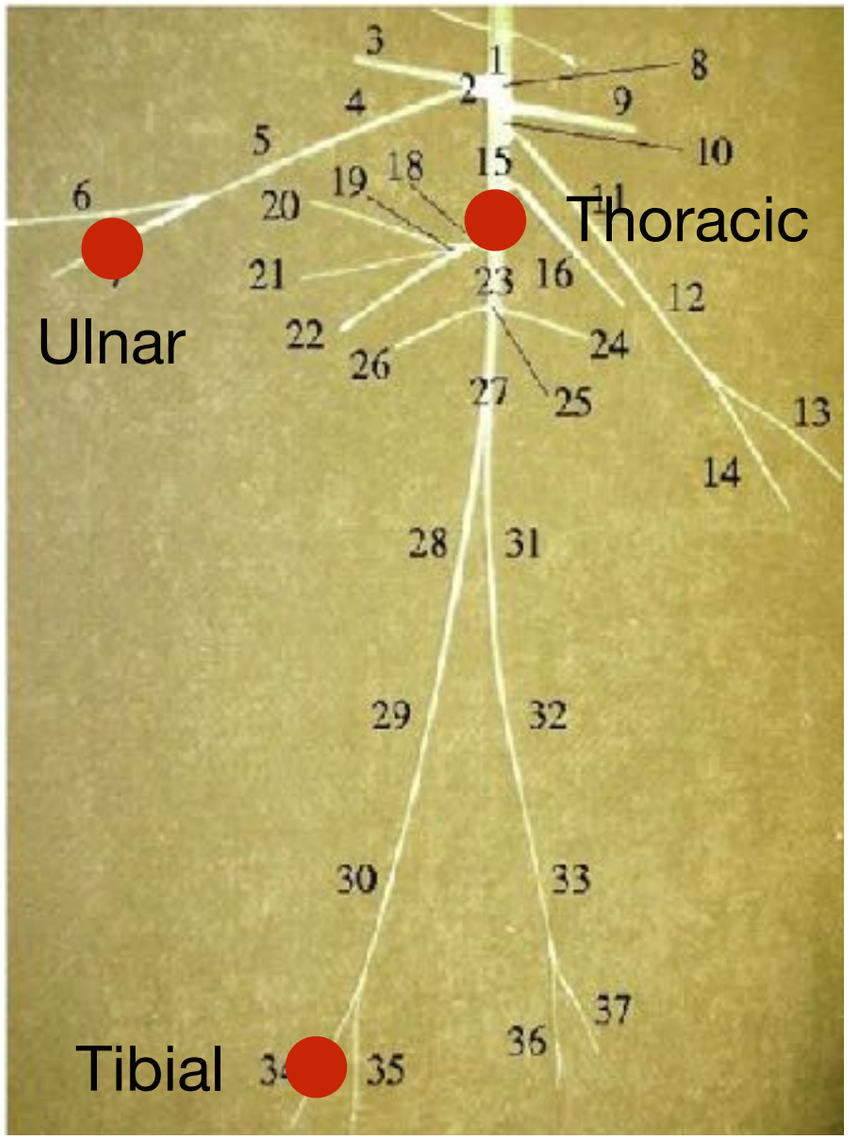

Alastruey & al., J Biomech (2011)

9 arteries network

Saito & al., J Biomech Eng (2011)

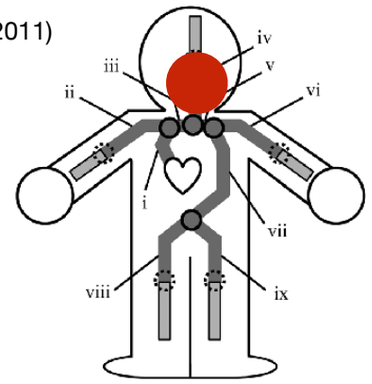

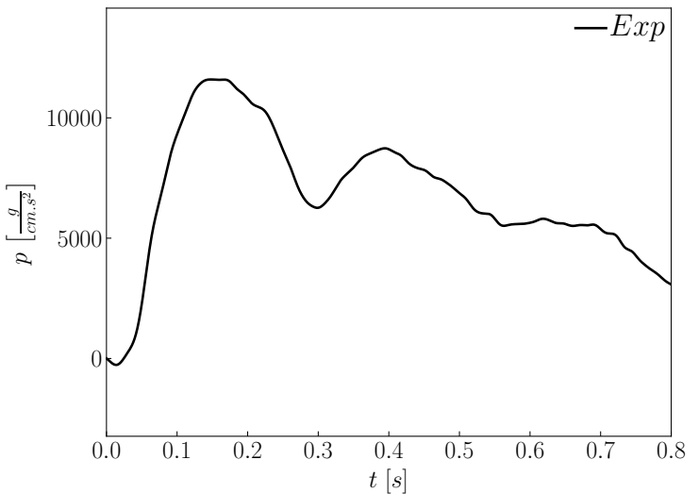

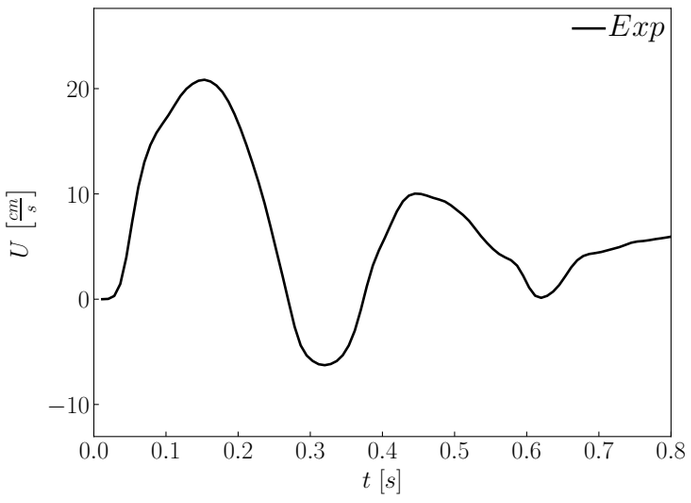

Experimental data

37 arteries network

Alastruey & al., J Biomech (2011)

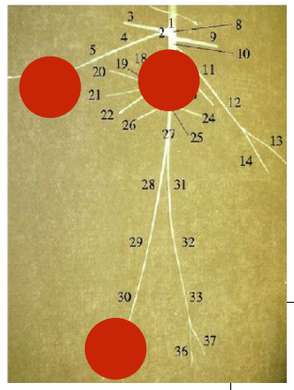

Ulnar

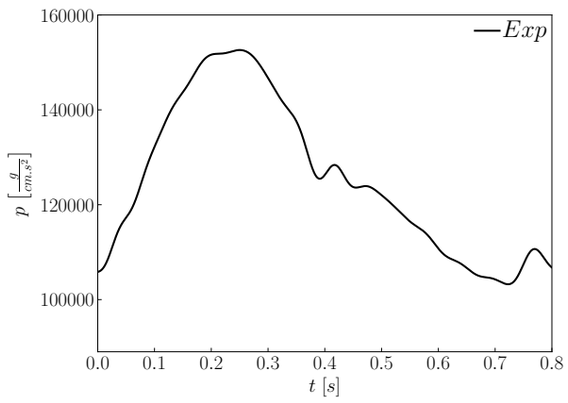

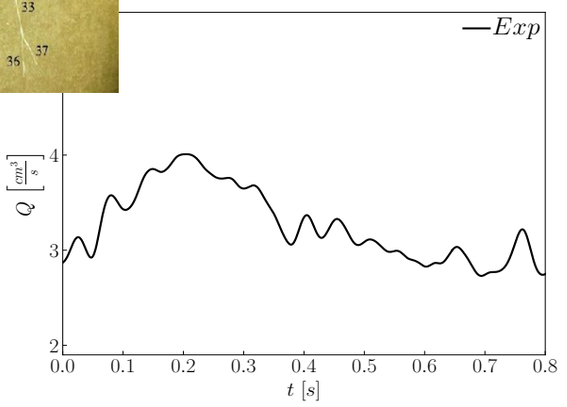

Thoracic

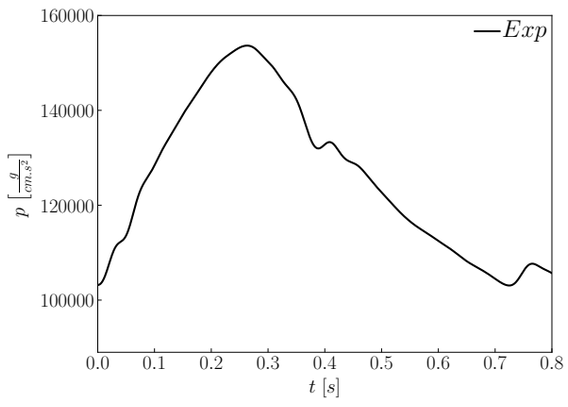

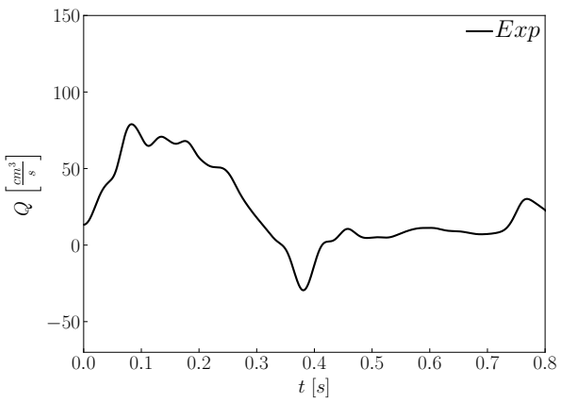

Tibial

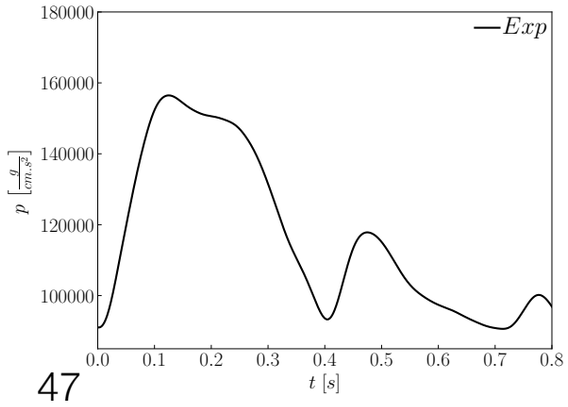

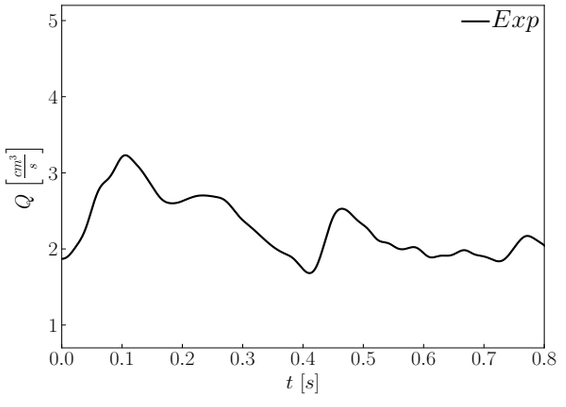

9 arteries network

Saito & al., J Biomech Eng (2011)

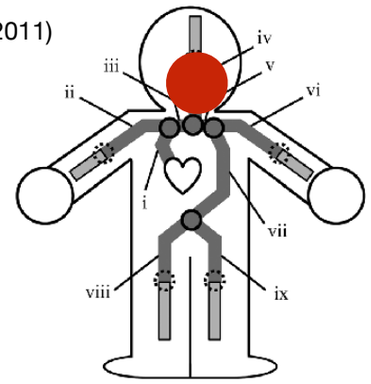

37 arteries network

Alastruey & al., J Biomech (2011)

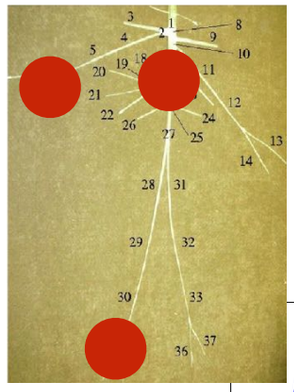

Wave propagation & reflection

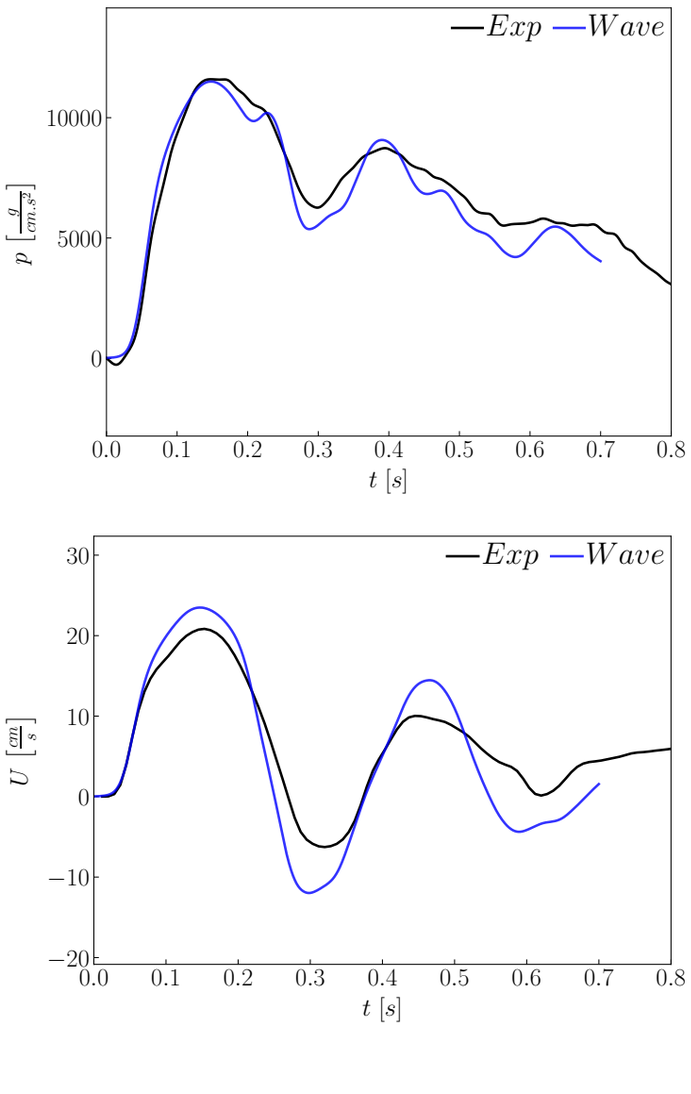

Ulnar

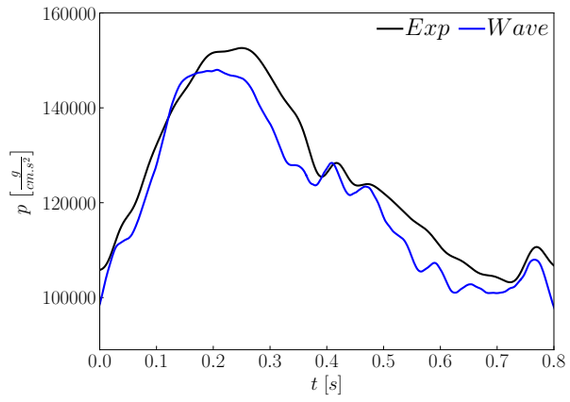

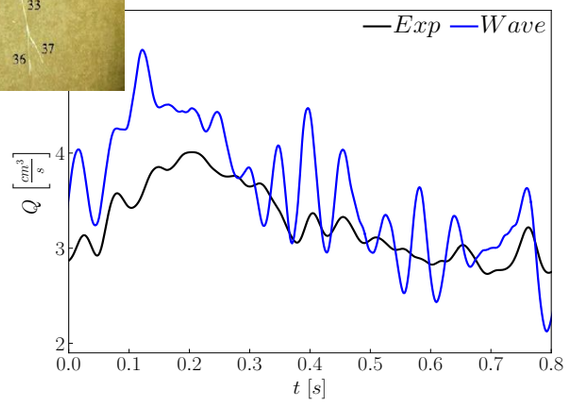

Thoracic

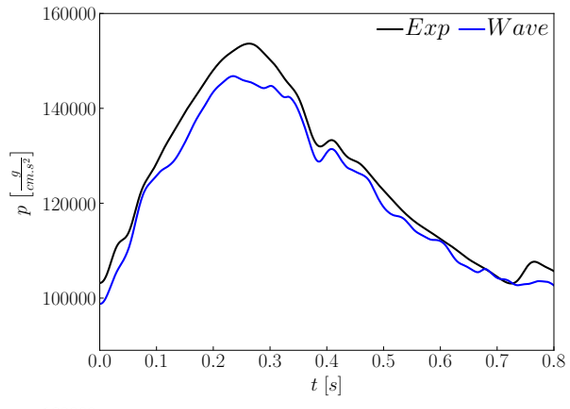

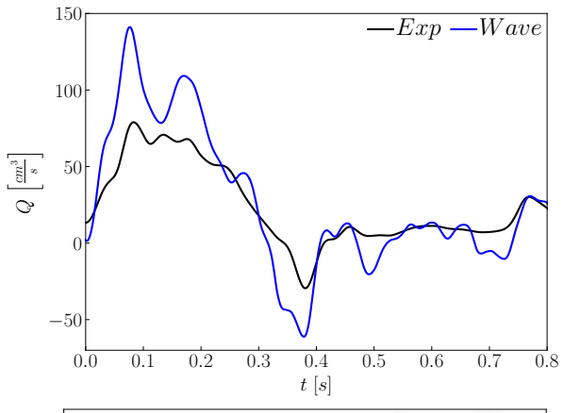

Tibial

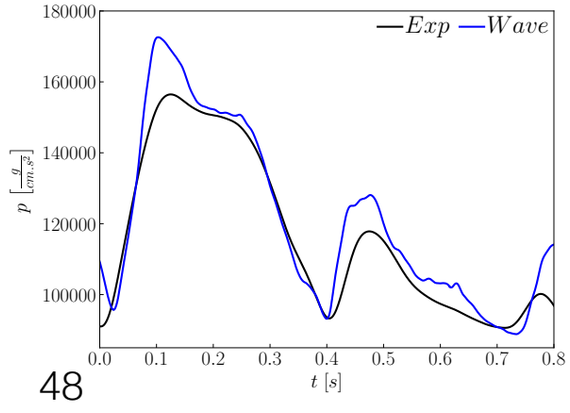

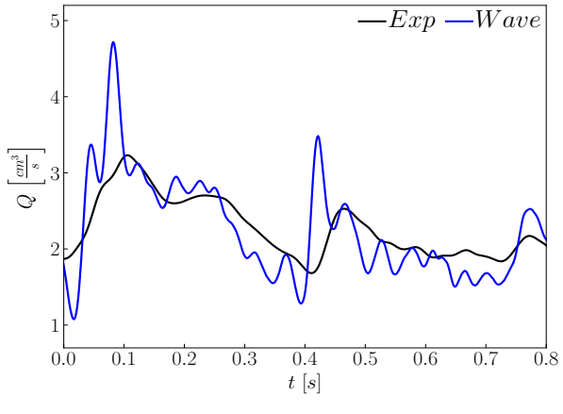

9 arteries network

Saito & al., J Biomech Eng (2011)

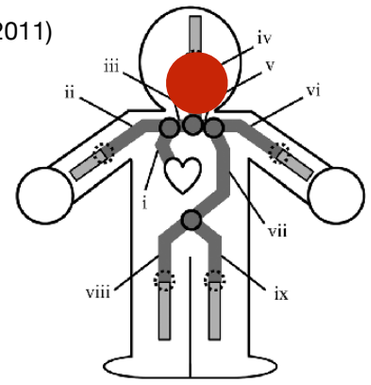

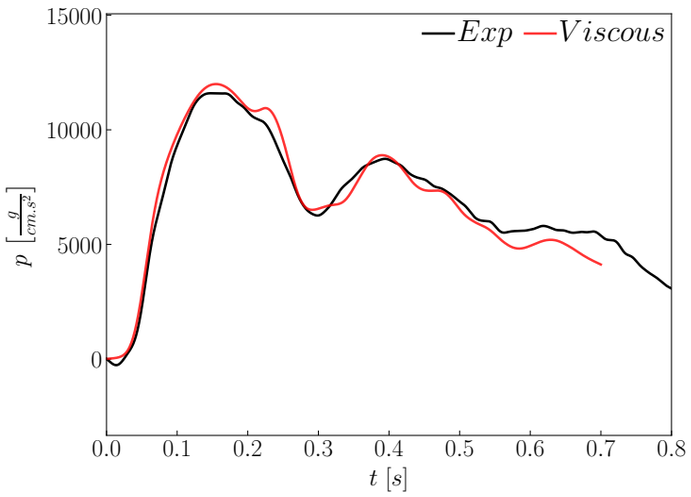

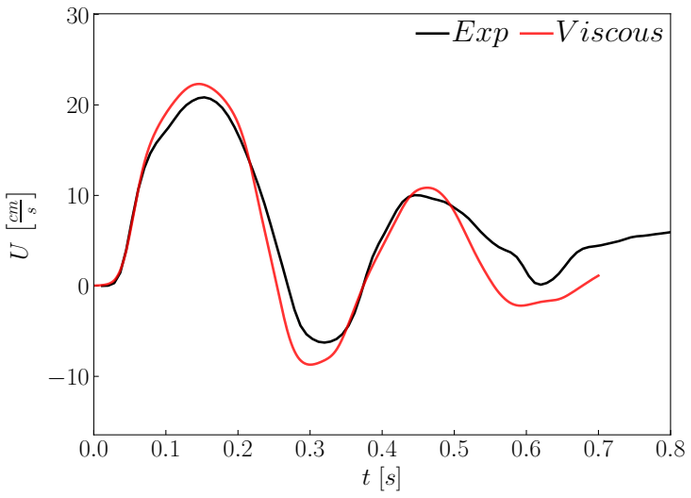

Viscous dissipation

37 arteries network

Alastruey & al., J Biomech (2011)

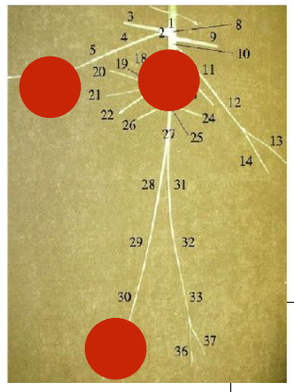

Ulnar

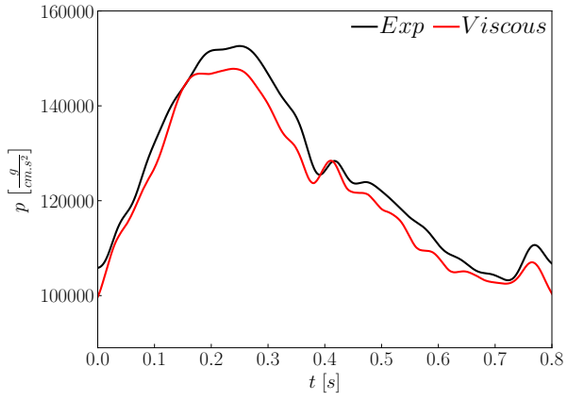

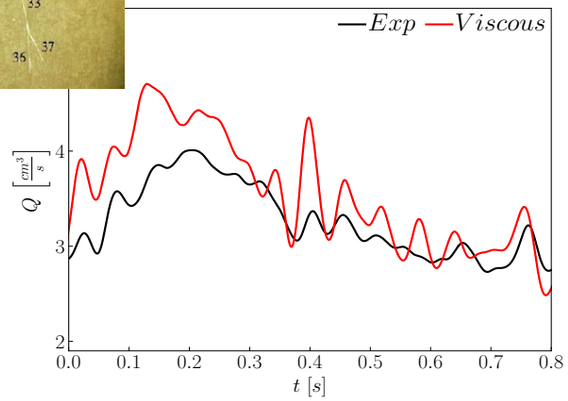

Thoracic

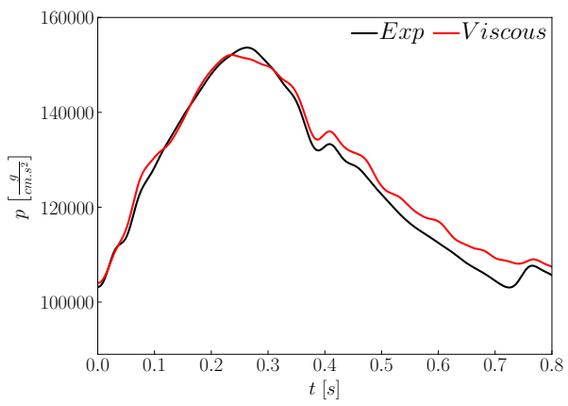

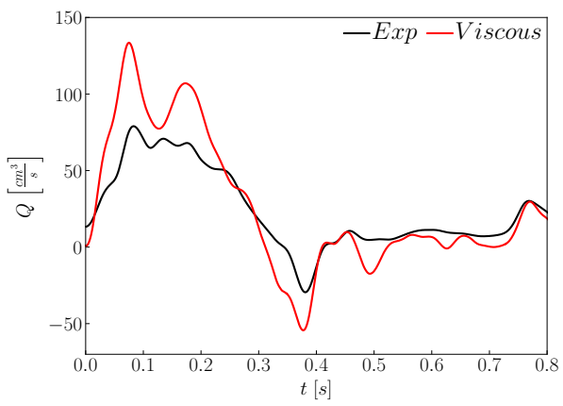

Tibial

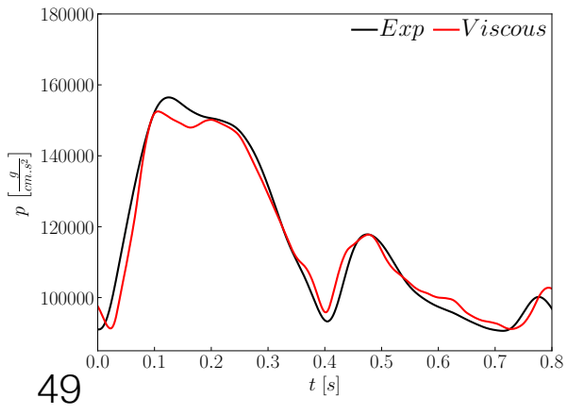

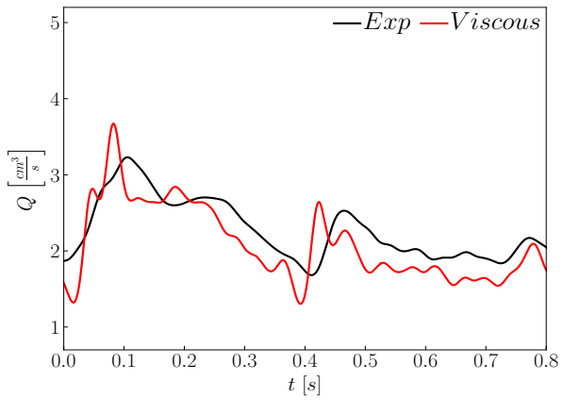

9 arteries network

Saito & al., J Biomech Eng (2011)

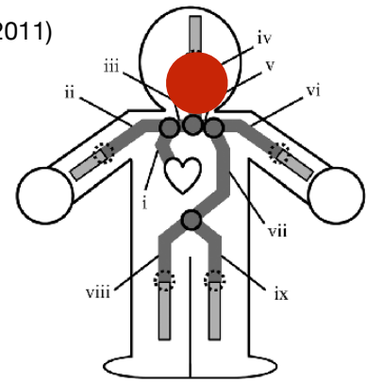

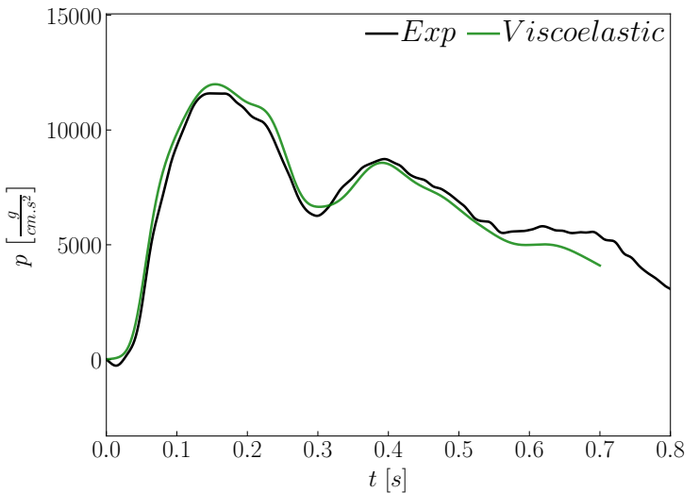

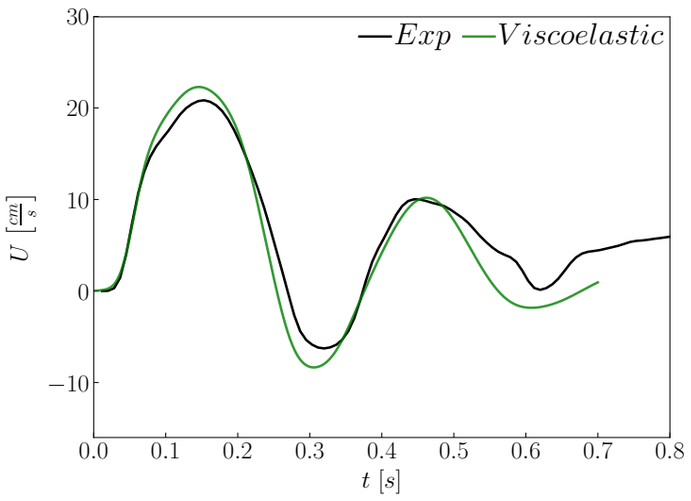

Viscoelastic diffusion

37 arteries network

Alastruey & al., J Biomech (2011)

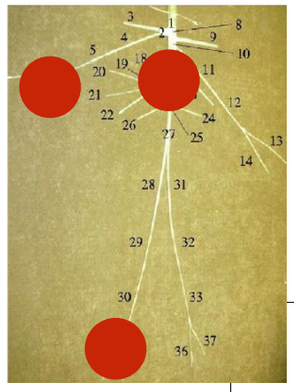

Ulnar

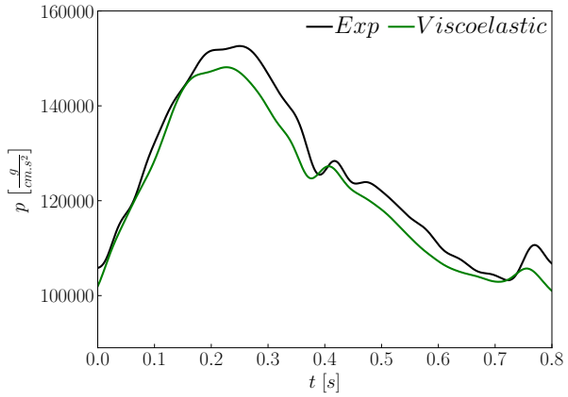

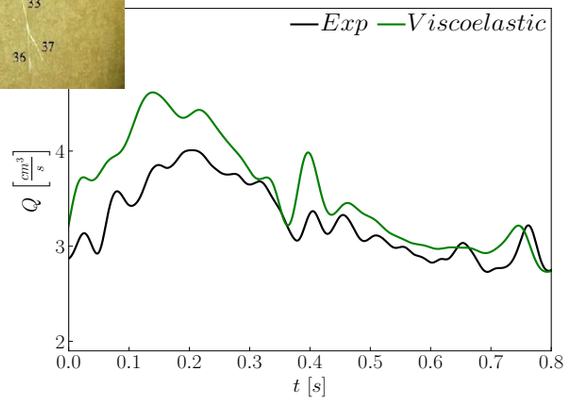

Thoracic

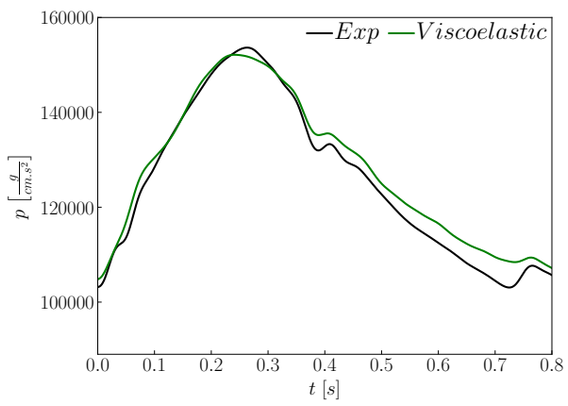

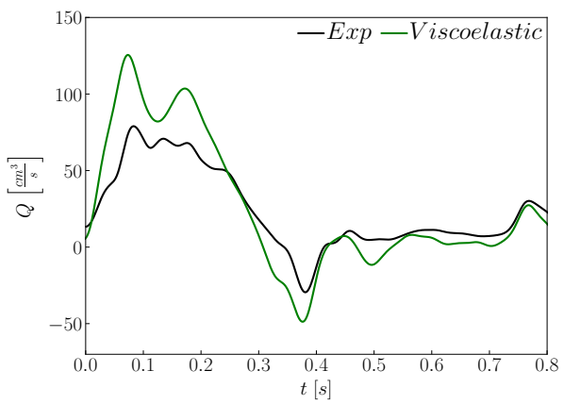

Tibial

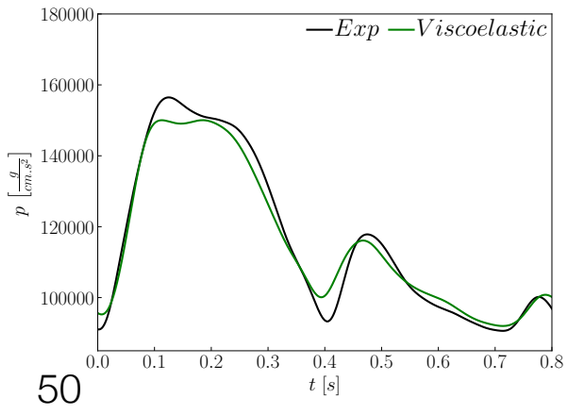

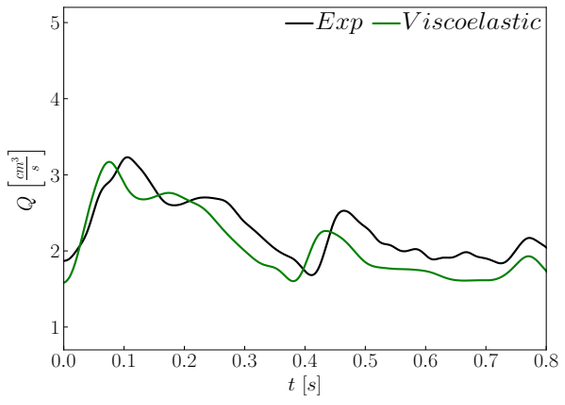

1D Model: Global Analysis — Stenosis of the iliac artery

Ghigo, et al. CMBBE 2015

55 arteries network

Sane

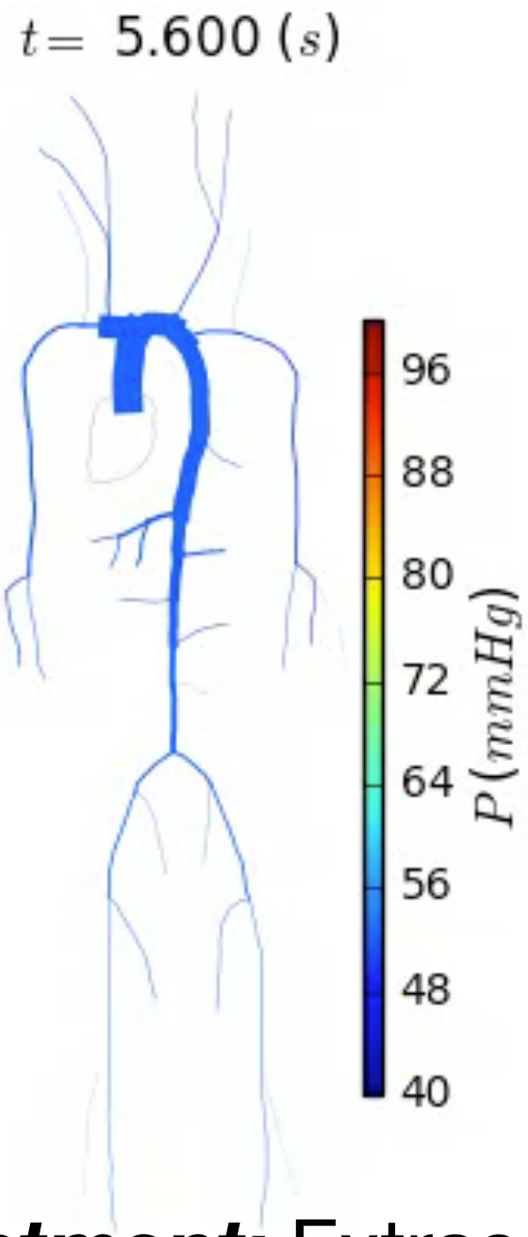

Stenosis of Iliac artery

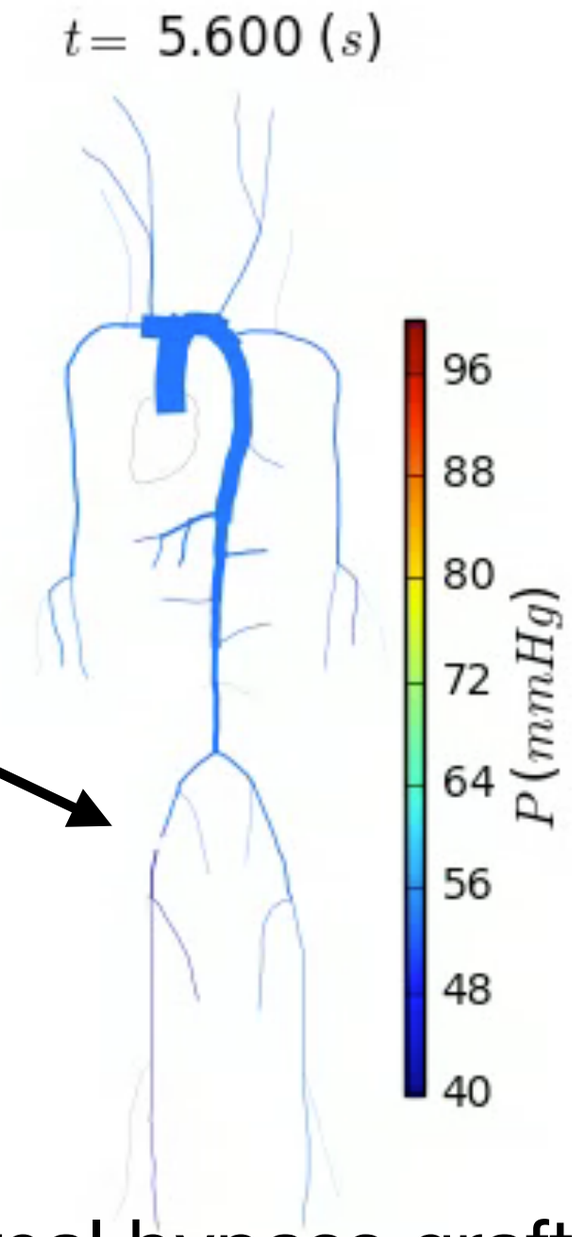

Axillo-Femoral bypass graft

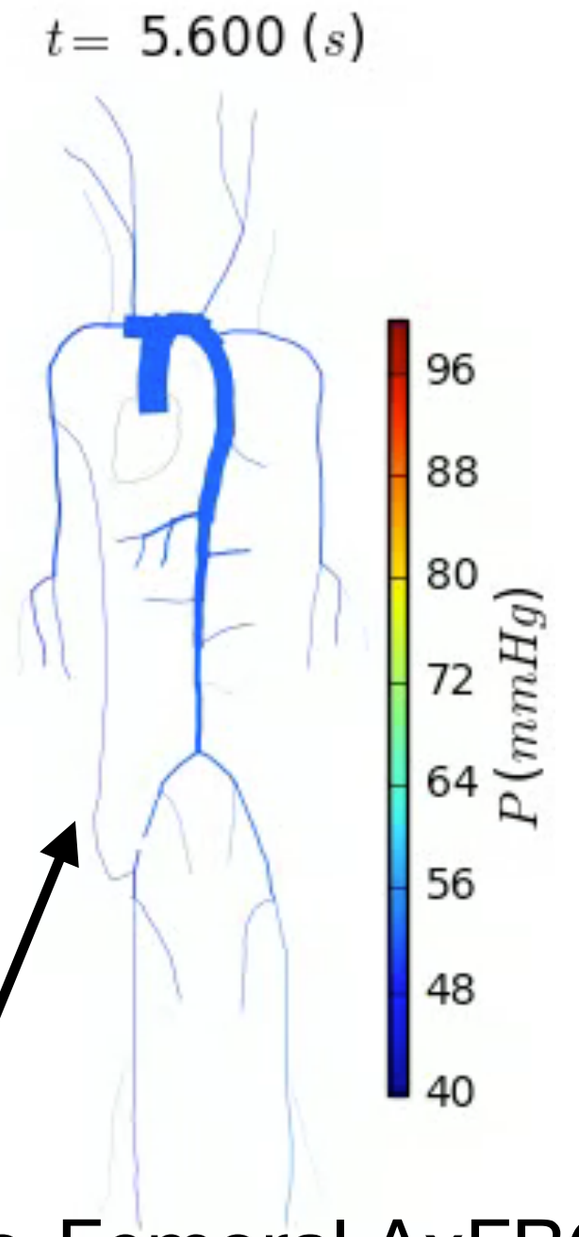

Treatment: Extracorporeal bypass graft (Axillo-Femoral AxFBG)

1D Model: Global Analysis — Stenosis of the iliac artery

Ghigo, et al. CMBBE 2015

55 arteries network

Sane

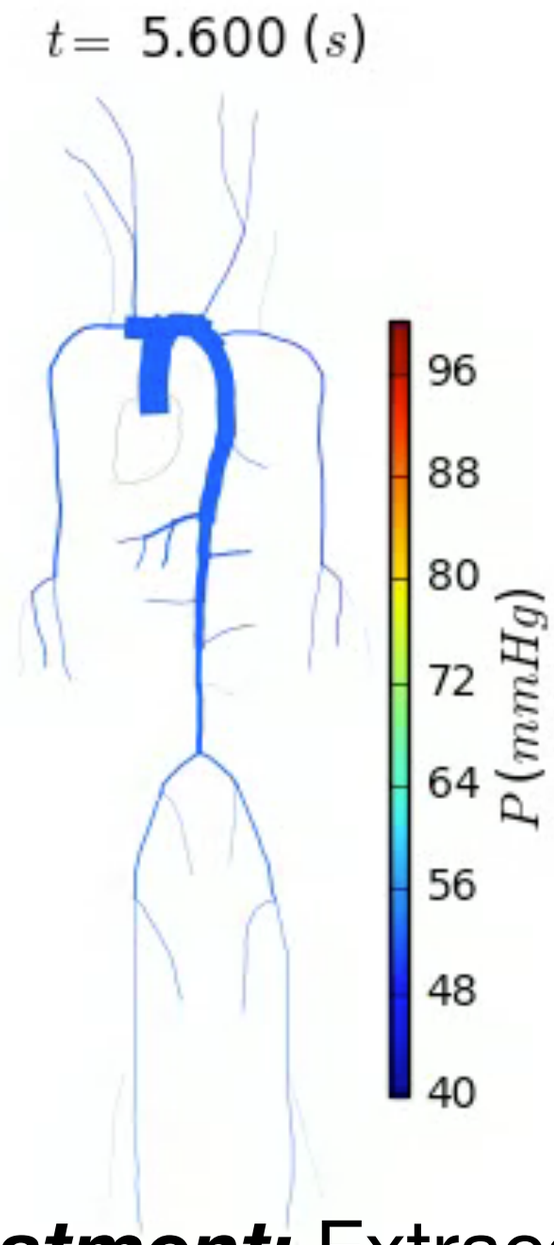

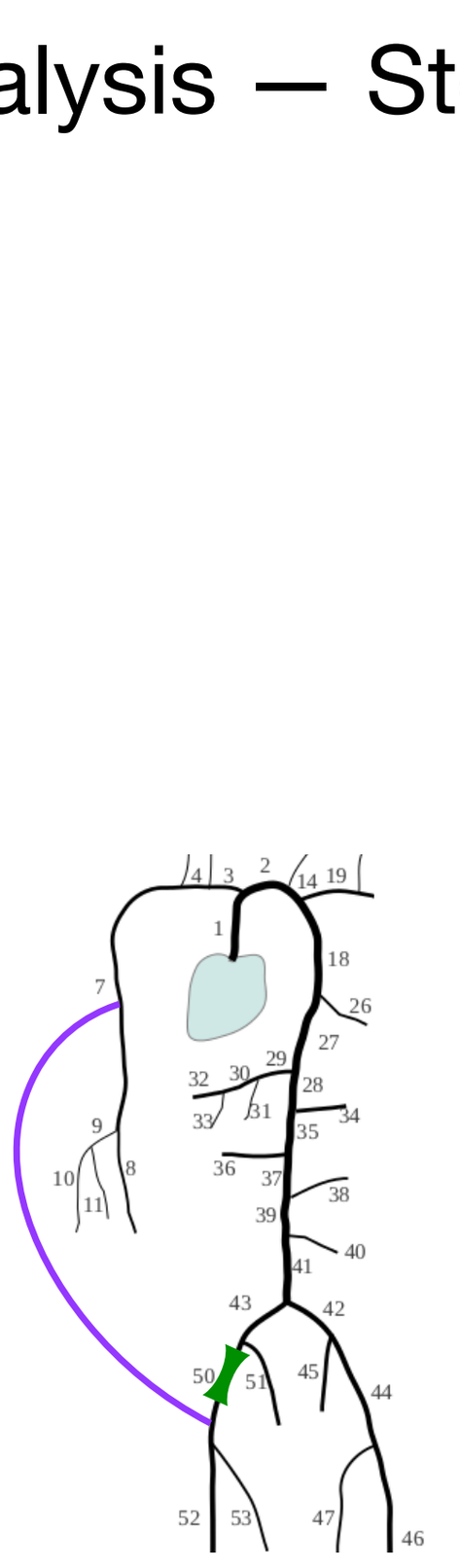

Treatment: Extracorporeal bypass graft (Axillo-Femoral AxFBG)

Application: clamping (*clampage*): change of blood network during an operation

Ventre et al. IJNMB 2020

Politi et al JSR 2019

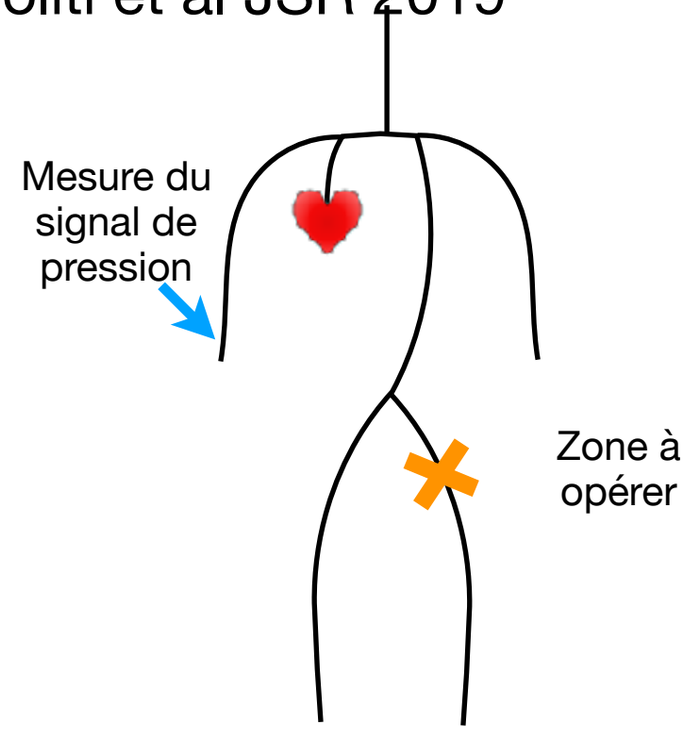

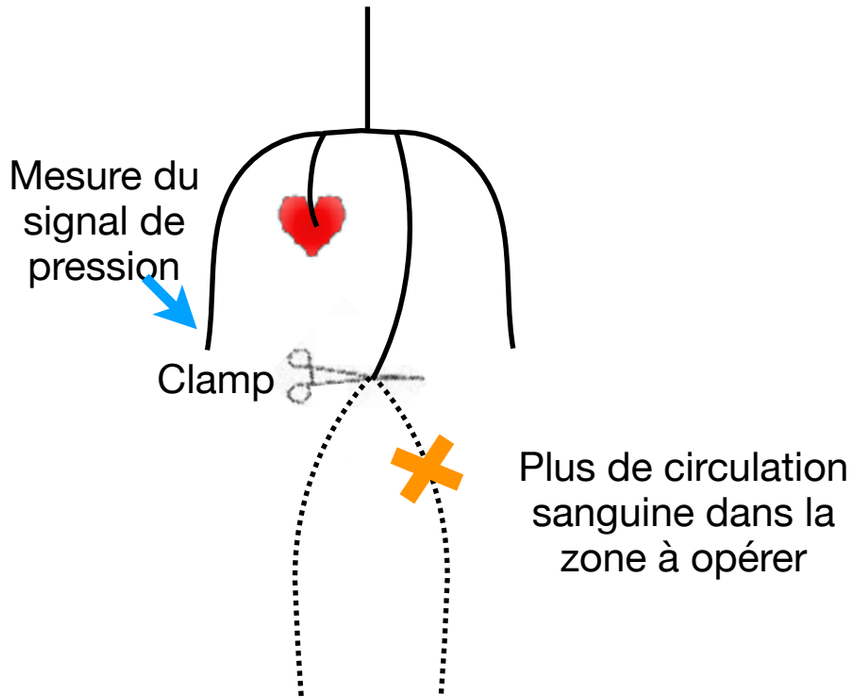

before

during

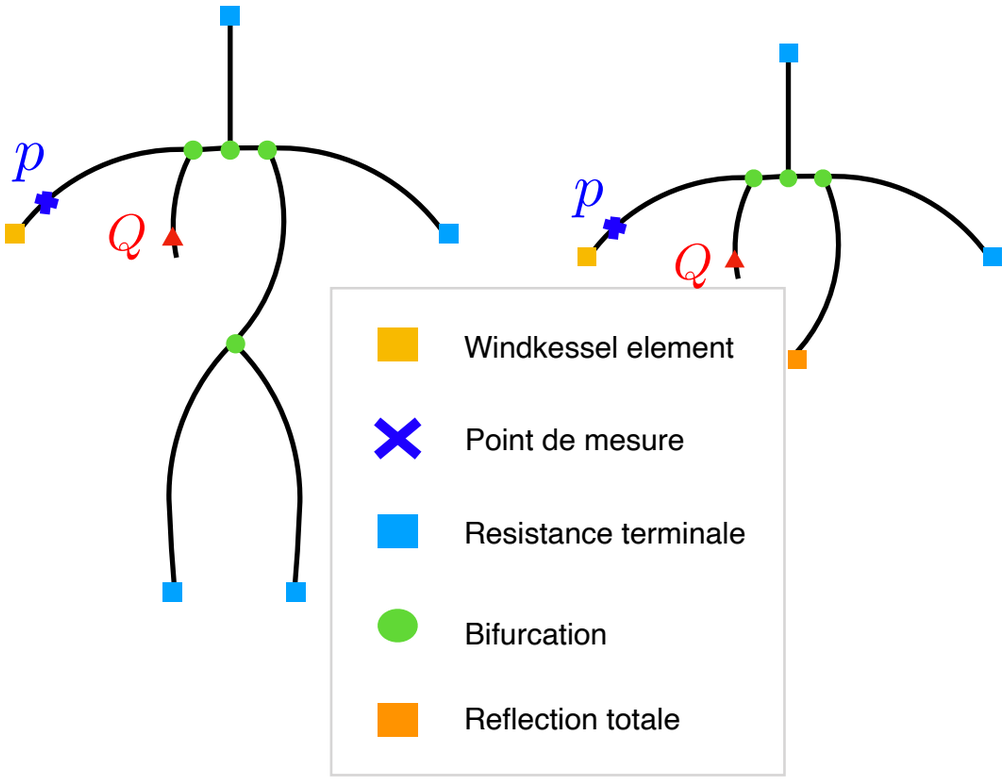

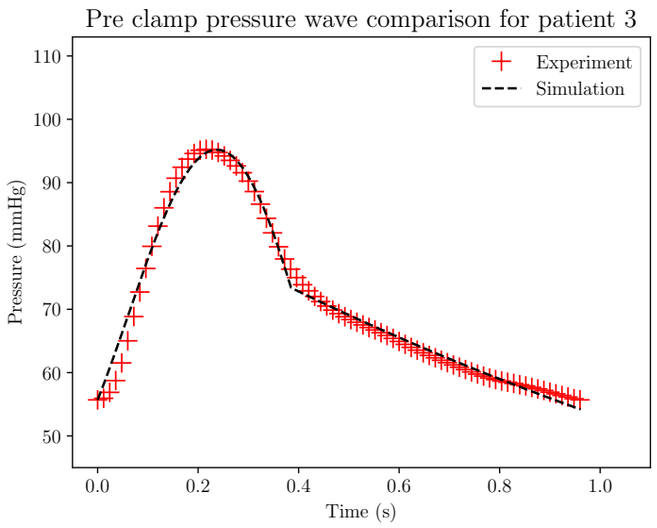

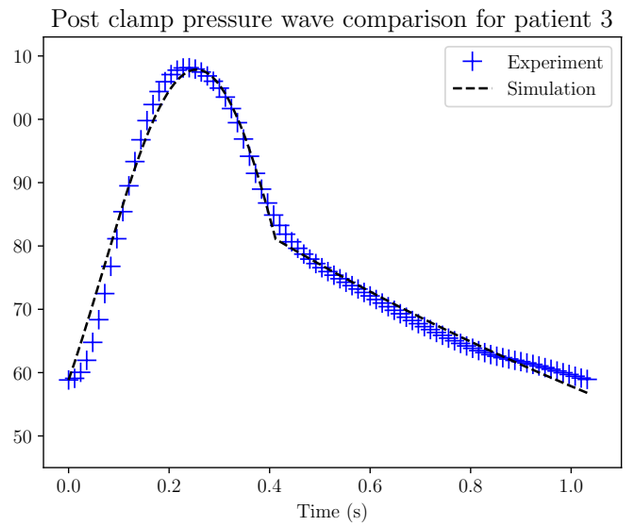

✓ Validation of model on cohort study of 5 "in vivo" patients

Collaboration : Faculté de Médecine de Buenos Aires, Argentine

So far, so good

1D models works well for engineering applications (flood and blood)

So far, so good

1D models works well for engineering applications (flood and blood)

But depends on the choice of the closure Gamma and friction

come back to free surface flows

Boussinesq or shape coefficient $$\Gamma = \frac{\frac{1}{h}\int_0^h u^2 dy}{\left(\frac{1}{h}\int_0^h u dy\right)^2}$$

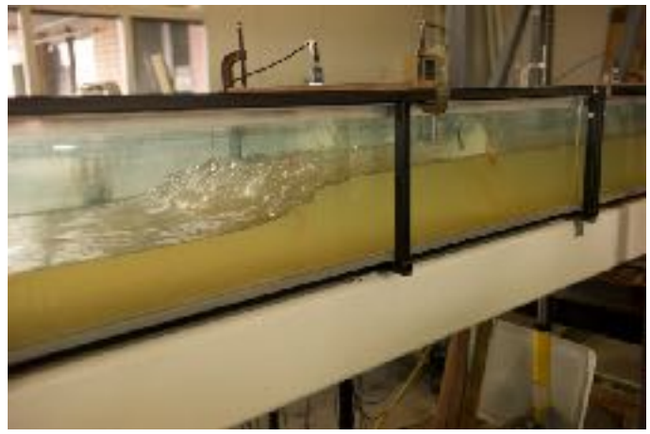

shear at the wall is $$\tau = \mu \left(\frac{\partial u}{\partial y}\right)_0$$

how the shape factor (Boussinesq coeff.) Γ and the wall shear stress τ are related to the flow rate and the depth?

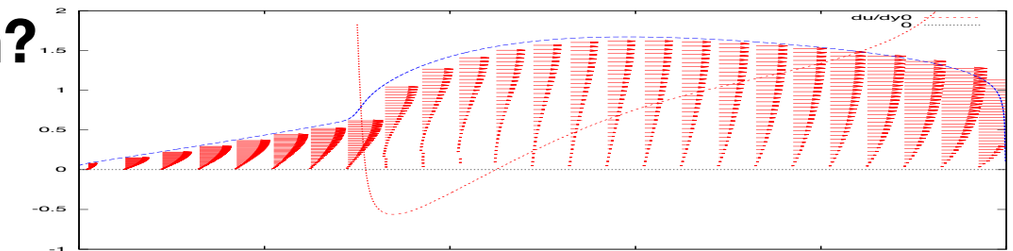

SHALLOW WATER Saint Venant

Closure relations

how the shape factor (Boussinesq coeff.) Γ and the wall shear stress τ are related to the flow rate and the depth?

suppose Poiseuille profile $\Gamma = \frac{6}{5}$ and $\tilde{\tau}_b = \frac{3}{Re}\frac{\tilde{Q}}{\tilde{h}^2}$.

suppose "turbulent flat" profile $\Gamma = 1$ and $\tilde{\tau}_b = \frac{c_f}{2}\frac{\tilde{Q}^2}{\tilde{h}^2}$,

suppose Watson profile $\Gamma = 1.25697$ and $\tilde{\tau}_b = \frac{2.2799}{Re}\frac{\tilde{Q}}{\tilde{h}^2}$.

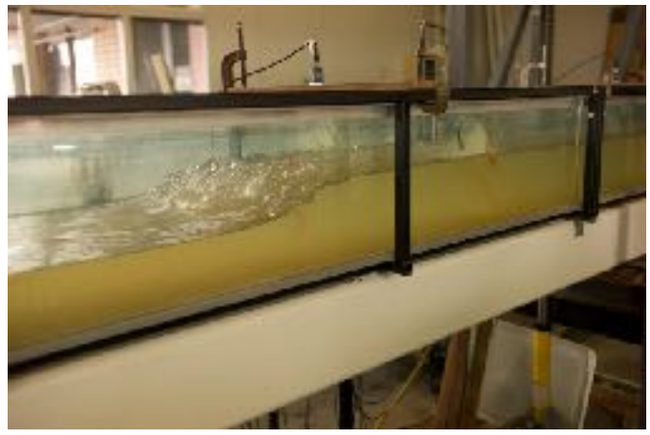

problem of choice? Which one is the best?

same question for Bingham flows, artery flows…

for granular: Bagnold profile…
for Bingham: Plug + half Poiseuille
for arteries Womersley profiles…

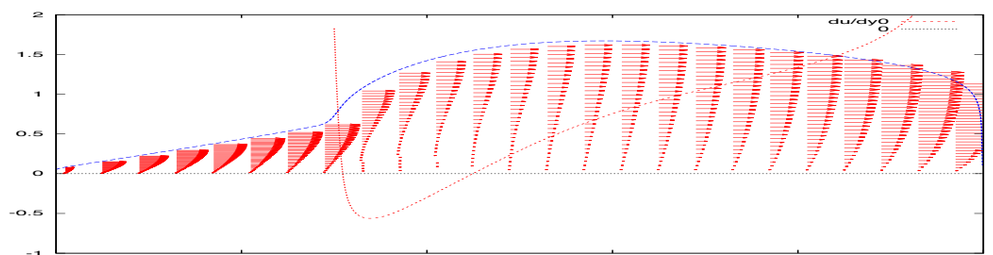

SHALLOW WATER Saint Venant

Closure relations

how the shape factor (Boussinesq coeff.) Γ and the wall shear stress τ are related to the flow rate and the depth?

suppose Poiseuille profile $\Gamma = \frac{6}{5}$ and $\tilde{\tau}_b = \frac{3}{Re}\frac{\tilde{Q}}{\tilde{h}^2}$.

suppose "turbulent flat" profile $\Gamma = 1$ and $\tilde{\tau}_b = \frac{c_f}{2}\frac{\tilde{Q}^2}{\tilde{h}^2}$,

suppose Watson profile $\Gamma = 1.25697$ and $\tilde{\tau}_b = \frac{2.2799}{Re}\frac{\tilde{Q}}{\tilde{h}^2}$.

problem of choice? Which one is the best?

same question for Bingham flows, artery flows…

for granular: Bagnold profile…
for Bingham: Plug + half Poiseuille
for arteries Womersley profiles…

-> compute Γ and t τ from numerical resolution of full Prandtl system

Numerical strategy: resolution of Prandtl

solve the last full system of equations (just before averaging)

$$\frac{\partial u}{\partial x} + \frac{\partial v}{\partial y} = 0$$

$$\rho\Big(\frac{\partial u}{\partial t} + \frac{\partial u^2}{\partial x} + \frac{\partial uv}{\partial y}\Big) = -\frac{\partial p}{\partial x} + \frac{\partial \tau_{xy}}{\partial y} + \rho g \sin\theta$$

$$0 = -\rho g \cos\theta - \frac{\partial p}{\partial y}$$

Prandtl system is not so simple to solve:
- singularity at separation
- finite time singularity
- spurious instabilities
- coupling
...

coupling of several "shallow water systems" with interaction (Audusse Bristeau Perthame Sainte-Marie 2011)

decompose the equations in several artificial interacting Saint-Venant layers

Numerical strategy: "Multilayer" resolution of Prandtl

solve the last full system of equations (just before averaging)

$$\frac{\partial u}{\partial x} + \frac{\partial v}{\partial y} = 0$$

$$\rho\Big(\frac{\partial u}{\partial t} + \frac{\partial u^2}{\partial x} + \frac{\partial uv}{\partial y}\Big) = -\frac{\partial p}{\partial x} + \frac{\partial \tau_{xy}}{\partial y} + \rho g \sin\theta$$

$$0 = -\rho g \cos\theta - \frac{\partial p}{\partial y}$$

"Multilayer" resolution:
integrate on fraction of height

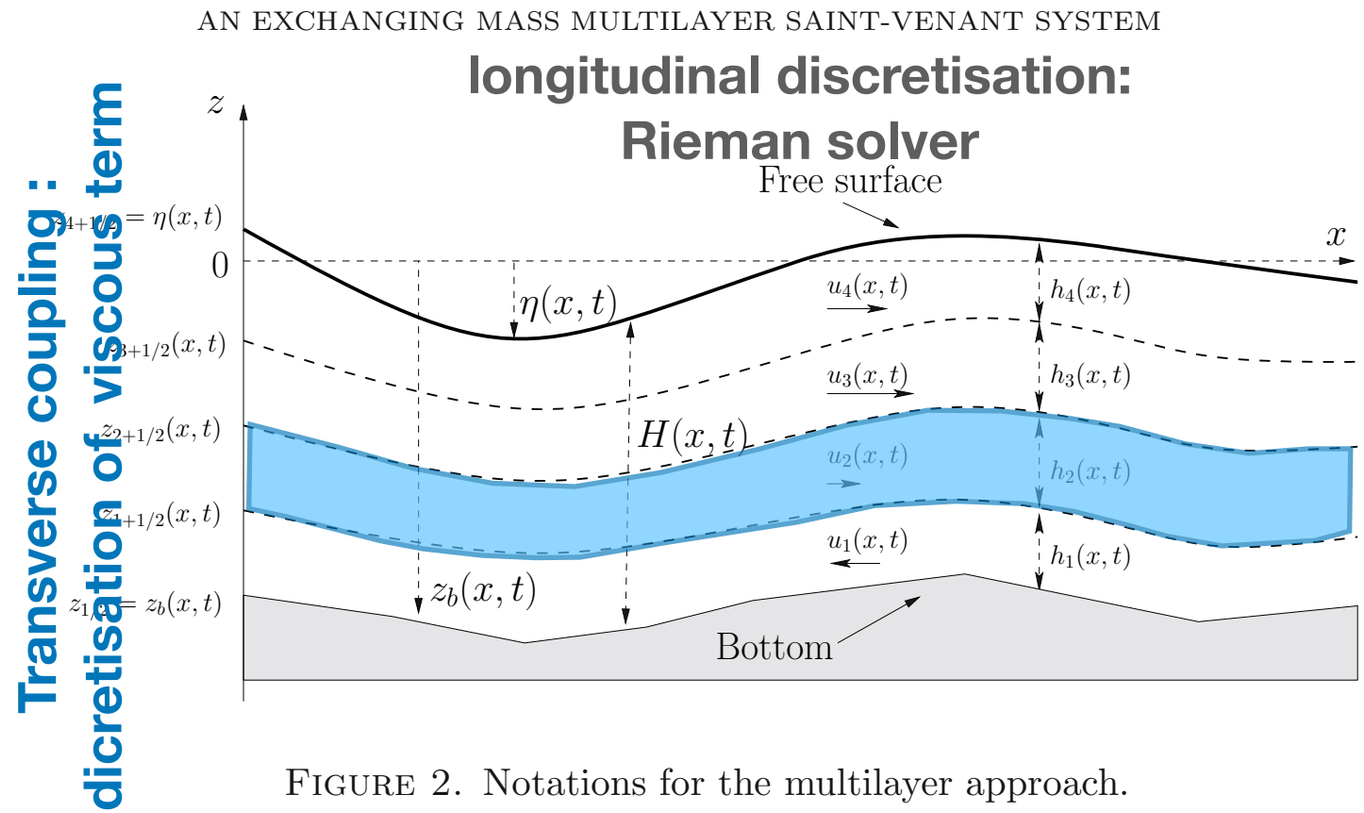

FIGURE 2. Notations for the multilayer approach.

coupling of several "shallow water systems" with interaction (Audusse Bristeau Perthame Sainte-Marie 2011)

$$\underbrace{\begin{aligned}\frac{\partial h_\alpha}{\partial t} + \frac{\partial h_\alpha u_\alpha}{\partial x} &= G_{\alpha+1/2} - G_{\alpha-1/2},\\ \frac{\partial h_\alpha u_\alpha}{\partial t} + \frac{\partial}{\partial x}\left(h_\alpha \langle u^2\rangle_\alpha\right) + g h_\alpha \frac{\partial H}{\partial x} &= -g h_\alpha \frac{\partial z_b}{\partial x} + u_{\alpha+1/2} G_{\alpha+1/2} - u_{\alpha-1/2} G_{\alpha-1/2}\end{aligned}}_{\text{"a shallow water layer"}} \underbrace{+ \frac{2\nu_\alpha}{l_{\alpha+1}+l_\alpha}\frac{u_{\alpha+1}-u_\alpha}{h} - \frac{2\nu_{\alpha-1}}{l_\alpha + l_{\alpha-1}}\frac{u_\alpha - u_{\alpha-1}}{h}}_{\text{dicretisation of viscous term}}$$

"mass/ mom. coupling the layers"

Testing the Multilayer Resolution of Prandtl

- newtonian: lubrication case (Huppert 82,82)
- newtonian: hydraulic jump (Higuera 94)
- non newtonian: Bingham Collapse (Balmforth…)
- newtonian: Arteries
- non newtonian: granular μ(I) avalanches

- newtonian: lubrication (Huppert 82,82)

De Vita et al. EJFM 2020

$$\frac{\partial h}{\partial t} - \frac{1}{3}\frac{\partial}{\partial x} h^3 \frac{\partial h}{\partial x} = 0$$

flood wave

Huppert JFM82

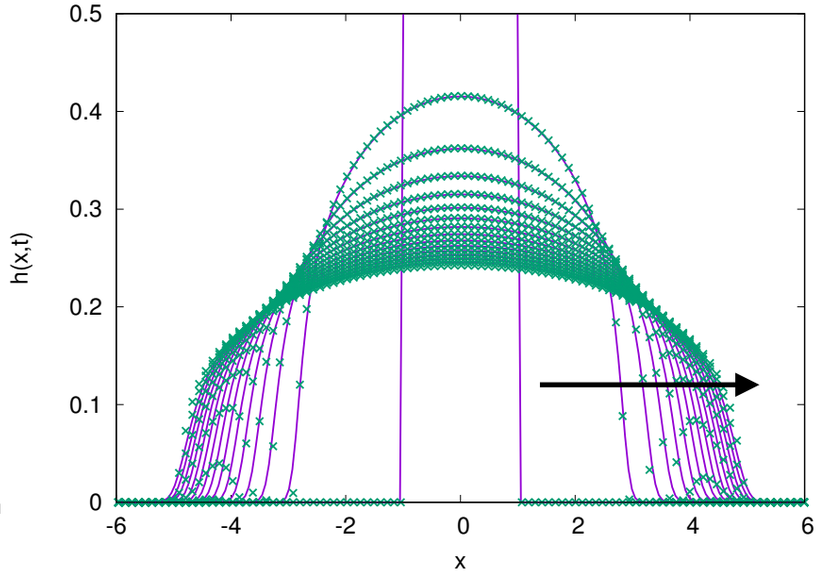

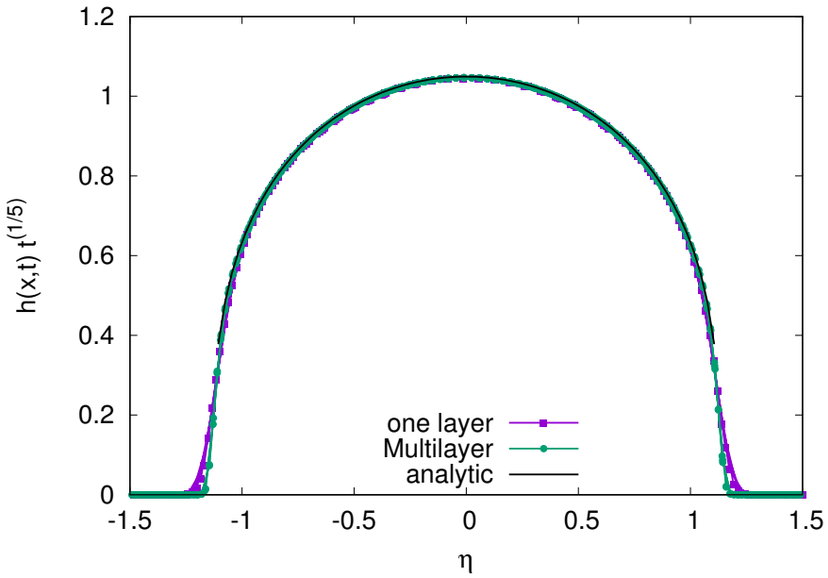

comparaison numerical 1D, Huppert, 2D RNSP Multilayer

$$\frac{\partial h}{\partial t} + h^2 \frac{\partial h}{\partial x} = 0$$

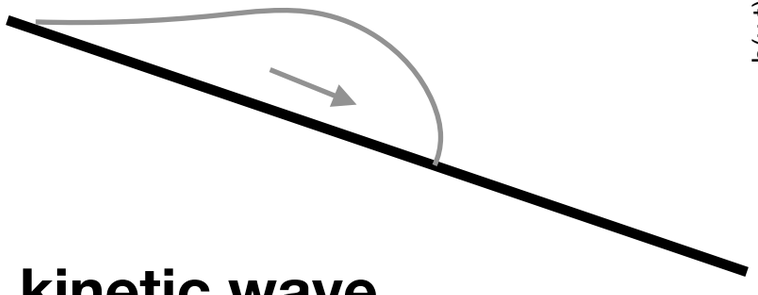

kinetic wave

Huppert Nat82

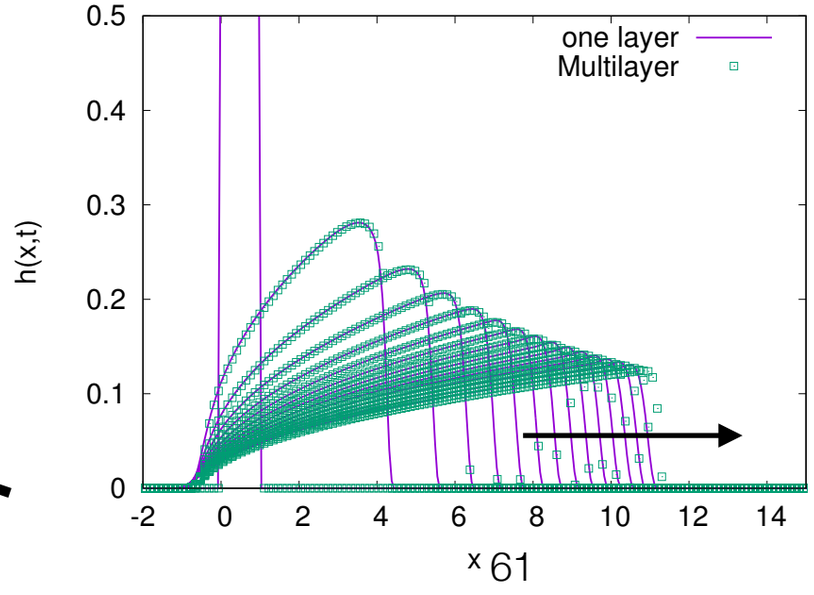

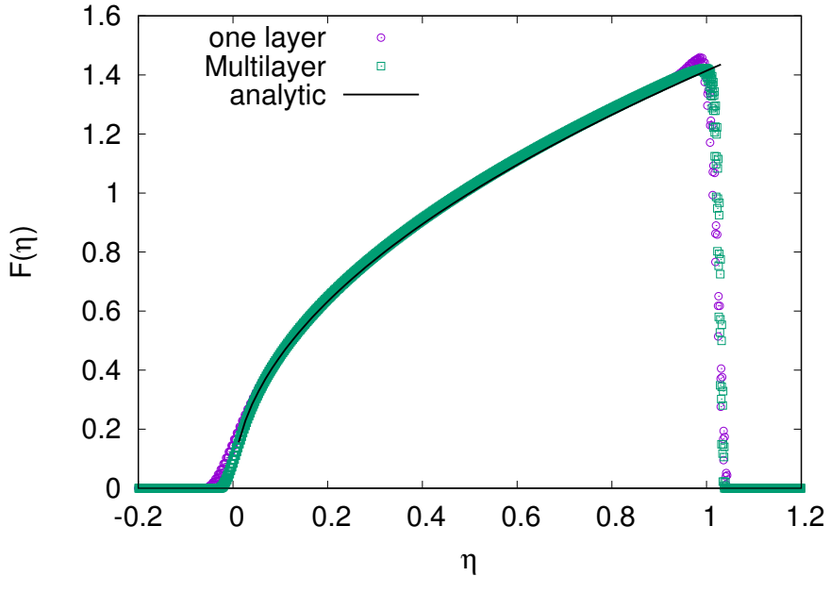

- newtonian: 2D hydraulic jump (Higuera 94)

De Vita et al. EJFM 2020

$$\frac{\partial \tilde{u}}{\partial \tilde{x}} + \frac{\partial \tilde{w}}{\partial \tilde{z}} = 0,\ \frac{\partial \tilde{u}}{\partial \tilde{t}} + \frac{\partial \tilde{u}^2}{\partial \tilde{x}} + \frac{\partial \tilde{u}\tilde{w}}{\partial \tilde{z}} = -\frac{\partial \tilde{h}}{\partial \tilde{x}} + \frac{\partial^2 \tilde{u}}{\partial \tilde{z}^2} \text{ given } \int_0^{\tilde{h}} \tilde{u} d\tilde{z} = \tilde{Q}.$$

$$\frac{\partial \bar{u}}{\partial \bar{x}} + \frac{\partial \bar{w}}{\partial \bar{z}} = 0,\ \bar{u}\frac{\partial \bar{u}}{\partial \bar{x}} + \bar{w}\frac{\partial \bar{u}}{\partial \bar{z}} = -S\frac{\partial \bar{h}}{\partial \bar{x}} + \frac{\partial^2 \bar{u}}{\partial \bar{z}^2} \text{ given } \int_0^{\bar{h}} \bar{u} d\bar{z} = 1,$$

$$S^{-1/2} = \tilde{Q}^{5/2}$$

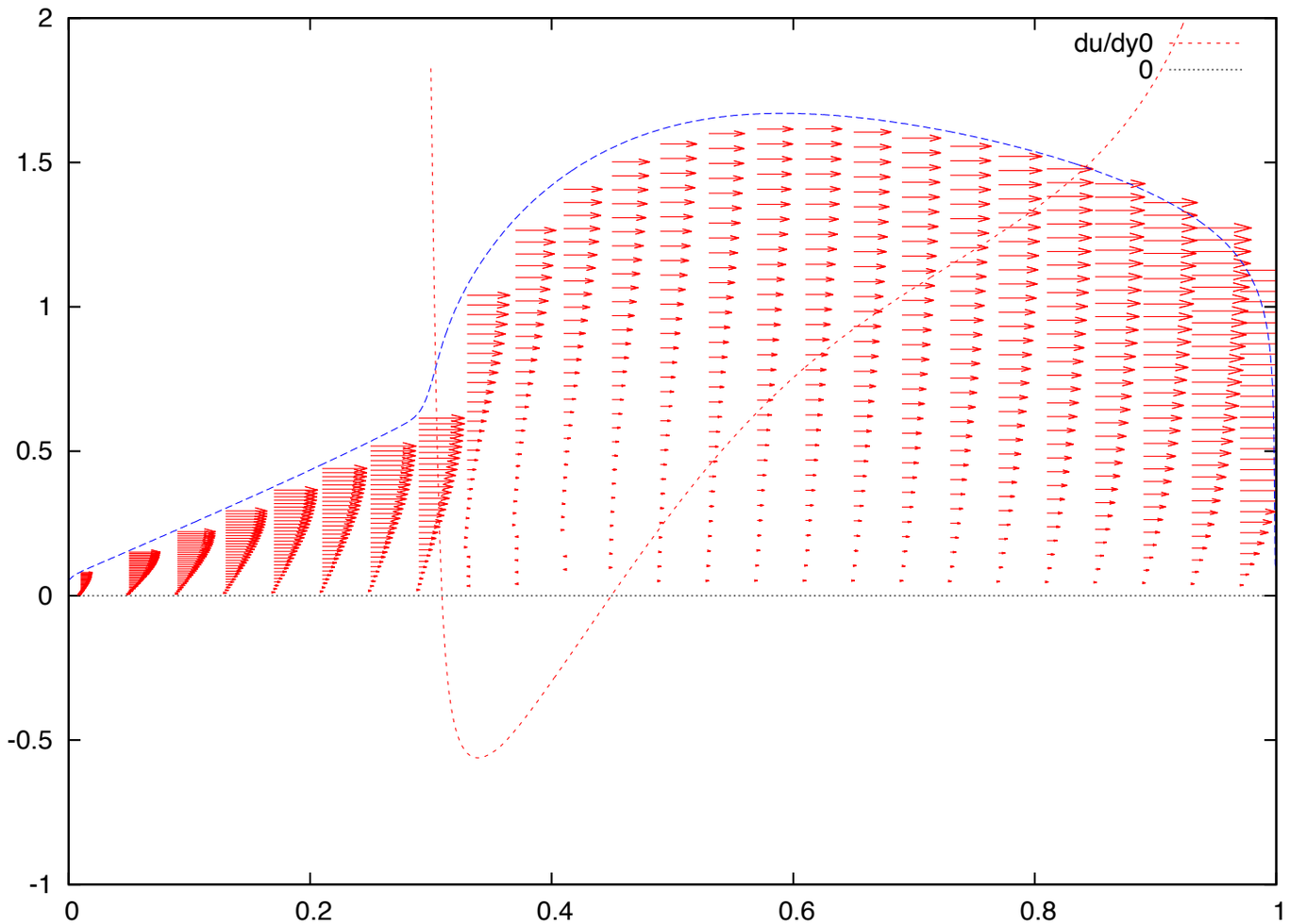

- newtonian: 2D hydraulic jump (Higuera 94)

De Vita et al. EJFM 2020

$$\frac{\partial \tilde{u}}{\partial \tilde{x}} + \frac{\partial \tilde{w}}{\partial \tilde{z}} = 0, \; \frac{\partial \tilde{u}}{\partial \tilde{t}} + \frac{\partial \tilde{u}^2}{\partial \tilde{x}} + \frac{\partial \tilde{u}\tilde{w}}{\partial \tilde{z}} = \qquad + \frac{\partial^2 \tilde{u}}{\partial \tilde{z}^2} \text{ given } \int_0^{\tilde{h}} \tilde{u} d\tilde{z} = \tilde{Q}.$$

$$S^{-1/2} = \tilde{Q}^{5/2}$$

self similar viscous solution
with no pressure gradient

$$u_w = \frac{1}{x} f(\eta) \text{ with } \eta = y/x.$$

$f''' = -f^2$ with $f(0) = 0$, $f'(H_w) = 0$ for a unit flow rate $\int_0^{H_w} f(\eta) d\eta = 1$.

$$\tilde{h}(\tilde{x}) = 1.8138\tilde{x}$$

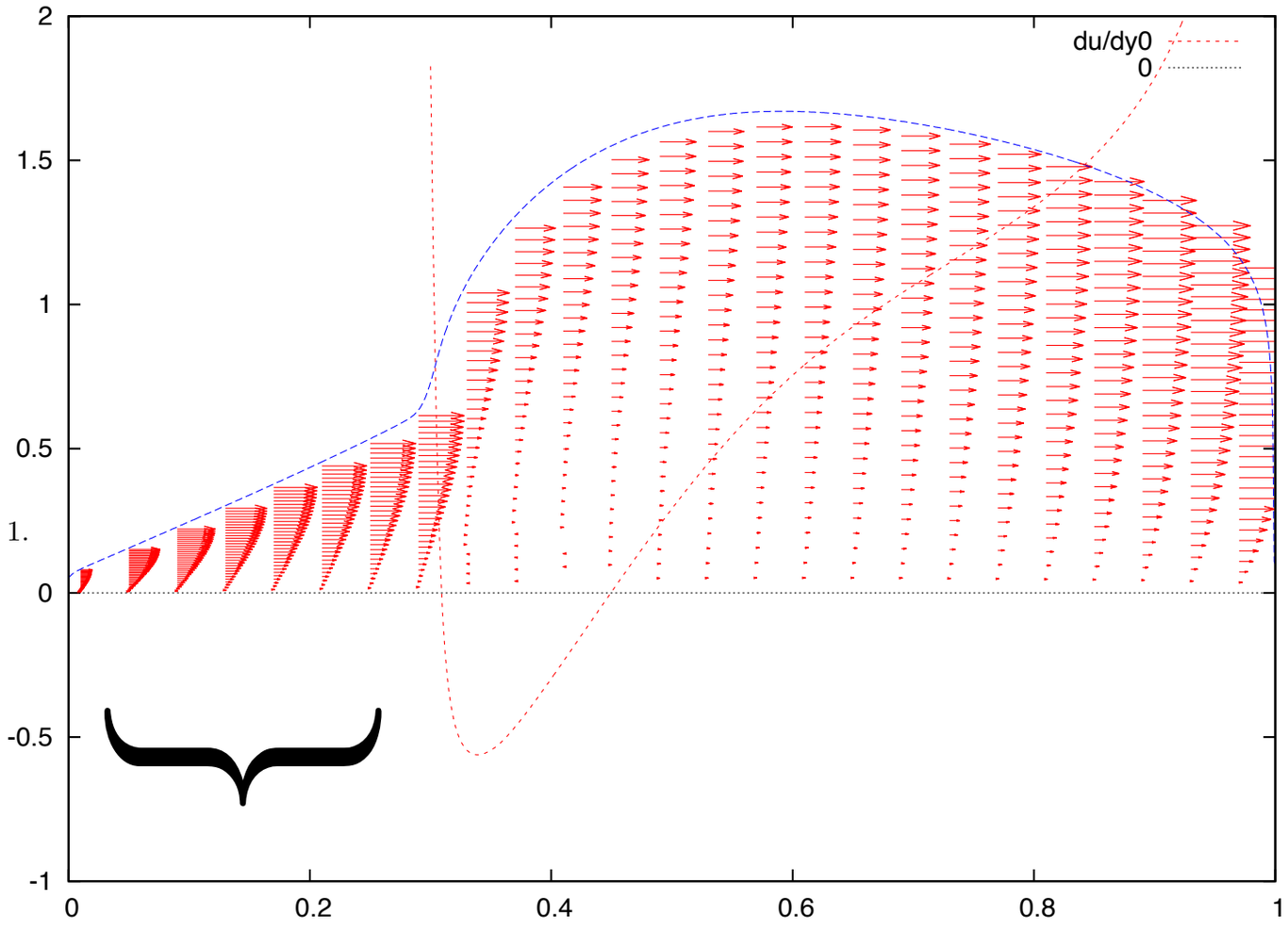

Watson regime

- newtonian: 2D hydraulic jump (Higuera 94)

De Vita et al. EJFM 2020

$$\frac{\partial \tilde{u}}{\partial \tilde{x}} + \frac{\partial \tilde{w}}{\partial \tilde{z}} = 0, \qquad 0 = -\frac{\partial \tilde{h}}{\partial \tilde{x}} + \frac{\partial^2 \tilde{u}}{\partial \tilde{z}^2} \text{ given } \int_0^{\tilde{h}} \tilde{u} d\tilde{z} = \tilde{Q}.$$

$$S^{-1/2} = \tilde{Q}^{5/2}$$

no inertia, viscous solution with pressure gradient

$$\tilde{u} = -\tilde{h}^2 \frac{\partial \tilde{h}}{\partial \tilde{x}} \frac{(\tilde{y})}{2\tilde{h}} (2 - \frac{(\tilde{y})}{\tilde{h}}), \quad \tilde{Q} = -\frac{\tilde{h}^3}{3} \frac{\partial \tilde{h}}{\partial \tilde{x}}$$

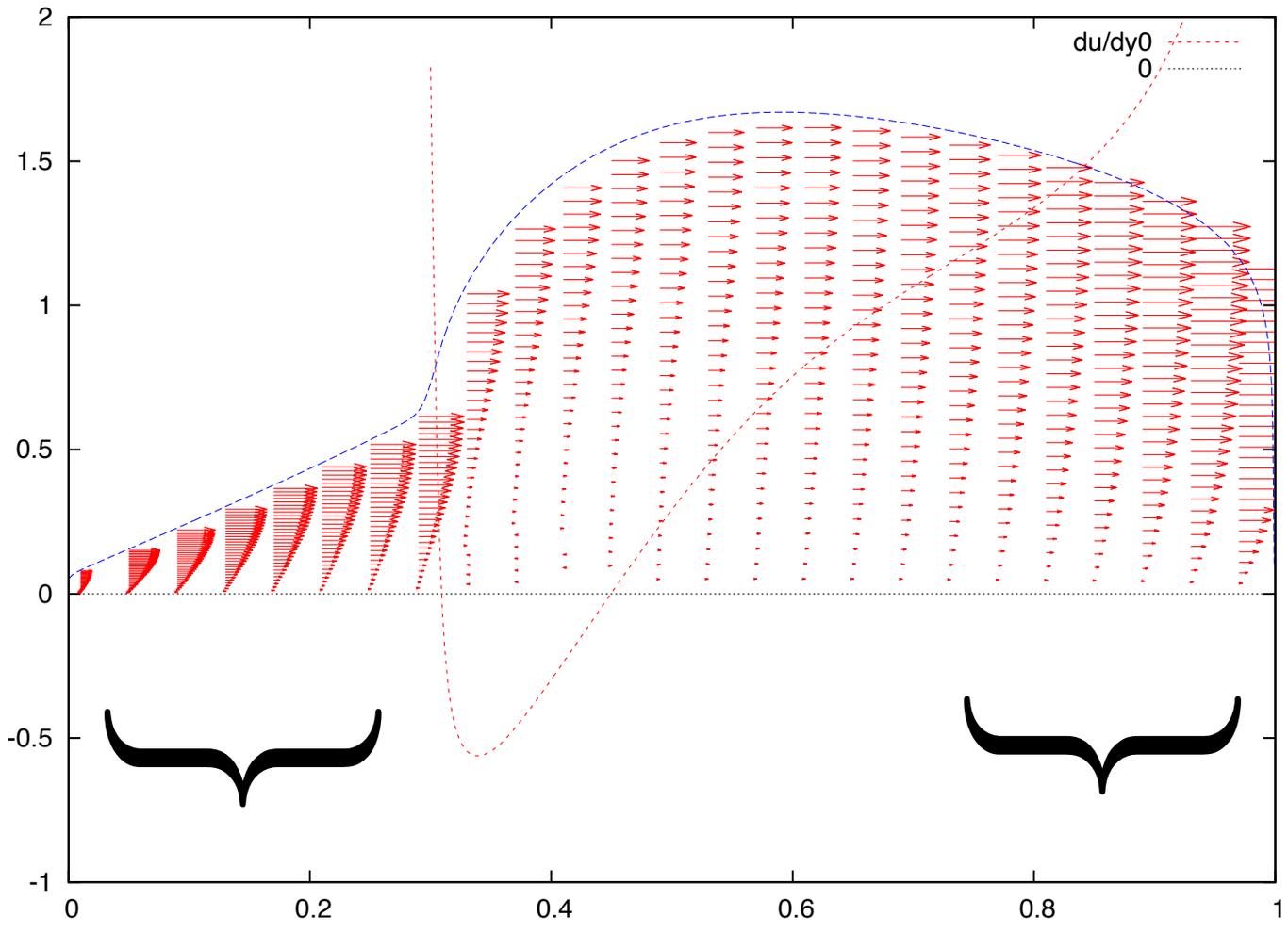

Watson regime **almost Poiseuille regime**

- newtonian: 2D hydraulic jump (Higuera 94)

De Vita et al. EJFM 2020

$$\frac{\partial \tilde{u}}{\partial \tilde{x}} + \frac{\partial \tilde{w}}{\partial \tilde{z}} = 0, \ \frac{\partial \tilde{u}}{\partial \tilde{t}} + \frac{\partial \tilde{u}^2}{\partial \tilde{x}} + \frac{\partial \tilde{u}\tilde{w}}{\partial \tilde{z}} = -\frac{\partial \tilde{h}}{\partial \tilde{x}} + \frac{\partial^2 \tilde{u}}{\partial \tilde{z}^2} \text{ given } \int_0^{\tilde{h}} \tilde{u} d\tilde{z} = \tilde{Q}.$$

$$S^{-1/2} = \tilde{Q}^{5/2}$$

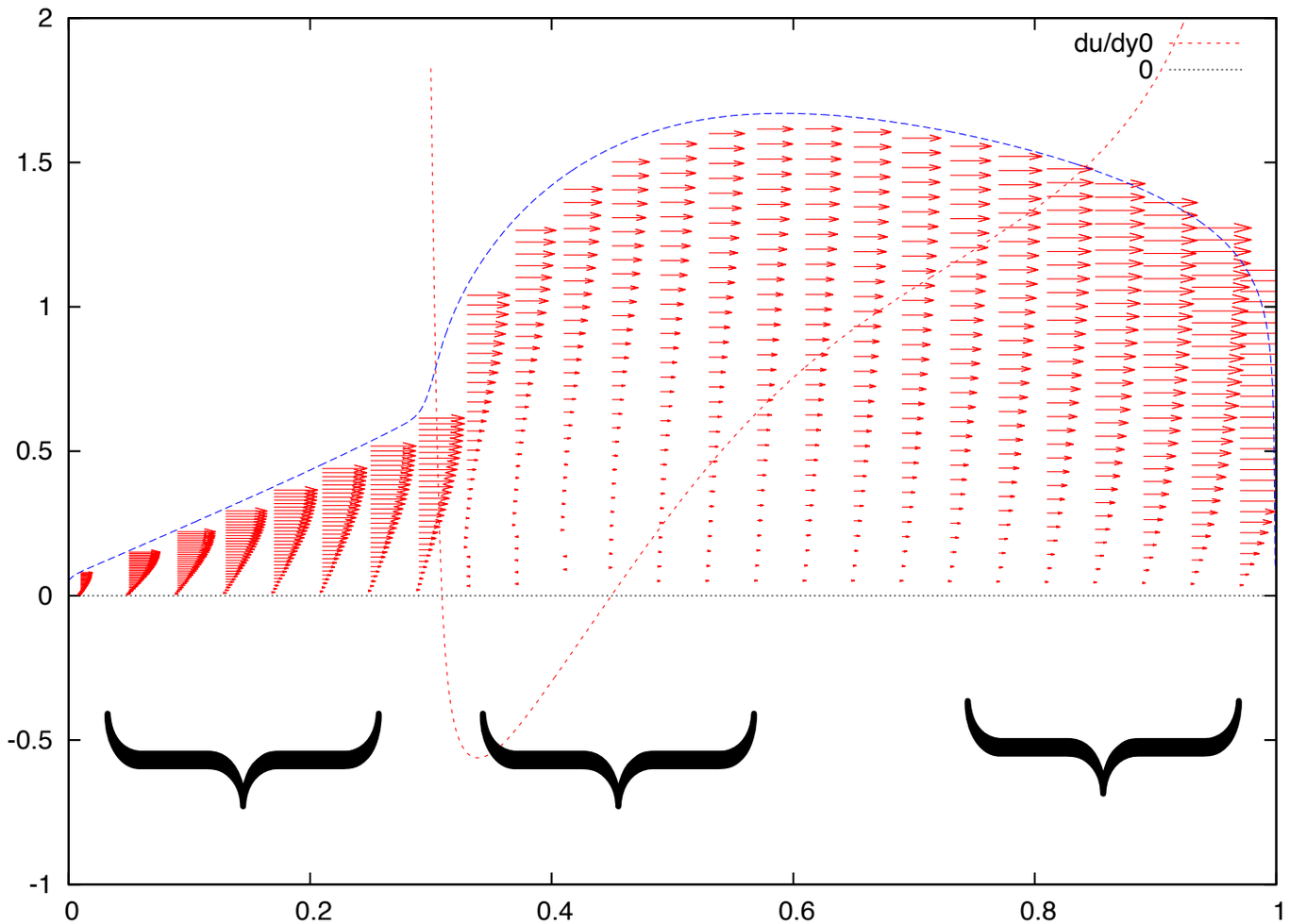

Watson regime **almost Poiseuille regime**

jump and separation

- newtonian: 2D hydraulic jump (Higuera 94)

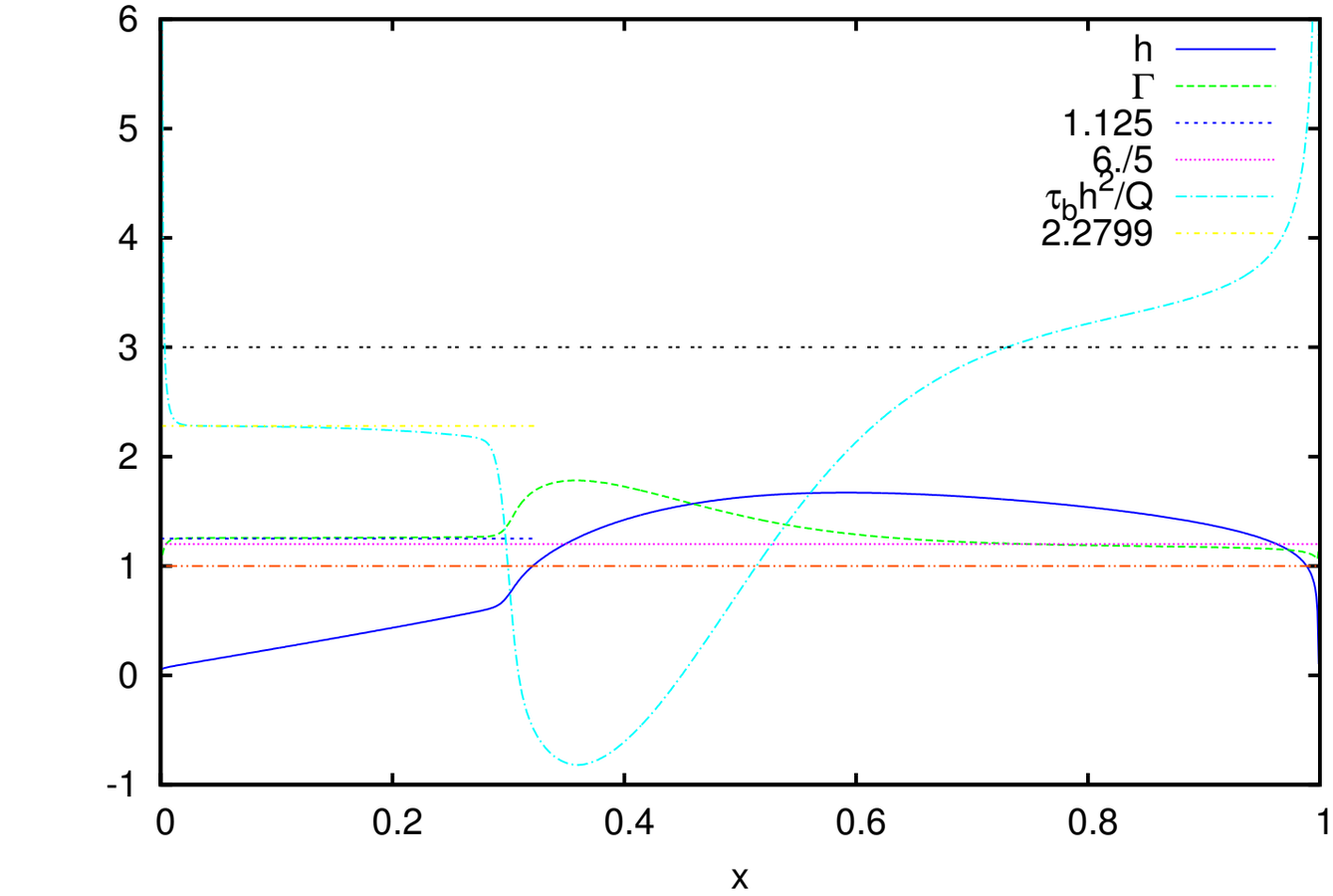

Watson & Poiseuille

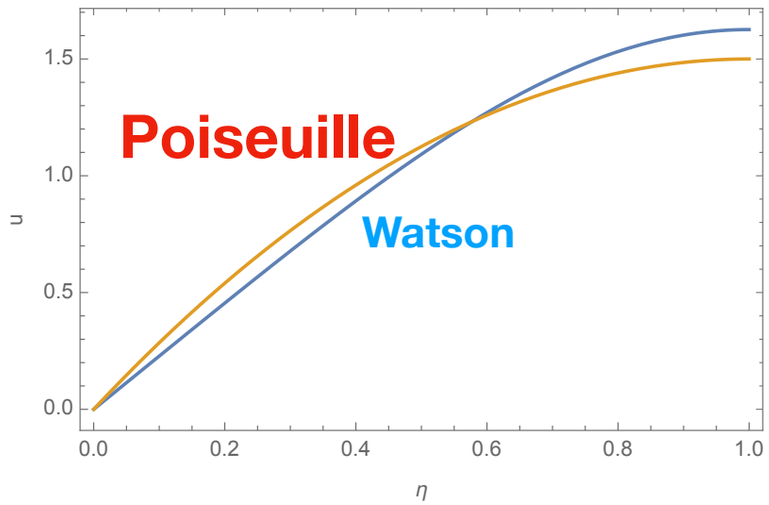

From the numerics we check the values of coefficients

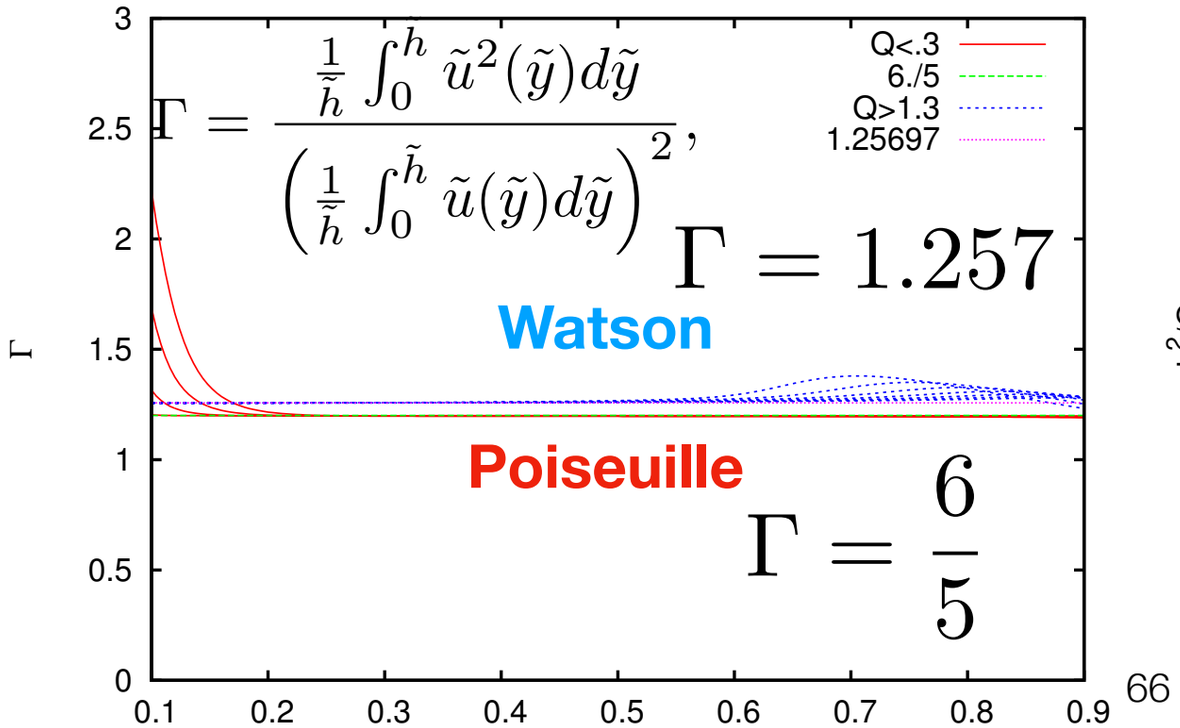

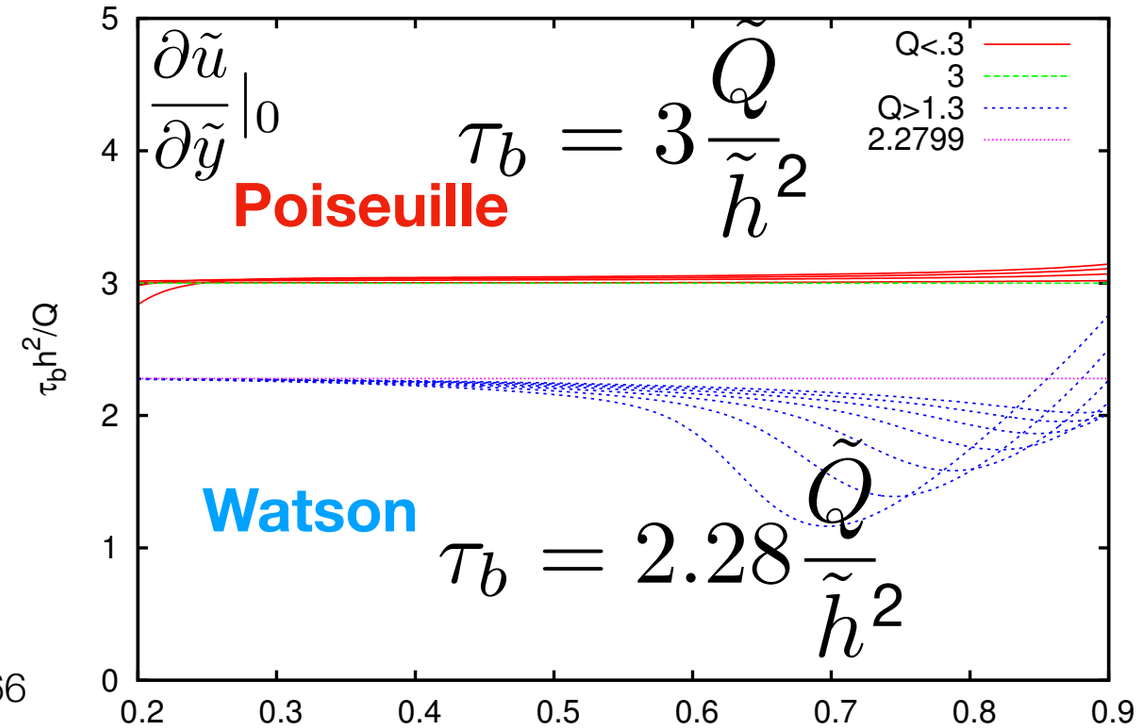

- newtonian: 2D hydraulic jump (Higuera 94)

come back to Shallow Water, note that $\Gamma = 1$ is mandatory

compare full resolution to Shallow Water with two closures for τ_b Watson & Poiseuille

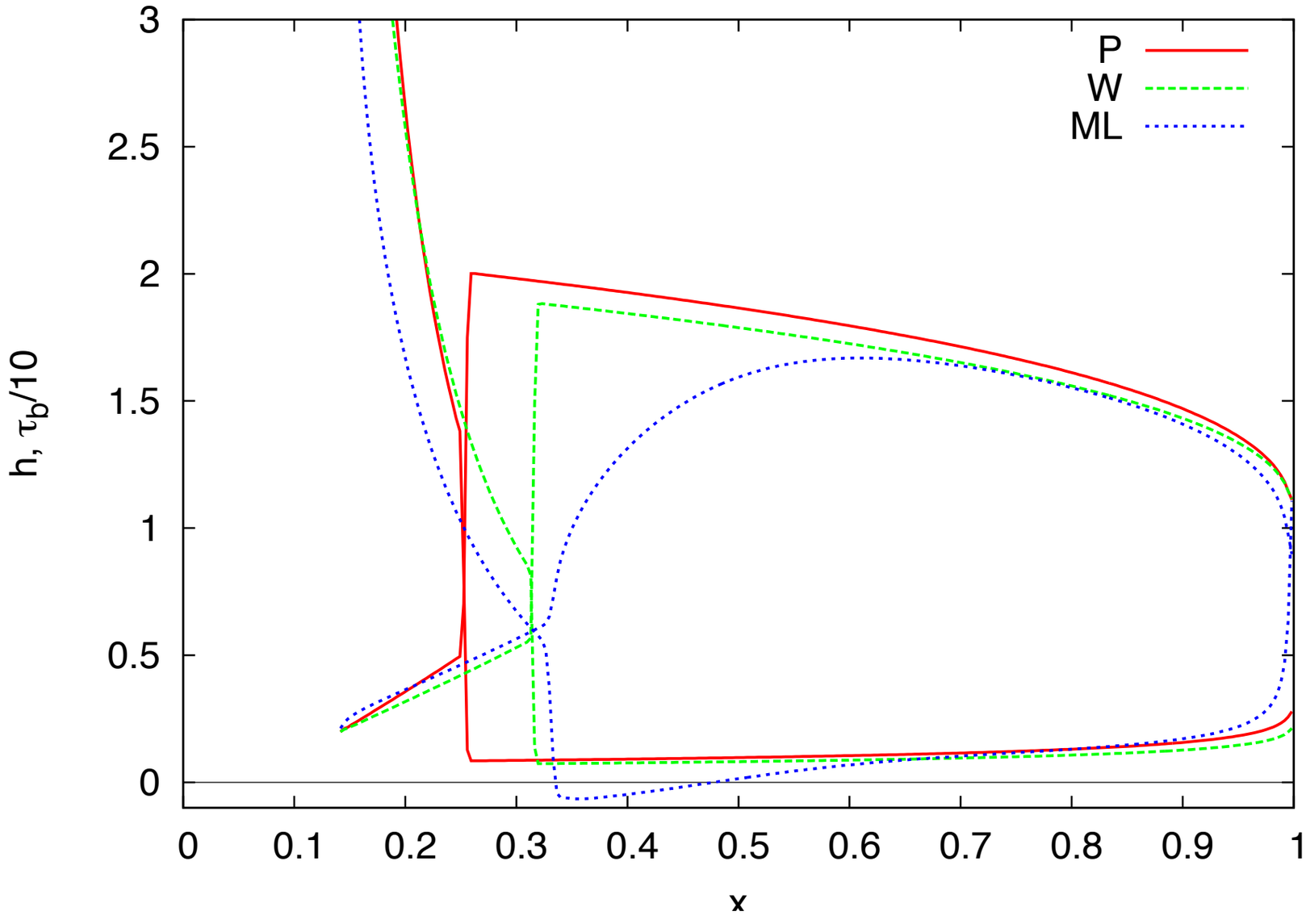

$$\frac{\partial \tilde{h}}{\partial \tilde{t}} + \frac{\partial \tilde{Q}}{\partial \tilde{x}} = 0$$

$$\frac{\partial \tilde{Q}}{\partial \tilde{t}} + \frac{\partial}{\partial \tilde{x}}\left(\Gamma \frac{\tilde{Q}^2}{\tilde{h}} + \frac{\tilde{h}^2}{2}\right) = -\tilde{\tau}_b$$

$$\Gamma = 1$$

$$\tau_b = 3\frac{\tilde{Q}}{\tilde{h}^2}$$

$$\tau_b = 2.28\frac{\tilde{Q}}{\tilde{h}^2}$$

Testing the Multilayer Resolution of Prandtl

- newtonian: lubrication case (Huppert 82,82)
- newtonian: hydraulic jump (Higuera 94)
- non newtonian: Bingham Collapse (Balmforth…)
- newtonian: Arteries
- non newtonian: granular μ(I) avalanches

- non newtonian: Bingham Collapse (Balmforth…)

lubrication

$$\tau = B + \frac{\partial u}{\partial y}$$

$$\frac{\partial h}{\partial t} + \frac{\partial}{\partial x}[\frac{Uh}{3}(3 - \frac{Y}{h})] = 0$$

$$U = \frac{1}{\mu}(S - \frac{\partial h}{\partial x})\frac{Y^2}{2}$$

$$Y = max(h - \frac{B}{|S - \frac{\partial h}{\partial x}|}, 0)$$

S slope, B Bingham number , Y yield height

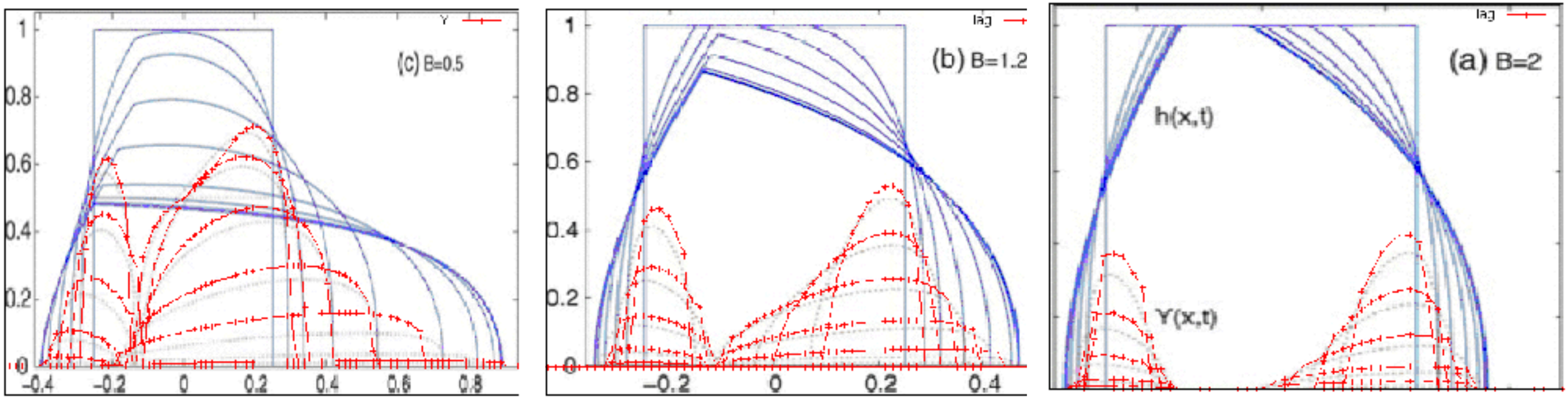

- N. Balmforth, R. Craster, A. Rust, R. Sassi [“Viscoplastic flow over an inclined surface”](), J. Non-Newtonian Fluid Mech. 139 (2006) 103–127

- non newtonian: Bingham Collapse (Balmforth…)

Bingham compare 2D RNSP 1D

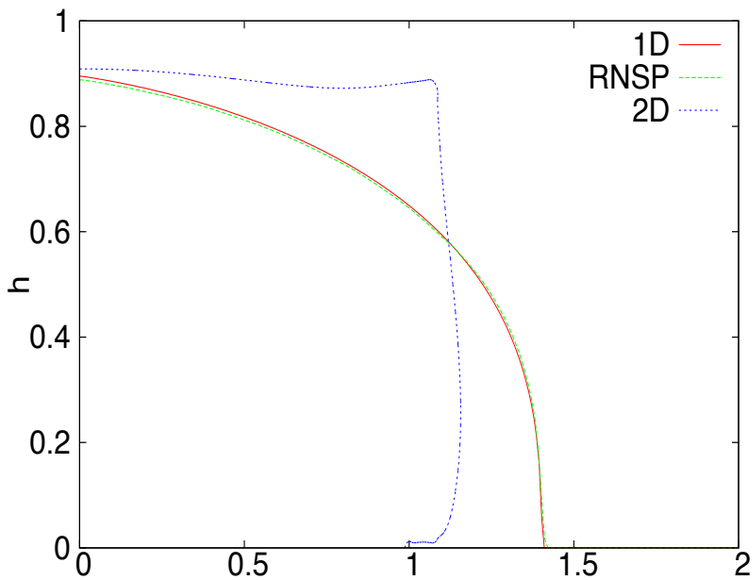

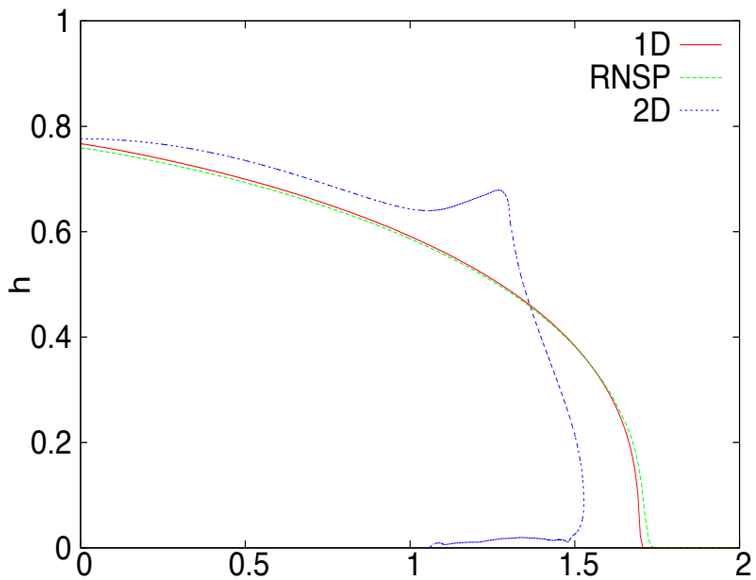

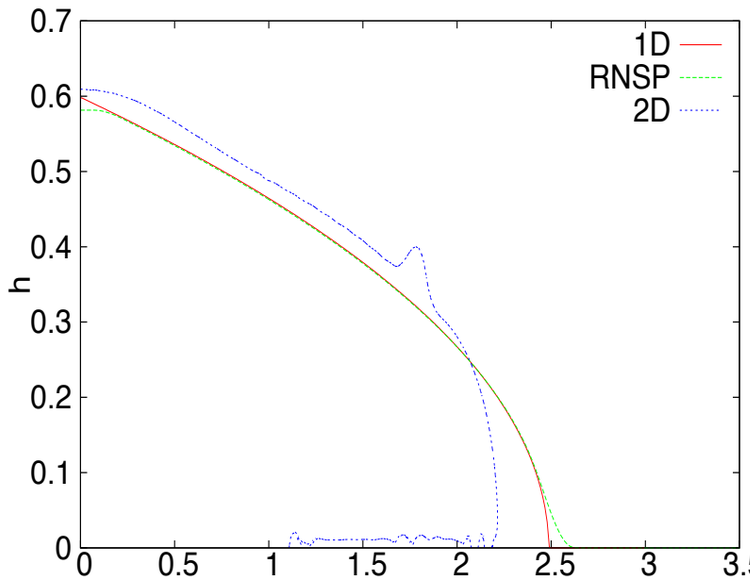

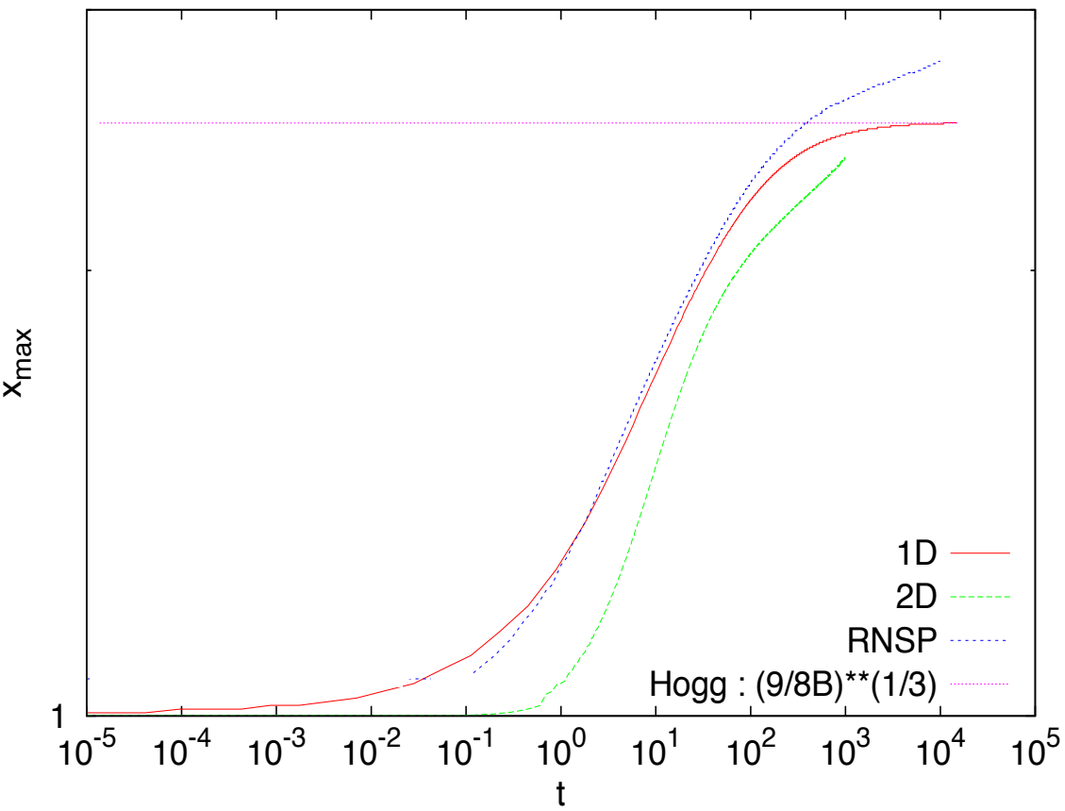

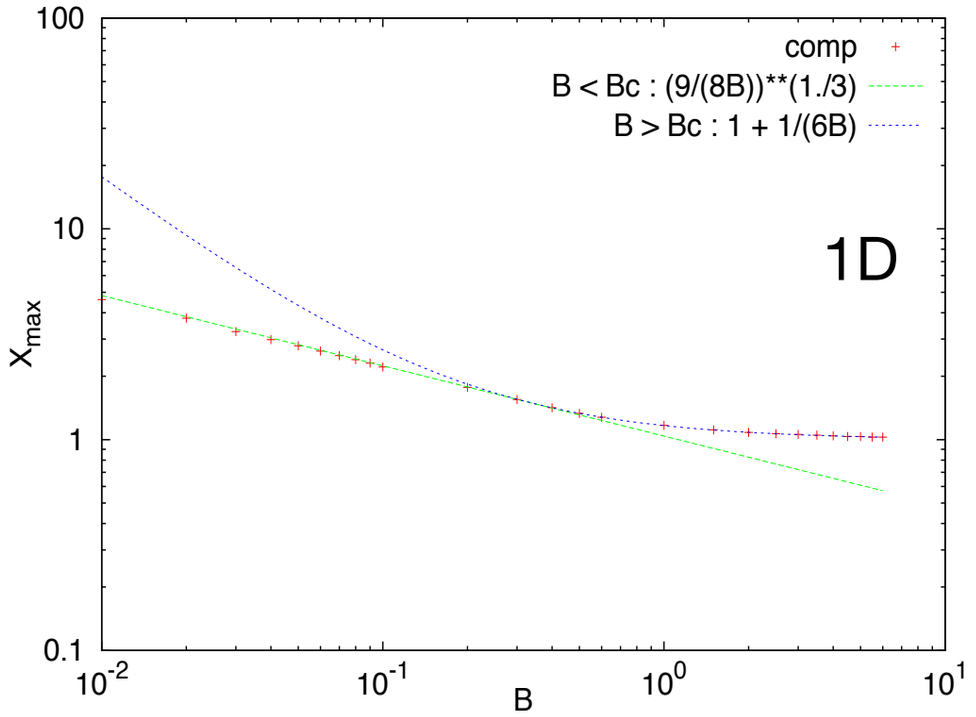

Hogg & Matson JNFM 2009

Testing the Multilayer Resolution of Prandtl

- newtonian: lubrication case (Huppert 82,82)
- newtonian: hydraulic jump (Higuera 94)
- non newtonian: Bingham Collapse (Balmforth…)
- newtonian: Arteries
- non newtonian: granular μ(I) avalanches

- newtonian: Arteries

multilayer -> multiring !

Ghigo et al. JCP 2017

$$\frac{1}{r}\frac{\partial}{\partial r}\left[ru_r\right] + \frac{\partial u_x}{\partial x} = 0$$

$$\frac{\partial u_x}{\partial t} + u_r\frac{\partial u_x}{\partial r} + u_x\frac{\partial u_x}{\partial x} = -\frac{1}{\rho}\frac{\partial p}{\partial x} + \frac{\nu}{r}\frac{\partial}{\partial r}\left[r\frac{\partial u_x}{\partial r}\right]$$

$$p\left(x,t\right) - p_0 = K(R(x,t) - R_0)$$

shear stress in a aneurism

shear stress in a stenosis

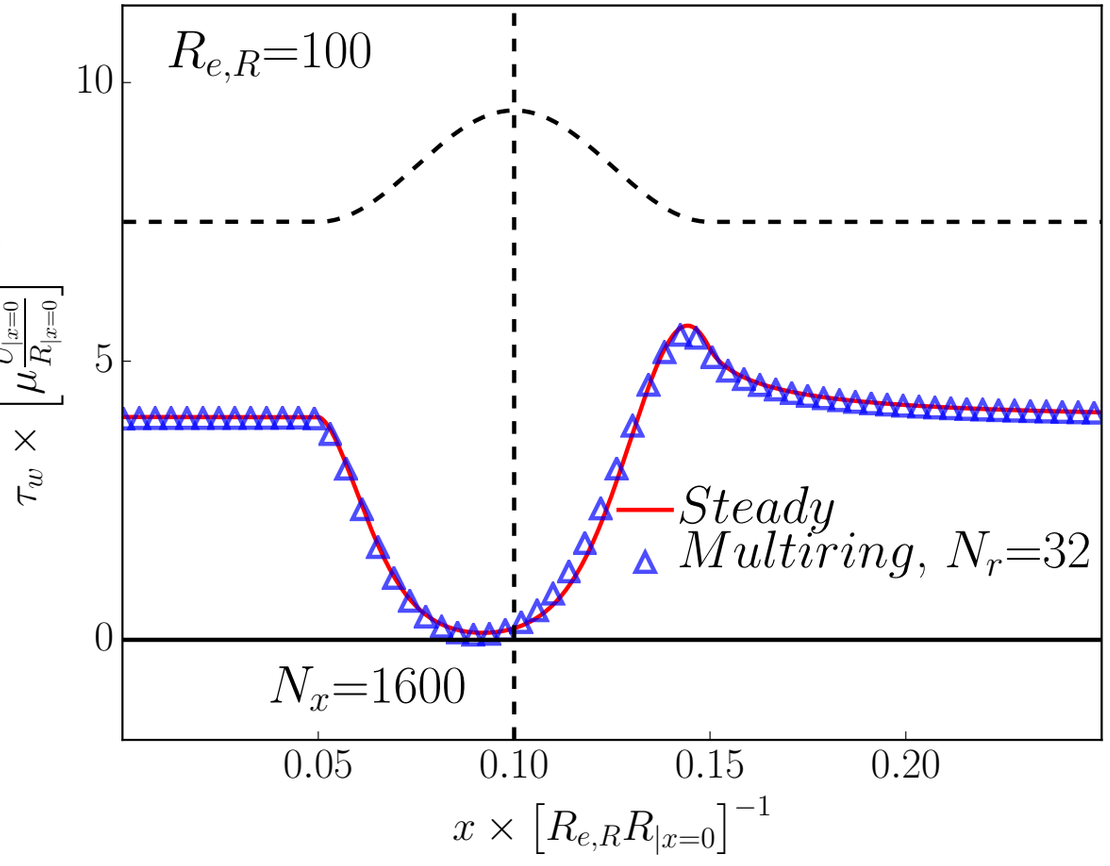

$K = 10^7$

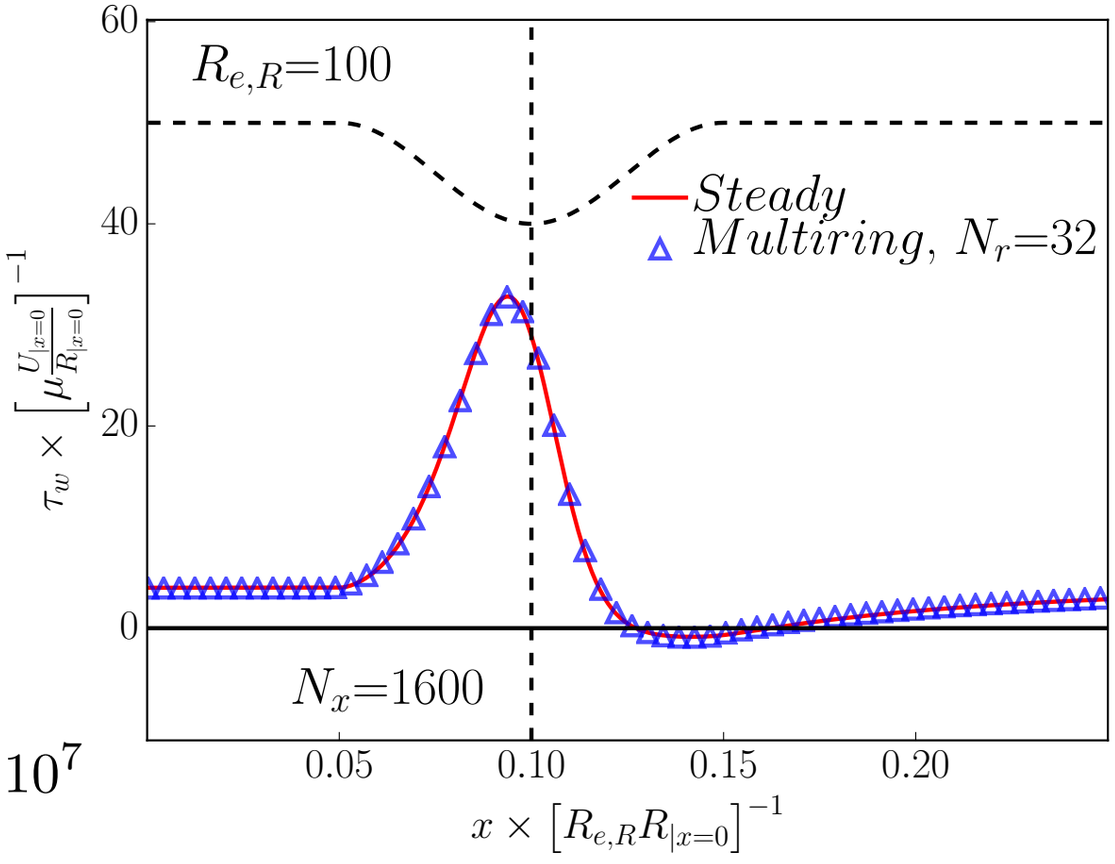

Steady wall shear stress (WSS)

- newtonian: Arteries

multilayer -> multiring !

Ghigo et al. JCP 2017

$$\frac{1}{r}\frac{\partial}{\partial r}\left[ru_r\right] + \frac{\partial u_x}{\partial x} = 0$$

$$\frac{\partial u_x}{\partial t} + u_r\frac{\partial u_x}{\partial r} + u_x\frac{\partial u_x}{\partial x} = -\frac{1}{\rho}\frac{\partial p}{\partial x} + \frac{\nu}{r}\frac{\partial}{\partial r}\left[r\frac{\partial u_x}{\partial r}\right]$$

$$p\left(x,t\right) - p_0 = K(R(x,t) - R_0)$$

shear stress in a aneurism

shear stress in a stenosis

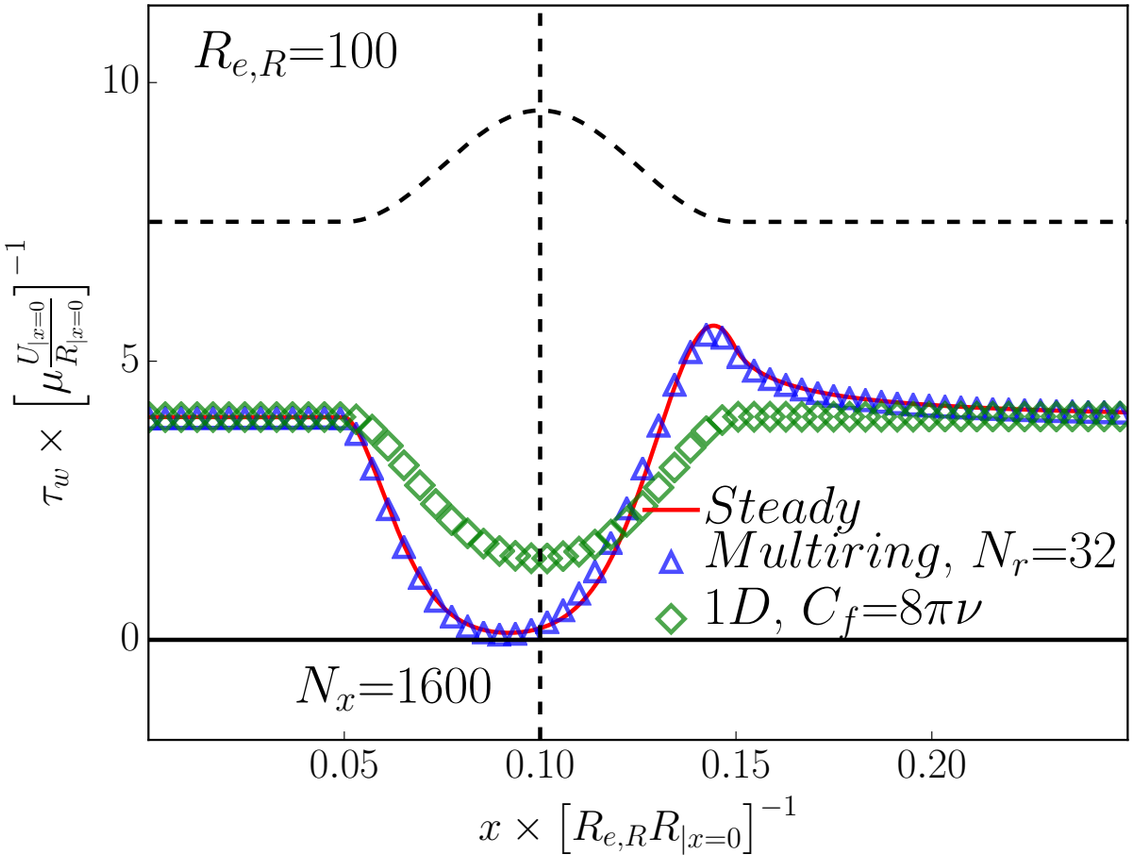

$K = 10^7$

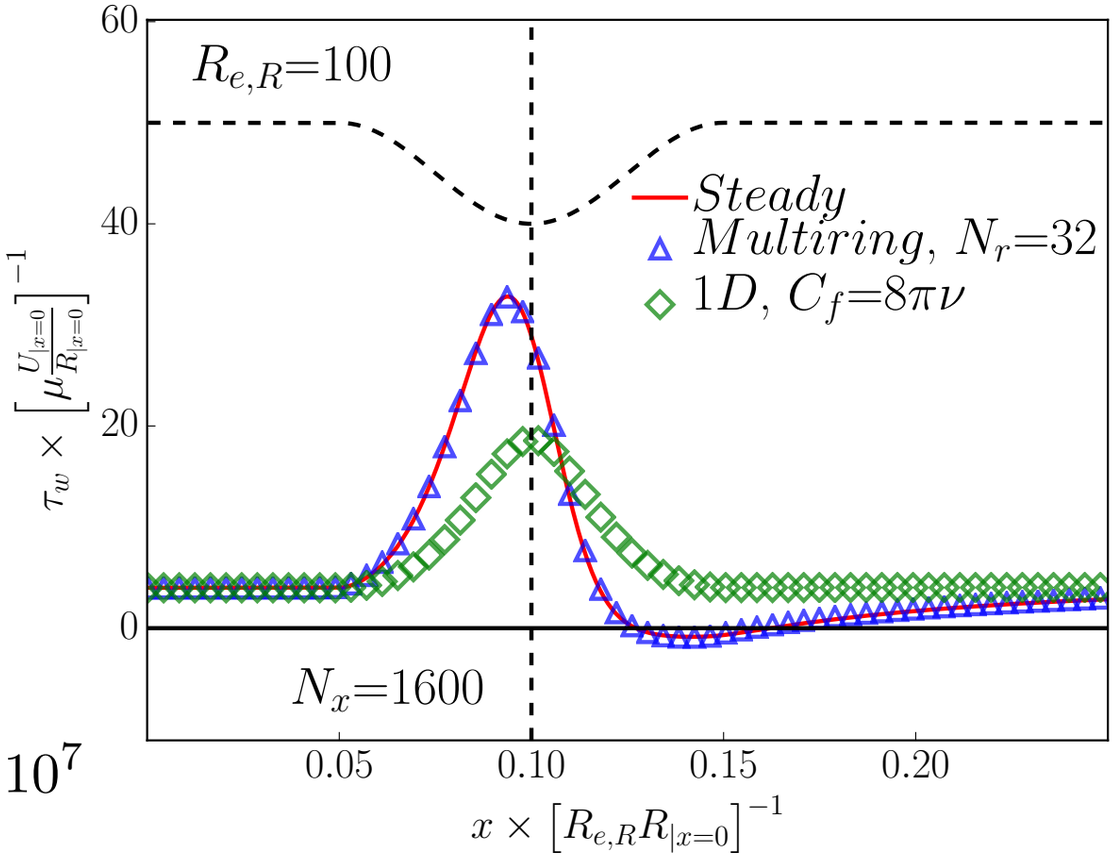

Steady wall shear stress (WSS)

- newtonian: Arteries

multilayer -> multiring !

Ghigo et al. JCP 2017

$$\frac{1}{r}\frac{\partial}{\partial r}\left[ru_r\right] + \frac{\partial u_x}{\partial x} = 0$$

$$\frac{\partial u_x}{\partial t} + u_r\frac{\partial u_x}{\partial r} + u_x\frac{\partial u_x}{\partial x} = -\frac{1}{\rho}\frac{\partial p}{\partial x} + \frac{\nu}{r}\frac{\partial}{\partial r}\left[r\frac{\partial u_x}{\partial r}\right]$$

$$p\,(x,t)\, - p_0 = K(R(x,t) - R_0)$$

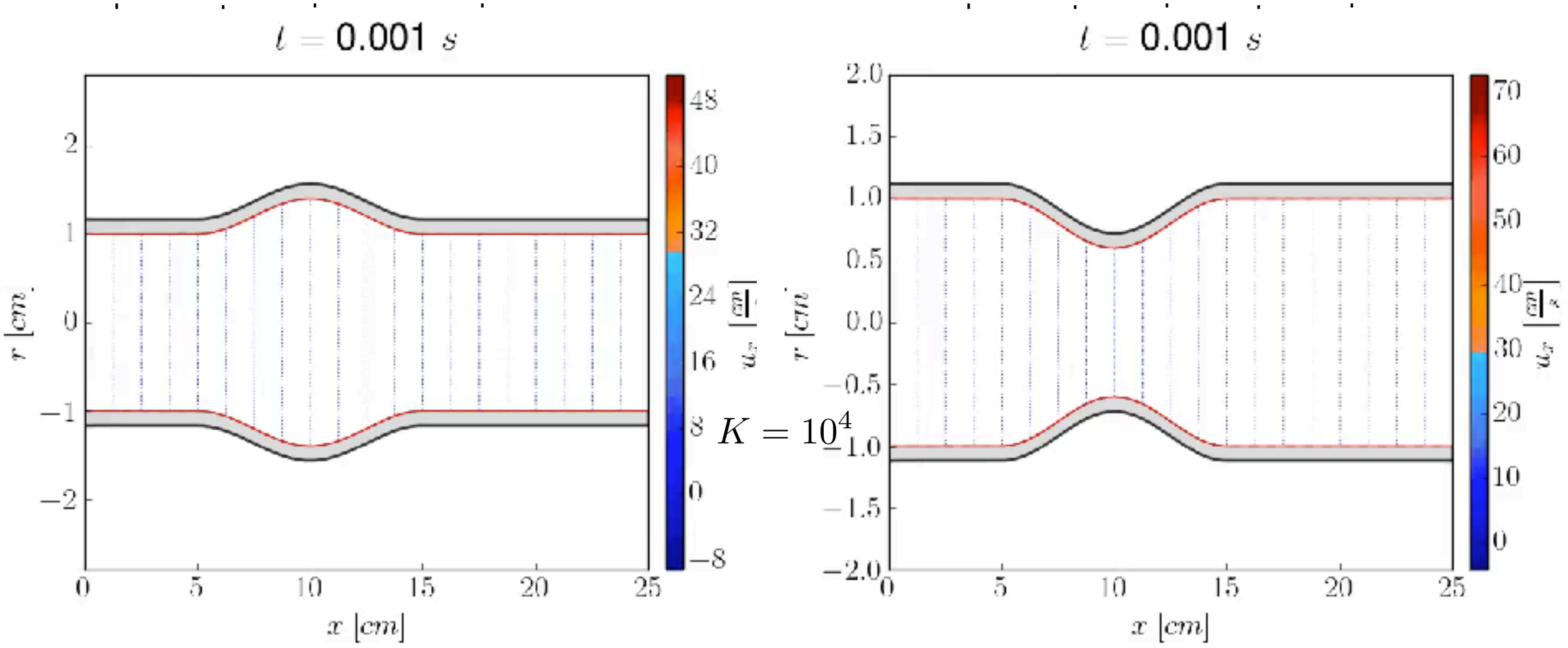

Unsteady wall shear stress (WSS)

Testing the Multilayer Resolution of Prandtl

- newtonian: lubrication case (Huppert 82,82)
- newtonian: hydraulic jump (Higuera 94)
- non newtonian: Bingham Collapse (Balmforth…)
- newtonian: Arteries
- non newtonian: granular μ(I) avalanches

Front in Savage Hutter St Venant

Experimental set up:
Pouliquen 99 & 99

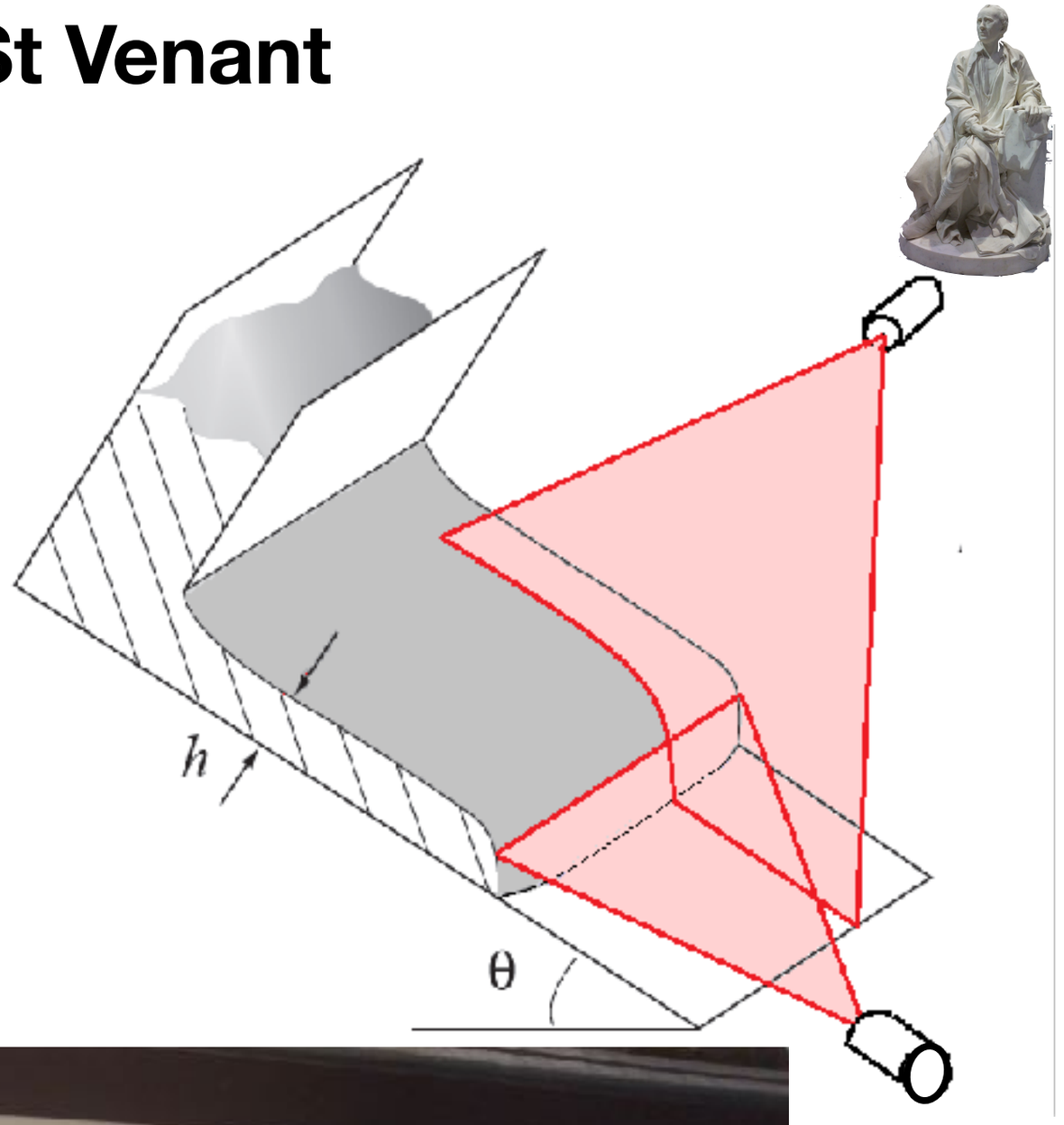

With Stéphanie Deboeuf and Guillaume Saingier

Front in Savage Hutter St Venant

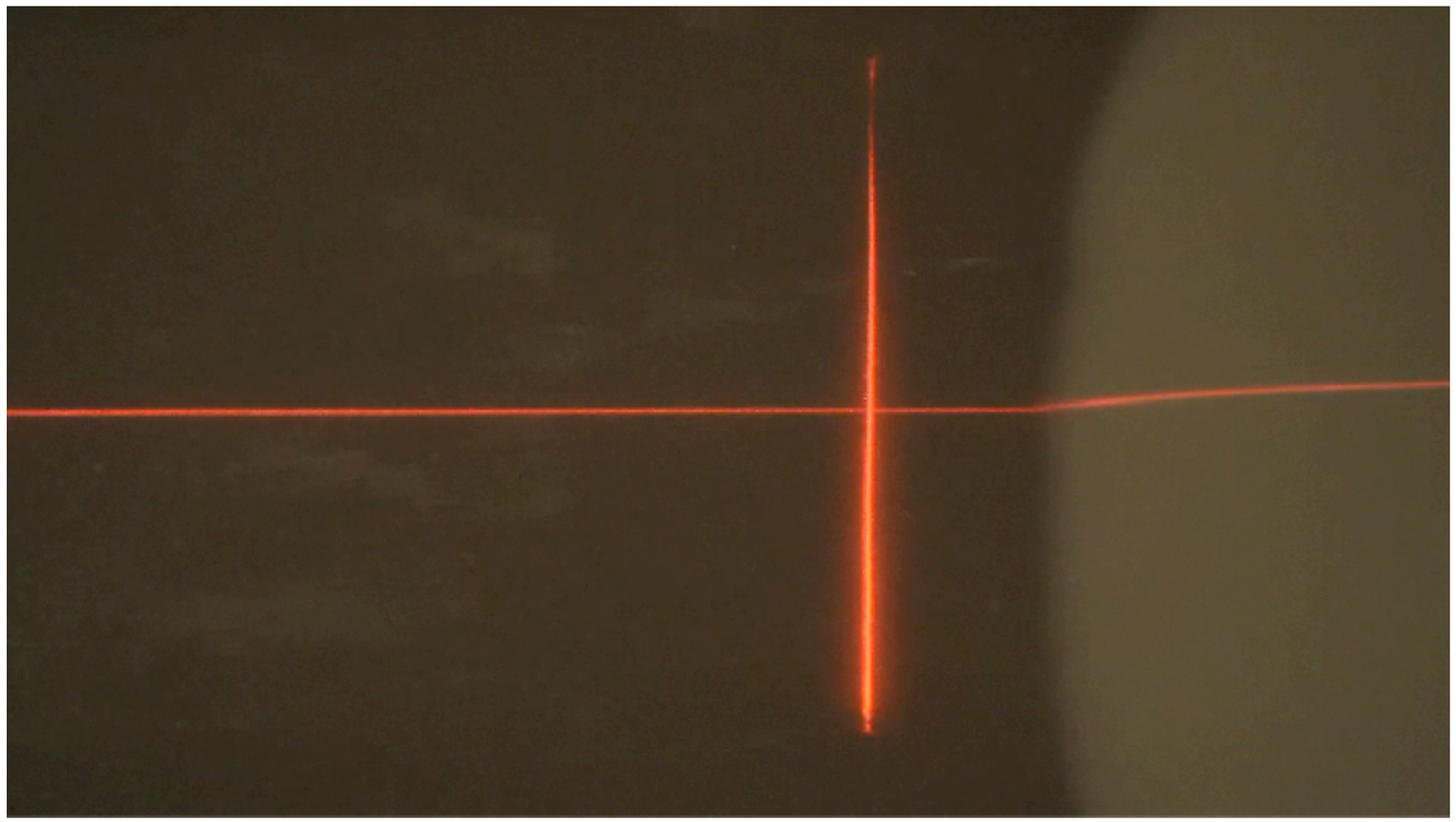

glass bead 400μm

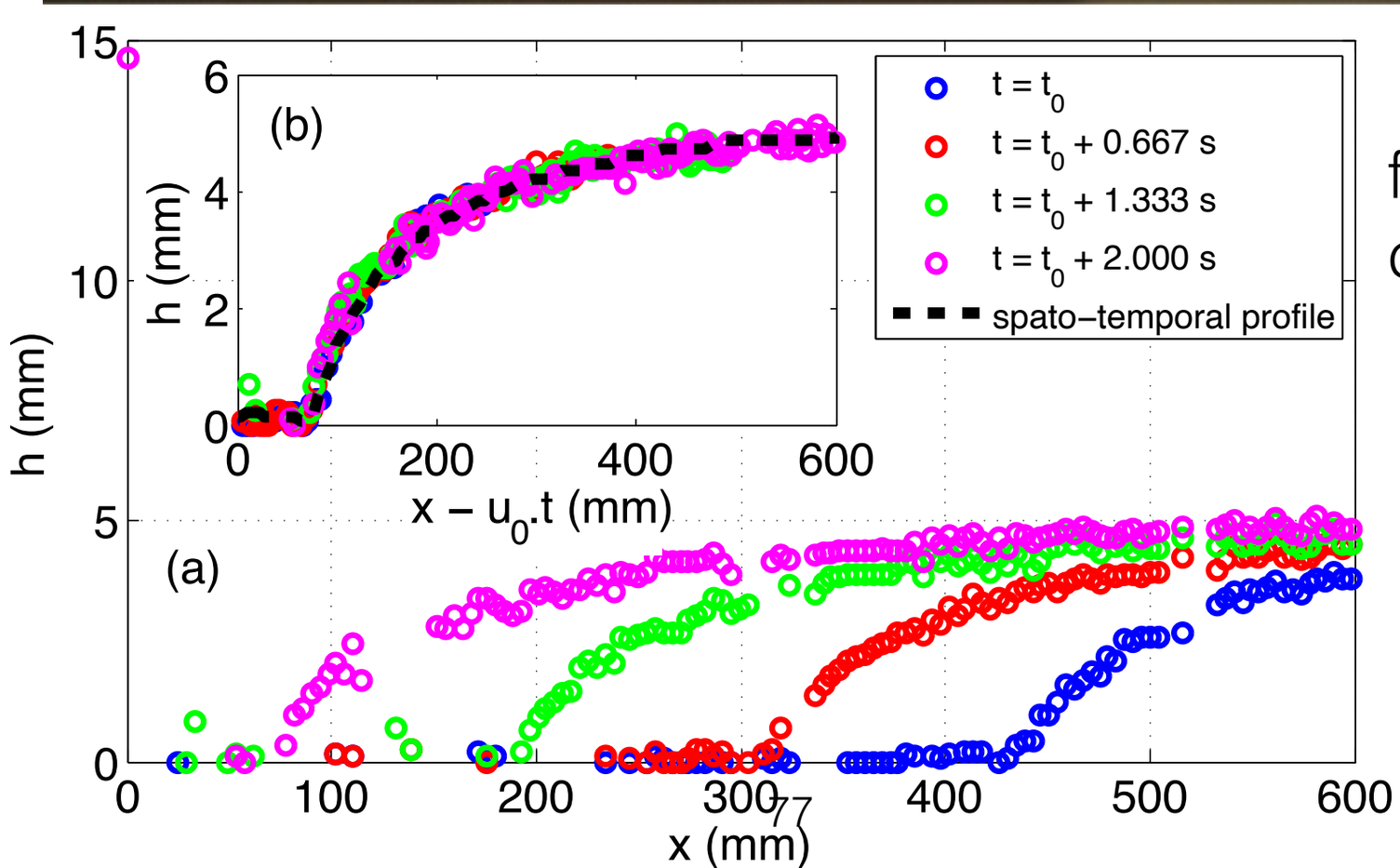

front moving at constant velocity u_0

Front in Savage Hutter St Venant

$$\frac{\partial u}{\partial x} + \frac{\partial v}{\partial y} = 0$$

$$\frac{\partial u}{\partial t} + \frac{\partial u^2}{\partial x} + \frac{\partial uv}{\partial y} = -g\tan\theta - \frac{\partial p}{\rho\partial x} + \frac{\partial \tau}{\partial y}$$

$$0 = -\frac{\partial p}{\rho\partial y} - g$$

usual full system before averaging

use GDR MiDi/ Jop et al. mu(I) rheology $\tau = \mu(I)p$

averaging : "Savage Hutter" lithostatic equations $\tau = \mu(I)(\rho g h)$

$$\frac{\partial h}{\partial t} + \frac{\partial hu}{\partial x} = 0$$

$$\frac{\partial hu}{\partial t} + \Gamma\frac{\partial}{\partial x}hu^2 = gh(\tan\theta - \frac{\partial h}{\partial x} - \mu(I))$$

Closure (here use Bagnold profile), if flat profile Γ=1, if half Poiseuille Γ=6/5

$$\Gamma = \frac{\frac{1}{h}\int_0^h u^2 dy}{\left(\frac{1}{h}\int_0^h u dy\right)^2} \quad \Gamma = \frac{5}{4} \quad I = \frac{5}{2}\frac{u d_g}{h\sqrt{gh}} \quad \mu(I) = \mu_0 + \frac{\Delta\mu}{I_0/I + 1}$$

Front in Savage Hutter St Venant

Saingier et al. PoF 2016

In a moving framework

$$\xi = x - u_0 t$$

$$((\Gamma-1)Fr^2\frac{h_\infty}{h}+1)\frac{dh}{d\xi} = \tan\theta - \mu(I).$$

analytical implicit solution: $X = \frac{\xi(\tan\theta-\mu_0)}{h_\infty}, \quad H = \frac{h}{h_\infty}, \quad d = \frac{\mu_0-\tan\theta}{\Delta\mu},$

$$X(H) = X_0 - \frac{1}{3(-1+d)}(3H(d-1) - 2\sqrt{3}\tan^{-1}(\frac{1+2\sqrt{H}}{\sqrt{3}}) - 2\log(1-\sqrt{H}) + 3d(1-\Gamma)Fr^2\log(H) + \log(1+\sqrt{H}+H) - 2(1-\Gamma)Fr^2\log(1-H^{3/2})),$$

superposed on Pouliquen 99 (who supposed $\Gamma = 1$)

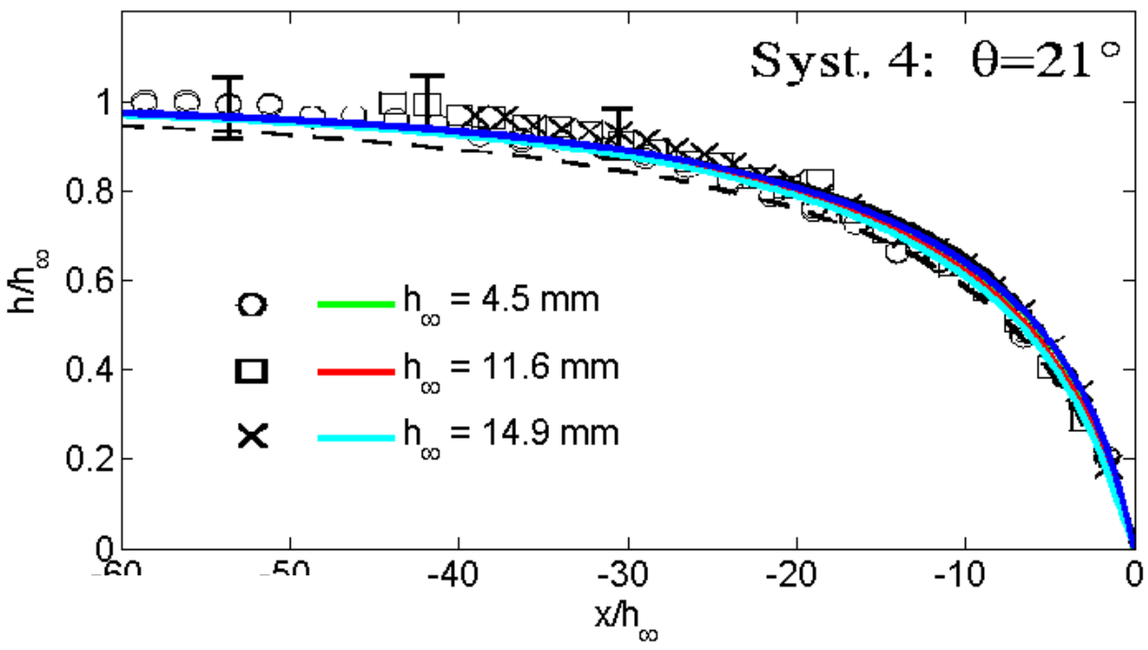

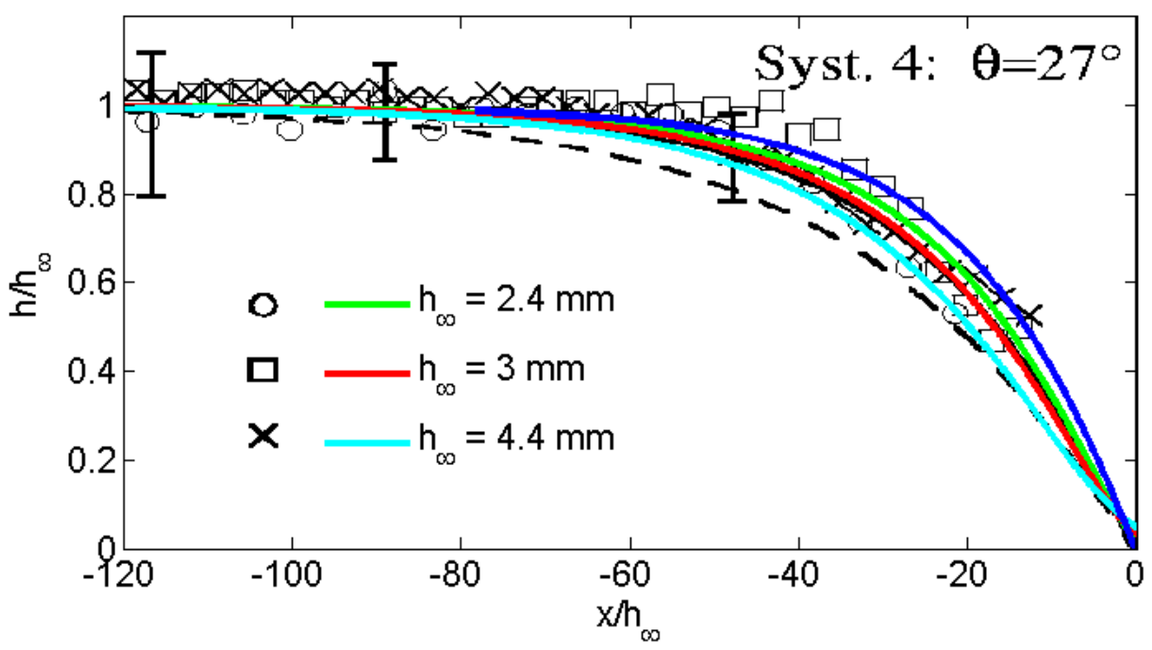

Front in Savage Hutter St Venant

with our inclined plane

$$((\Gamma - 1)Fr^2 \frac{h_\infty}{h} + 1)\frac{dh}{d\xi} = \tan\theta - \mu(I).$$

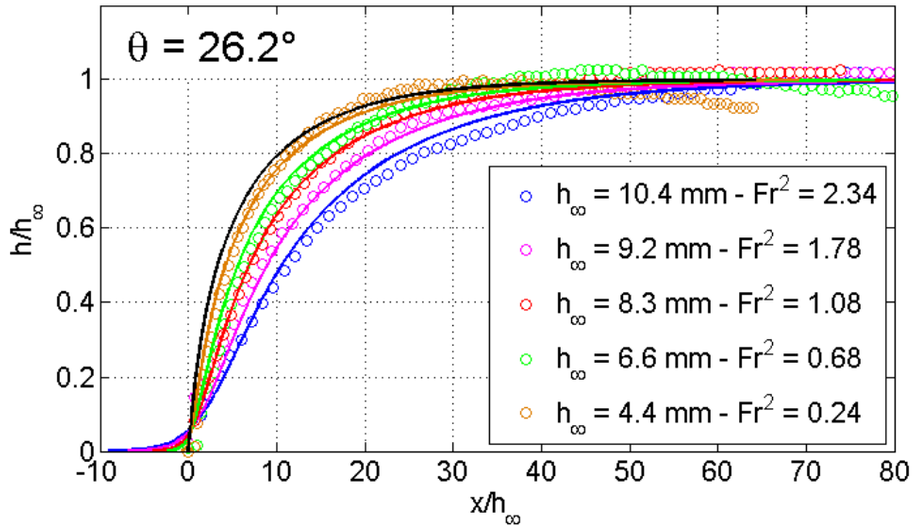

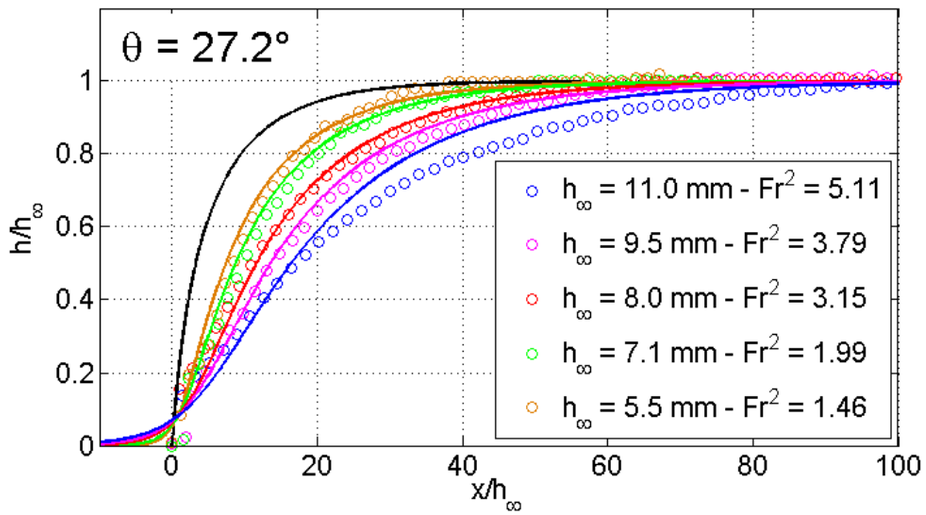

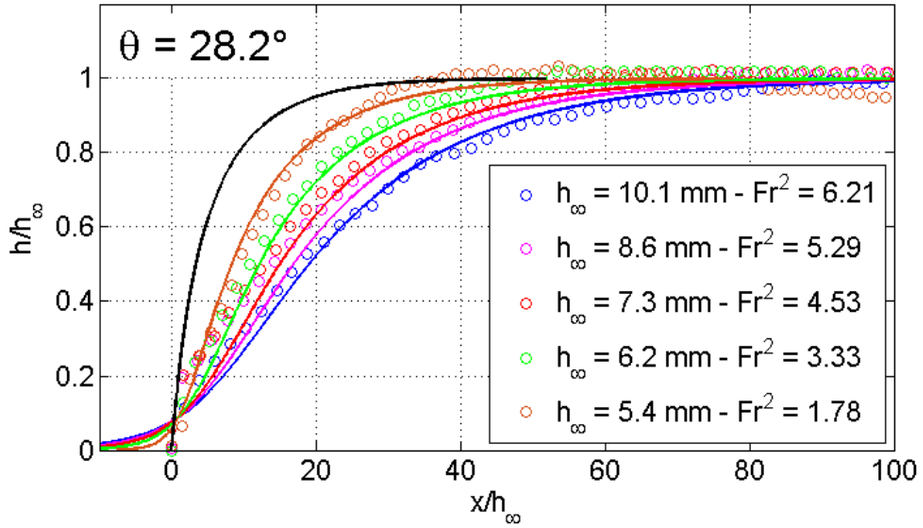

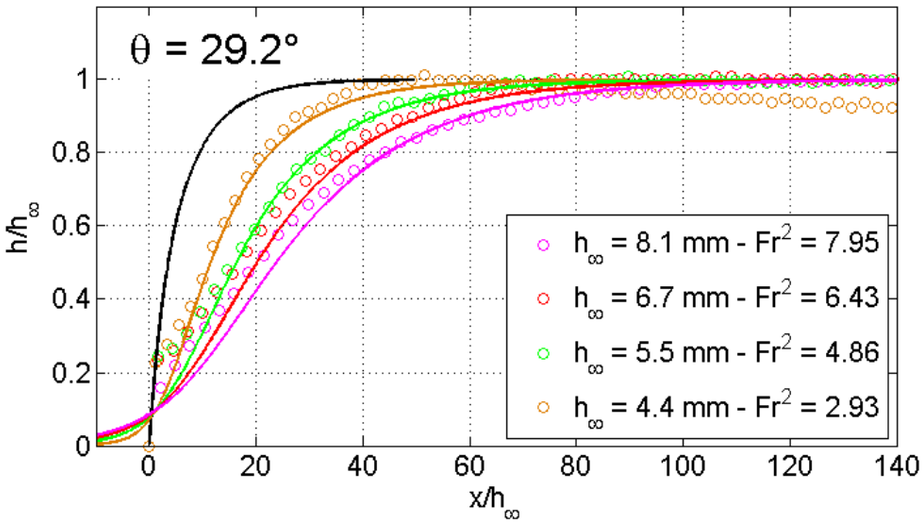

Rescaled granular profiles: comparison between experiments and analytical predictions for different inclinations and different thicknesses h_∞. Analytical solutions (colored lines) are calculated by using the thickness h_∞ and the front velocity u_0 measured for each experimental front (colored circles) with a shape factor $\mathbf{\Gamma} = 5/4$. The analytical solution evaluated for $\mathbf{\Gamma} = 1$ is plotted in black line.

importance of the up to now neglected inertial effects

Front in Savage Hutter St Venant

with our inclined plane

$$((\Gamma - 1)Fr^2 \frac{h_\infty}{h} + 1)\frac{dh}{d\xi} = \tan\theta - \mu(I).$$

unphysical exponential

precursor

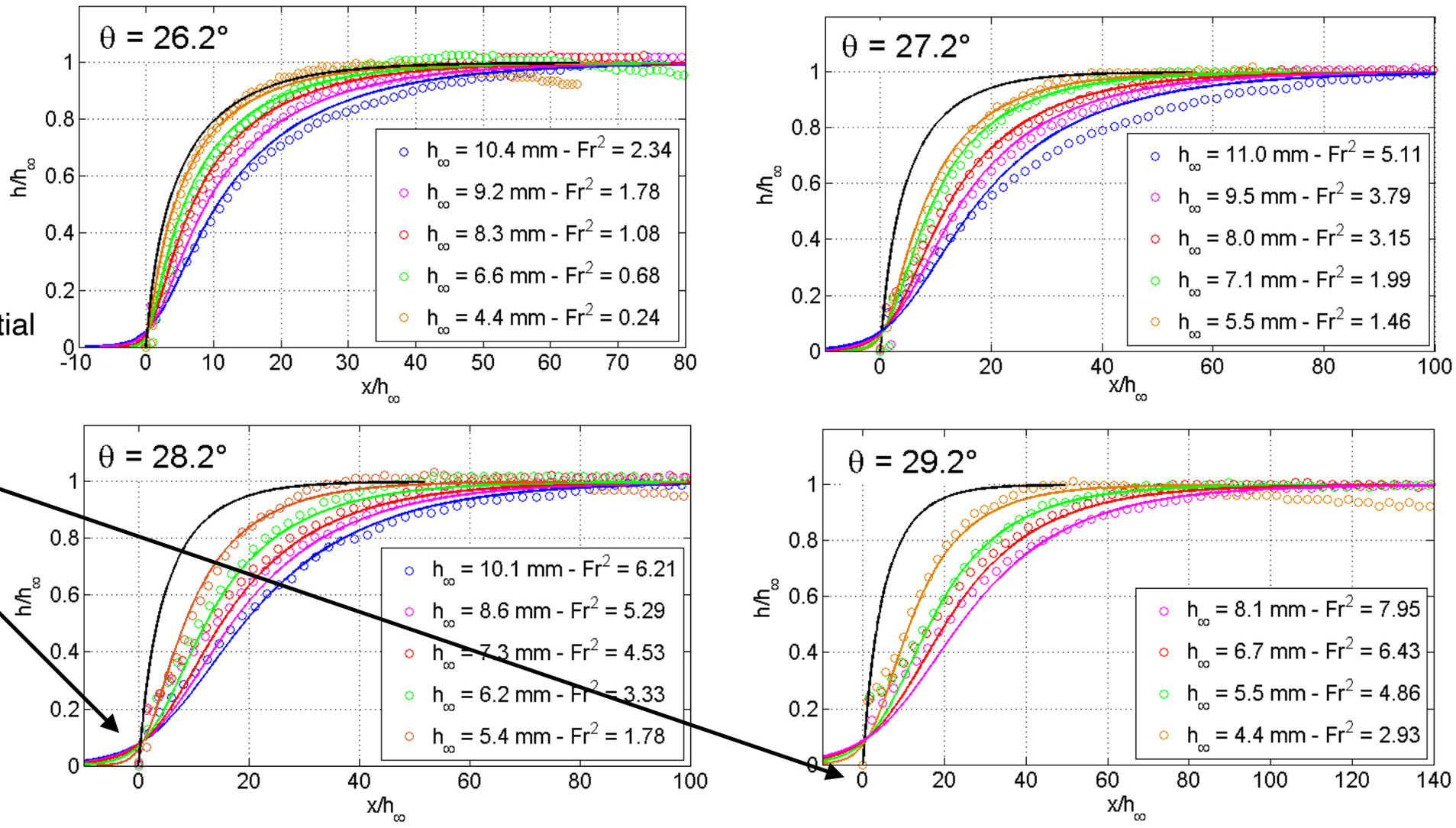

Figure 5: Rescaled granular profiles: comparison between experiments and analytical predictions for different inclinations and different thicknesses h_∞. Analytical solutions (colored lines) are calculated by using the thickness h_∞ and the front velocity u_0 measured for each experimental front (colored circles) with a shape factor $\mathbf{\Gamma} = 5/4$. The analytical solution evaluated for $\mathbf{\Gamma} = 1$ is plotted in black line.

importance of the up to now neglected inertial effects

Front in Savage Hutter St Venant

Lagrée et al. EPJ WoC 2017

$$\frac{\partial u}{\partial x}+\frac{\partial v}{\partial y}=0$$

$$\frac{\partial u}{\partial t}+\frac{\partial u^2}{\partial x}+\frac{\partial uv}{\partial y}=-g\tan\theta-\frac{\partial p}{\rho\partial x}+\frac{\partial \tau}{\partial y}$$

$$0=-\frac{\partial p}{\rho\partial y}-g$$

numerical resolution of the

full system before averaging

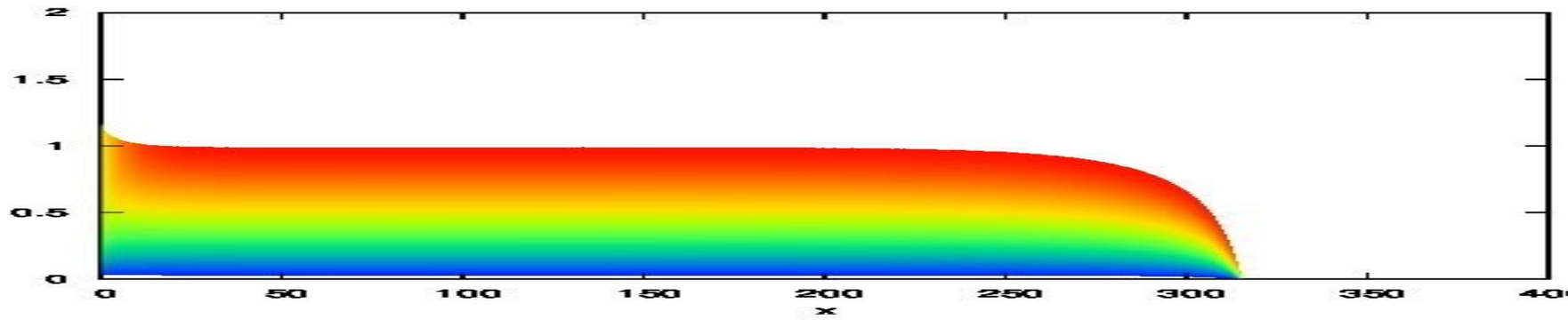

numerical multilayer resolution

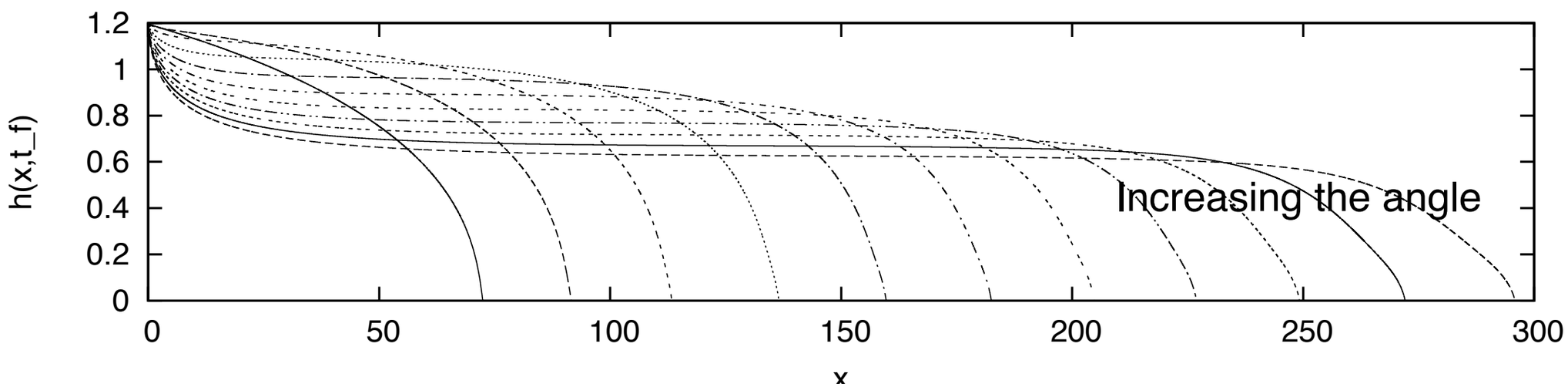

Front in Savage Hutter St Venant

Lagrée et al. EPJ WoC 2017

$$\frac{\partial u}{\partial x}+\frac{\partial v}{\partial y}=0$$

$$\frac{\partial u}{\partial t}+\frac{\partial u^2}{\partial x}+\frac{\partial uv}{\partial y}=-g\tan\theta-\frac{\partial p}{\rho\partial x}+\frac{\partial \tau}{\partial y}$$

$$0=-\frac{\partial p}{\rho\partial y}-g$$

numerical resolution of the

full system before averaging

RNSP (Reduced NS Prandtl)

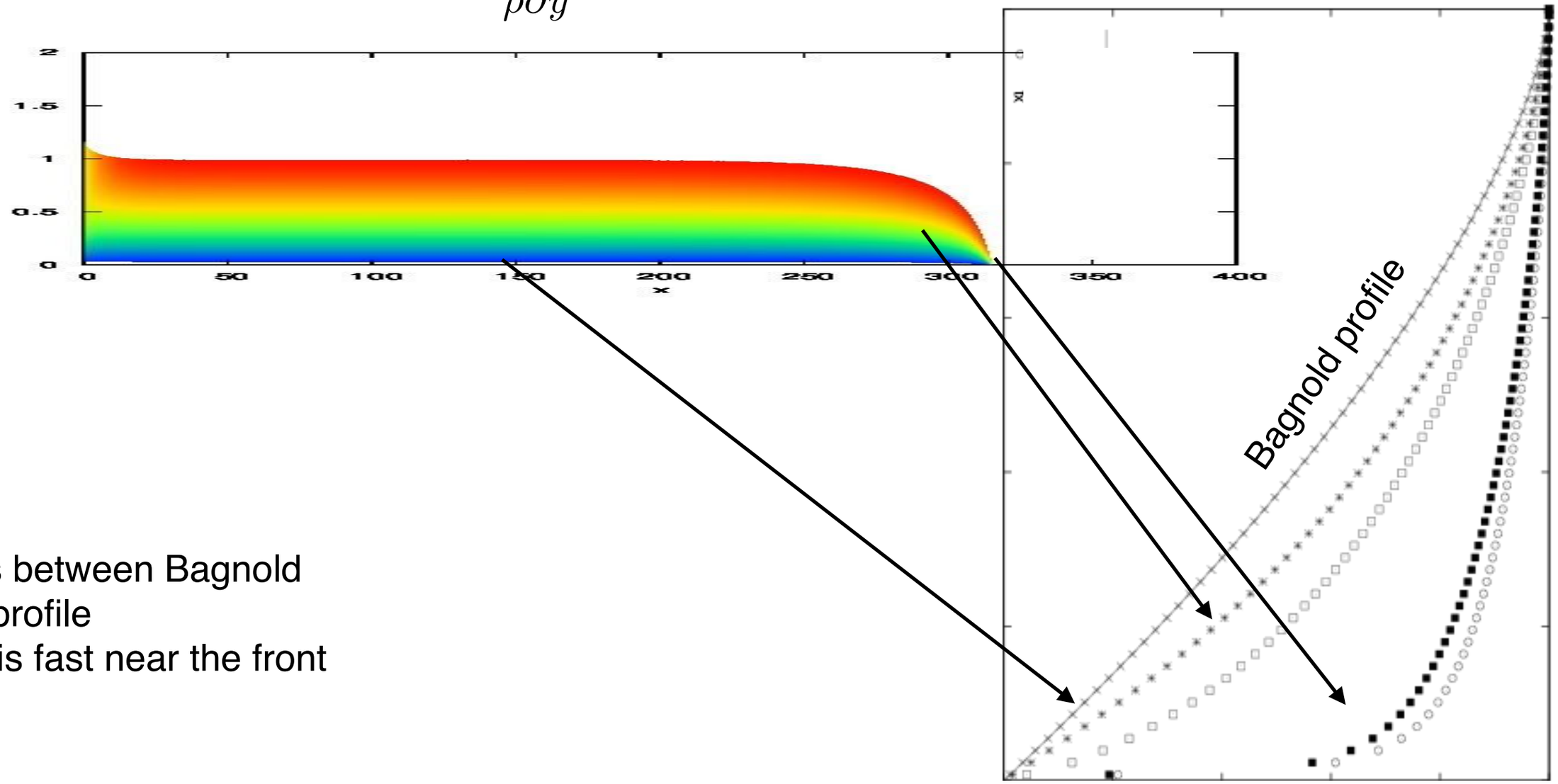

the profile is between Bagnold
and a “flat” profile
the change is fast near the front

Front in Savage Hutter St Venant

Lagrée et al. EPJ WoC 2017

$$\frac{\partial u}{\partial x}+\frac{\partial v}{\partial y}=0$$

$$\frac{\partial u}{\partial t}+\frac{\partial u^2}{\partial x}+\frac{\partial uv}{\partial y}=-g\tan\theta-\frac{\partial p}{\rho\partial x}+\frac{\partial \tau}{\partial y}$$

$$0=-\frac{\partial p}{\rho\partial y}-g$$

numerical resolution of the

full system before averaging

RNSP (Reduced NS Prandtl)

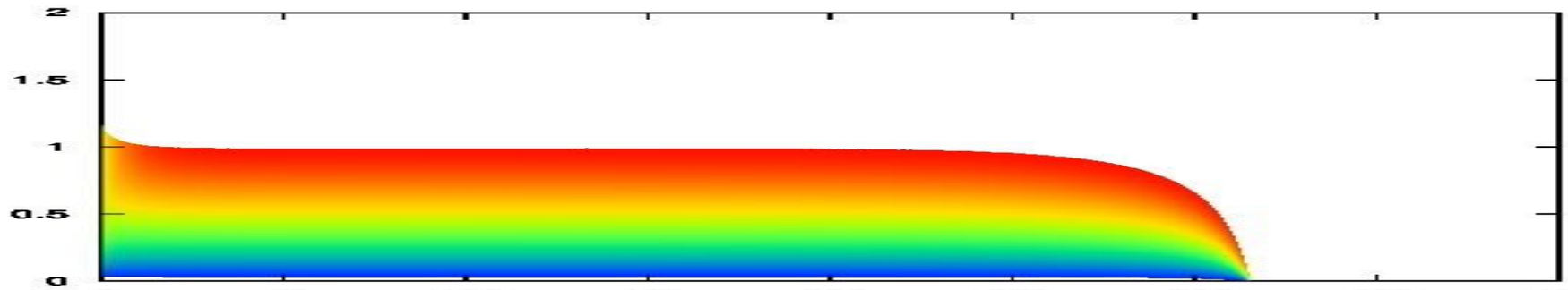

compute the shape factor:

the profile is between Bagnold
and a “flat” profile
the change is fast near the front

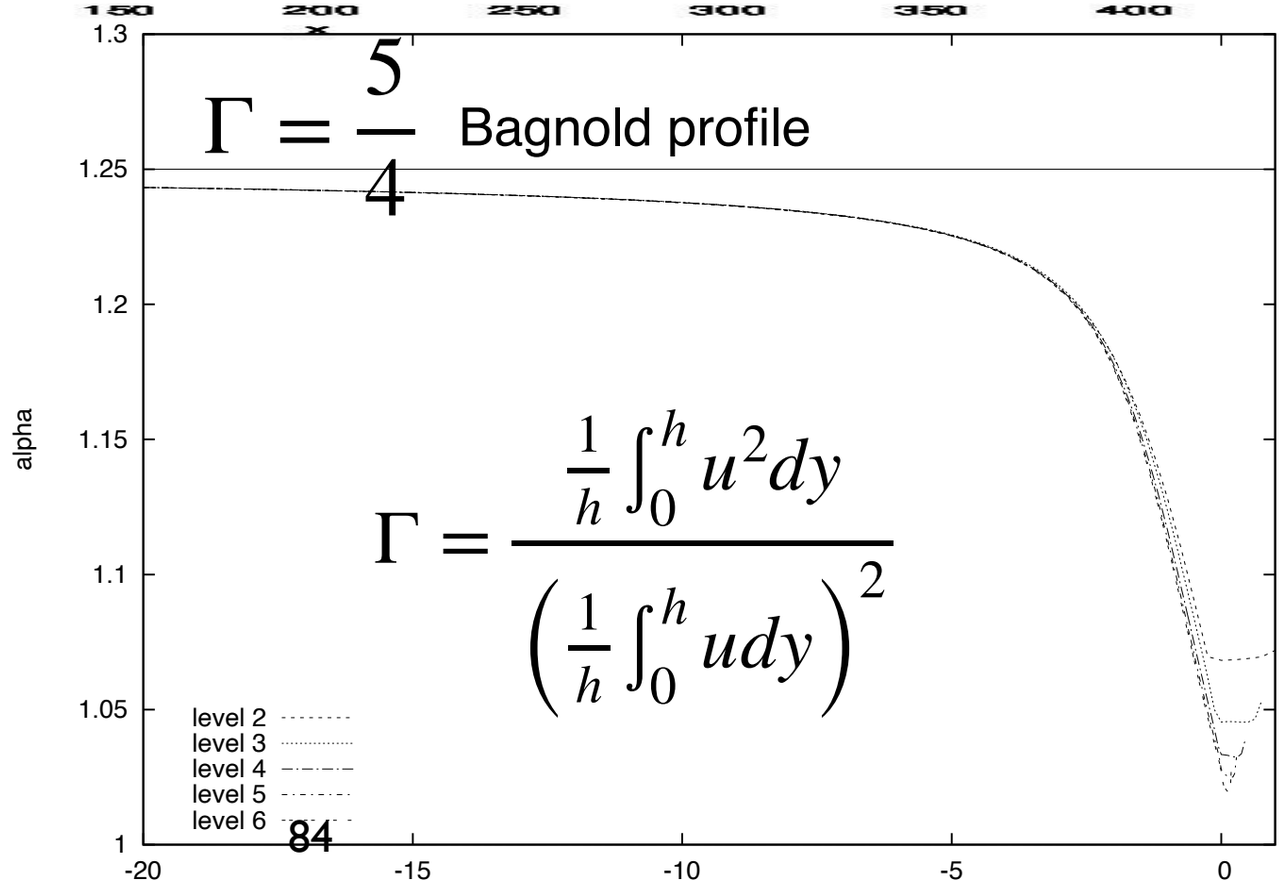

$\Gamma = 1$

Front in Savage Hutter St Venant

Lagrée et al. EPJ WoC 2017

$$\frac{\partial u}{\partial x}+\frac{\partial v}{\partial y}=0 \qquad 0=-\frac{\partial p}{\rho\partial y}-g$$

$$\frac{\partial u}{\partial t}+\frac{\partial u^2}{\partial x}+\frac{\partial uv}{\partial y}=-g\tan\theta-\frac{\partial p}{\rho\partial x}+\frac{\partial \tau}{\partial y}$$

numerical resolution of the full system before averaging

RNSP (Reduced NS Prandtl)

compared

with F=0 and Γ=1 (SHSV)
with the analytical solution F, Γ=5/4

Thin Layer (Boundary Layer) and integral SHSV are finally very close
there is a noticeable effect of inertia

Front in Savage Hutter St Venant

Lagrée et al. EPJ WoC 2017

$$\frac{\partial u}{\partial x}+\frac{\partial v}{\partial y}=0 \qquad 0=-\frac{\partial p}{\rho\partial y}-g$$

$$\frac{\partial u}{\partial t}+\frac{\partial u^2}{\partial x}+\frac{\partial uv}{\partial y}=-g\tan\theta-\frac{\partial p}{\rho\partial x}+\frac{\partial \tau}{\partial y}$$

numerical resolution of the full system before averaging

RNSP (Reduced NS Prandtl)

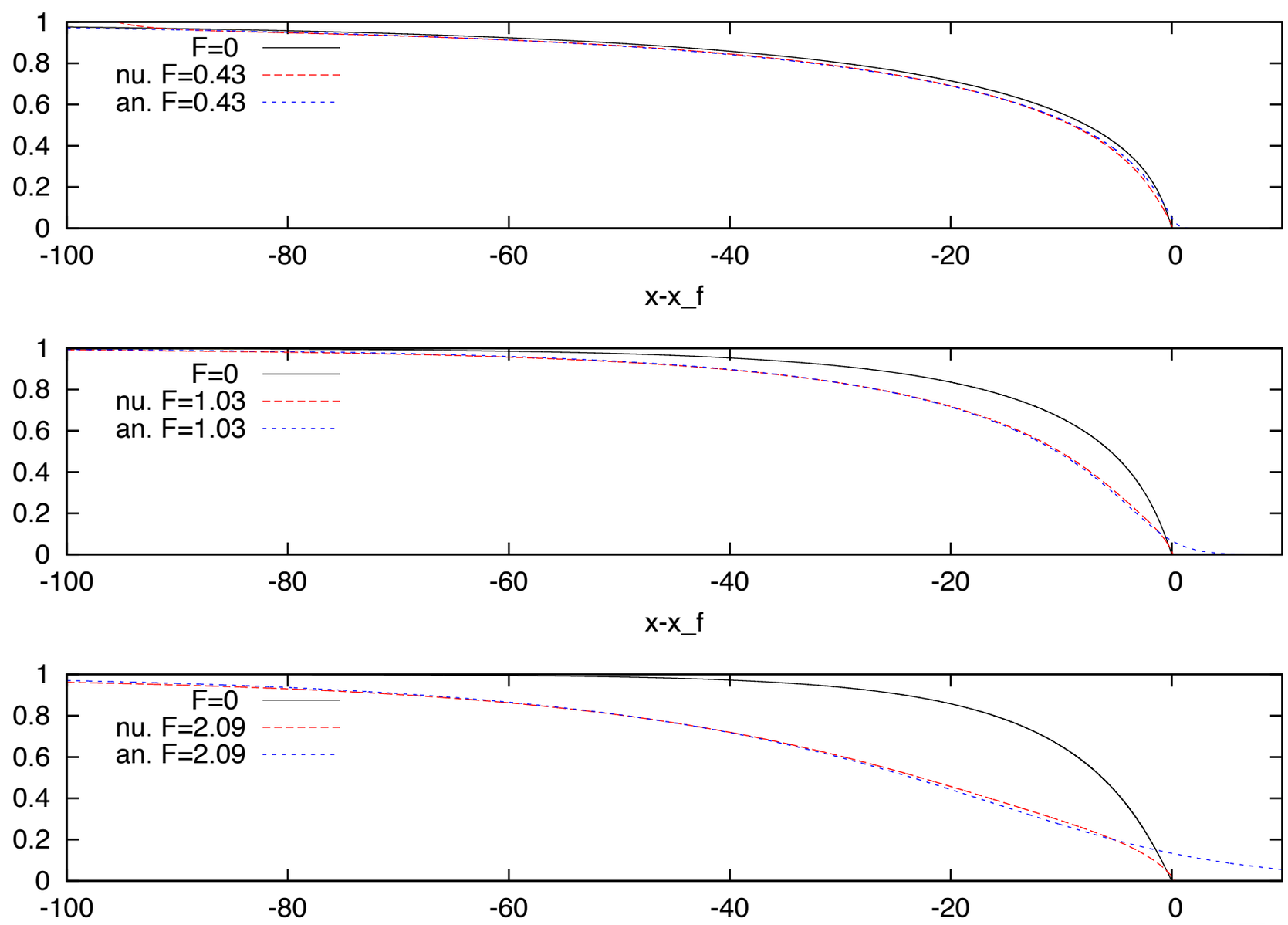

compared

with F=0 and Γ=1 (SHSV)
with the analytical solution F, Γ=5/4

Thin Layer (Boundary Layer) and integral SHSV with Γ=5/4 are finally very close
there is a noticeable effect of inertia

Front in Savage Hutter St Venant

- implementing the μ(I) friction law in Shallow Water (SVSH)
  - friction is only at the bottom
  - pay attention to the shape factor: should be Γ=5/4
  - but: Γ=1 in the SVSH for Galilean invariance (and entropy?) and practical use

- Widely used in geophysics with Γ=1
- 1 D model

Multilayer vs Multilayer

full system before averaging

$$\frac{\partial U_1}{\partial x} + \frac{\partial U_2}{\partial z} = 0$$

$$\rho(\frac{\partial}{\partial t}U_1 + \frac{\partial}{\partial x}U_1^2 + \frac{\partial}{\partial z}(U_1U_2)) = -\frac{\partial p}{\partial x} + \frac{\partial \tau_{12}}{\partial z} + ...$$

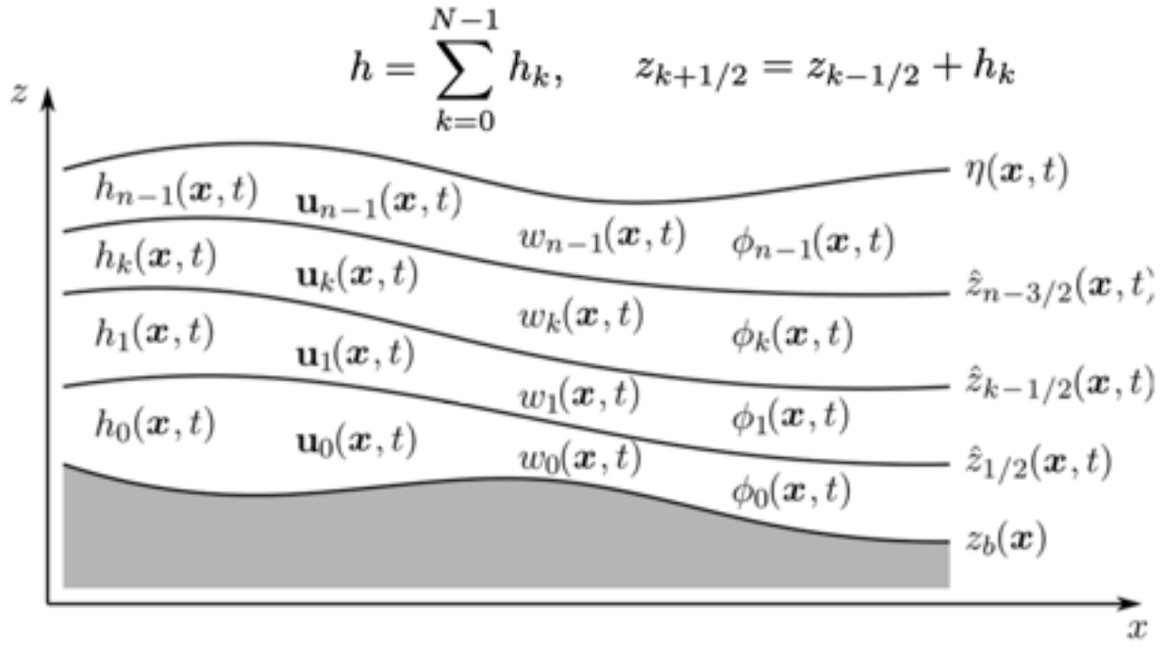

notation

$$\int_{z_{k-1/2}}^{z_{k+1/2}} \frac{\partial}{\partial z} q dz = q(x, z_{k+1/2}) - q(x, z_{k-1/2}) = [q]_k.$$

$$\begin{cases} \frac{\partial}{\partial x}(h_k u_k) + [U_2 - U_1 \frac{\partial}{\partial x} z]_k = 0. \\ \rho \frac{\partial}{\partial t}(h_k u_k) + \rho \frac{\partial}{\partial x}(h_k u_k^2) = -\frac{\partial}{\partial x}(h_k p_k) + [p \frac{\partial}{\partial x} z]_k + \rho[U_1(\frac{\partial}{\partial t} z + U_1 \frac{\partial}{\partial x} z - U_2)]_k + [\tau_{12}]_k. \end{cases}$$

Multilayer Saint-Venant system with mass exchanges", https://basilisk.fr/src/multilayer.h

$$\begin{cases} \frac{\partial h}{\partial t} + \sum_{\alpha=1}^{N} \frac{\partial (h_\alpha u_\alpha)}{\partial x} = 0, \\ \frac{\partial (h_\alpha u_\alpha)}{\partial t} + \frac{\partial}{\partial x}\left(h_\alpha u_\alpha^2 + \frac{g}{2} l_\alpha h^2\right) = -g h_\alpha \frac{\partial z_b}{\partial x} + u_{\alpha+1/2} G_{\alpha+1/2} - u_{\alpha-1/2} G_{\alpha-1/2} + (\tau_{\alpha+1/2} - \tau_{\alpha-1/2}) \end{cases}$$

$$G_{\alpha+1/2} = \frac{\partial z_{\alpha+1/2}}{\partial t} + u_{\alpha+1/2} \frac{\partial z_{\alpha+1/2}}{\partial x} - U_2\left(x, z_{\alpha+1/2}, t\right)$$

used here

Multilayer vs Multilayer

full system before averaging

$$\frac{\partial U_1}{\partial x} + \frac{\partial U_2}{\partial z} = 0$$

$$\rho(\frac{\partial}{\partial t}U_1 + \frac{\partial}{\partial x}U_1^2 + \frac{\partial}{\partial z}(U_1U_2)) = -\frac{\partial p}{\partial x} + \frac{\partial \tau_{12}}{\partial z} + ...$$

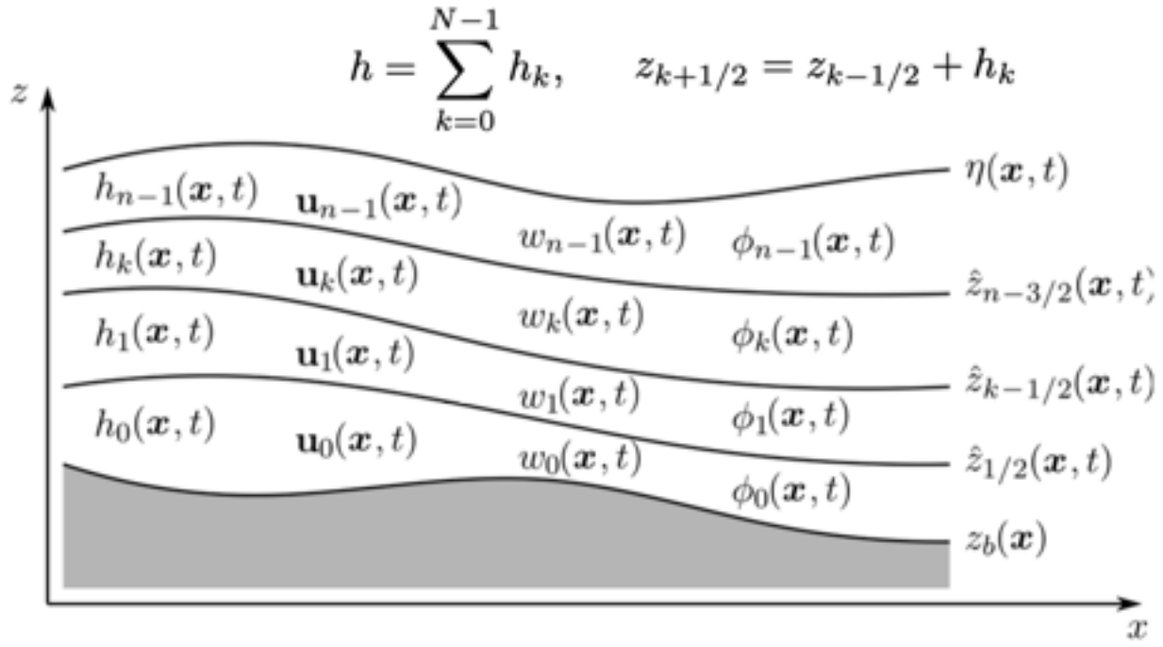

notation

$$\int_{z_{k-1/2}}^{z_{k+1/2}} \frac{\partial}{\partial z} q dz = q(x, z_{k+1/2}) - q(x, z_{k-1/2}) = [q]_k.$$

$$\begin{cases} \frac{\partial}{\partial x}(h_k u_k) + [U_2 - U_1 \frac{\partial}{\partial x} z]_k = 0. \\ \rho \frac{\partial}{\partial t}(h_k u_k) + \rho \frac{\partial}{\partial x}(h_k u_k^2) = -\frac{\partial}{\partial x}(h_k p_k) + [p \frac{\partial}{\partial x} z]_k + \rho[U_1(\frac{\partial}{\partial t} z + U_1 \frac{\partial}{\partial x} z - U_2)]_k + [\tau_{12}]_k. \end{cases}$$

Multilayer Euler-Lagrange”

https://basilisk.fr/src/layered/ hydro.h

$$\begin{cases} \frac{\partial}{\partial t} h_k + \frac{\partial}{\partial x}(h_k u_k) = 0. \\ \rho \frac{\partial}{\partial t}(h_k u_k) + \rho \frac{\partial}{\partial t}(h_k u_k^2) = -h_k g \frac{\partial \eta}{\partial x} + [\tau_{12}]_k. \end{cases}$$

$$G_{\alpha+1/2} = 0$$

Popinet 2020
work on progress for non newtonian flows

Conclusion Perspectives

A journey in the 1D system with application on flood, blood, and granular flows

closure: importance of the Boussinesq shape factor and friction depending on the problem

Multilayer is a compromise, faster than NS more precise than Saint-Venant
(There is always space for two layer description (James et al. 2019))

recent computations in Marseille on the same configuration (granular μ(I))
enstrophy approach: Deleage & Richard 2026

some possible **problems** (identified in Boundary layer):
- singularity at separation
- finite time singularity
- spurious instabilities (but removes ill posedness of μ(I)!)
- coupling

Perspectives

Multilayer Euler-Lagrange will be useful for multiphase flows :
- land slides due to rain: mud+water…
- Tsunamis generated by avalanche of grains + water…

a numerical code which switches from 2D…1D depending on the degree of precision

Félix Lecomte (1737-1817)
D'Alembert (1717-1783), auteur de l'Encyclopédie
Avant 1786 Sculpture Marbre
H. 1,50 m ; l. 0,95 m ; pr. 0,92 m
Don de Napoléon Ier à l'Institut de France, 1807

en arrière plan:
Eugène Delacroix
La Liberté guidant le peuple, 1830
260 × 325 cm

Masashi Saito, Xiaofei Wang, Arthur Ghigo, Jeanne Ventre, Teresa Politi, Fanshuo Ma,…

Geoffroy Kirstetter, Olivier Delestre, Mathilde Tavares,…

Stéphane Popinet, Jose Maria Fullana, Stéphanie Lebœuf…

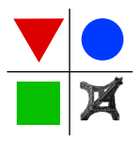

∂'Alembert
Institut Jean le Rond d'Alembert

SCIENCES SORBONNE UNIVERSITÉ

cnrs